INVESTIGATION OF HEMI-GAP-JUNCTION CHANNELS IN RETINAL HORIZONTAL CELLS

By

Ziyi Sun

Dissertation

Submitted to the Faculty of the

Graduate School of Vanderbilt University

in partial fulfillment of the requirements

for the degree of

DOCTOR OF PHILOSOPHY

in

Biological Sciences

December, 2009

Nashville, Tennessee

Approved:

Professor Terry L. Page

Professor Douglas G. McMahon

Professor David J. Calkins

Professor Joshua T. Gamse

Professor Laurence J. Zwiebel

For my husband Xiaoming and for my parents, whose love and support made this possible.

ACKNOWLEDGEMENTS

I would like to express my deepest and sincerest gratitude to my thesis advisor Dr. Douglas G. McMahon for his insightful advice, direction, and continuous supportiveness. Dr. McMahon's enthusiasm for science and broad knowledge has greatly inspired me. His positive attitude and scientific spirit has been enormous encouragement to me during my graduate studies. I would also like to thank my thesis committee members, Dr. Terry Page, Dr. Laurence Zwiebel, Dr. Joshua Gamse, and Dr. David Calkins for their time, effort, and dedication in the development of my thesis research.

I would also like to show my gratitude to my colleagues of the McMahon lab for their friendship and assistance, both past and present, during my time at Vanderbilt, specifically Dr. Dao-Qi Zhang, Dr. Karen Gamble, Dr. Gregg Allen, Dr. Bin Zhao, Dr. Guoxiang Ruan, Dr. Christopher Ciarleglio, Shi Meng, Richard Penny, Tongrong Zhou, and James Foster. Particularly, I am so grateful to Dr. Dao-Qi Zhang, who originally introduced me to electrophysiology, for his valuable input to my thesis project. I also appreciate the help and the friendship from the members of the Johnson lab, the Page lab, and the Yamazaki lab. I also want to say thanks to the members of zebrafish facility for their assistance with zebrafish maintenance and other zebrafish-related issues. My thanks also go to my fellow graduate student friends for their companionship and being always supportive.

Most importantly, I want to thank my husband, Xiaoming Zhou, for his undying love,

support and encouragement from the first day I met him. I also want to express my utmost gratitude to my parents and my sister for their love, understanding, and support during this arduous adventure of research and discovery.

Finally I would like to thank the financial support from the NEI grants R01 EY09256 to DGM.

TABLE OF CONTENTS

Page

LIST OF FIGURES

CHAPTER I

INTRODUCTION

We rely on sight more than any other sense to interact with the space around us. Our eyes allow us to appreciate all the beautiful changes of the world in which we exist. With only one glance, it is sufficient to perceive a good image and determine the location, size, color and shape; or to detect movement and judge the direction and speed of the object. With the help of eyes, not only can we obtain the information accurately from the environment, but we can also respond to the environment more efficiently. Thus, vision is one of the most important senses to humans.

We know that the visual system begins with the eye and half of the brain cortex in humans is involved in visual signal processing. The fundamental question is: how can we see through our eyes? The first step in the process of seeing is the transmission and refraction of light by the optics of the eye. Light is one kind of electromagnetic energy, which is emitted in the form of waves. These waves encounter objects and then they are absorbed, scattered, and reflected. Based on the nature of these waves and their interaction with the environment, eyes can extract information about the world.

As shown in **Figure 1-1A**, the eye is a fluid-filled sphere enclosed by three layers of tissue. The external layer, formed by the sclera and the cornea, is the outermost protective layer. This layer maintains the shape of the globe, offers resistance to internal

and external forces, and protects the eye from becoming dry. The intermediate layer is divided into two parts: the anterior chamber (the iris and the ciliary body) and the posterior chamber (the choroid). The iris gives our eyes color and defines the size of the pupil. Behind the iris is the lens, which is a transparent structure that aids in focus. The ciliary body releases aqueous humor within the eye and it contains the ciliary muscle to control the shape of the lens. The choroid contains blood vessels, which deliver oxygen and nutrients to the retina. The innermost layer is the retina, which is a multi-layered light sensory tissue that lines the back of the eye. Although all components of the eye are indispensable for perceiving an image or detecting an object, the retina is the most critical component for vision, since it is the only layer in the eye that contains light-sensitive neurons. If the eye acts as a camera to capture the image, the retina is very much like the film. Light is processed into an image by first passing through the cornea, and then being focused through the lens onto the retina, which contains the photoreceptors. Photoreceptors receive light signals, convert them into neural electric activities, and eventually trigger nerve impulses. The retina is a complex neural network, which is composed of different types of retinal neurons and multiple synaptic connections, that further modify and transform the electric signals into spatially and temporally dynamic neural output. After the visual signals are processed by the retina neural circuit, they are transmitted as action potentials by the axons of retinal neurons and are transferred to the brain for further processing, where they are finally interpreted as visual images.

Thus, to better understand how the eye works and the conditions that affect vision, it is

vital to learn the organization and function of the retina, which has been the goal of many vision scientists during the past century.

Section 1.1: The organization and function of the vertebrate retina

Despite its peripheral location, the retina is actually a part of the central nervous system and develops from a pouch of the embryonic forebrain. As a natural “brain slice”, the vertebrate retina is an ideal region to study the vertebrate brain and has long been used as a model system for studying the neuronal network.

As shown in **Figure 1-1B**, the vertebrate retina is a thin layer of soft tissue, which measures only half a millimeter thick and is located in the innermost layer of the eye. It is a highly ordered laminar structure that consists of three compact layers of neurons separated by two synaptic layers. From the outer to the inner retina, there are five types of neurons arranged in this order: photoreceptors (PRs), including rods and cones, which are located in the outer nuclear layer (ONL); bipolar cells (BCs), horizontal cells (HCs), and amacrine cells (ACs), which are located in the inner nuclear layer (INL); ganglion cells (GCs) and displaced amacrine cells, which are located in the ganglion cell layer (GCL). The processes and synaptic connections of these neurons are located in the outer plexiform layer (OPL) and the inner plexiform layer (IPL). In the outer plexiform layer, photoreceptors synapse with bipolar cells and HCs in different positions. In the inner plexiform layer, the short axonal processes of bipolar cells make synaptic contacts with the dendritic processes of ganglion cells.

Two types of photoreceptors are present in the vertebrate retina: the rod photoreceptors and the cone photoreceptors. Both rods and cones contain light-sensitive photopigments, which can absorb light, evoke changes in the photoreceptor membrane potential, initiate a reaction cascade and trigger electric activities. In most sensory systems, a stimulus causes the depolarization of the cell membrane and ultimately stimulates an action potential. In the retina, light activation causes a graded change in the membrane potential of photoreceptors. The phototransduction processes in rods and cones are virtually the same, and the only major difference is the opsins they contain in the outer segment. During light stimulation, 11-*cis* retinal, the chromophore of the photopigment, absorbs a photon and isomerizes to all-*trans* retinal. This photoisomerization causes a conformational change of a G-protein coupled receptor called opsin, which is the protein component of the photopigment. Opsin then activates the G-protein transducin (G_t), which in turn activates the effector enzyme called phosphodiesterase (PDE) and results in the reduction of an intracellular second messenger molecule, cyclic guanosine monophosphate (cGMP). The decrease of cGMP concentration leads to closure of membrane Na^+ channels and causes negative changes of the membrane potential (hyperpolarization). Compared to rods, which contain only one type of photopigment, different spectra types of cones contain different types of photopigments, which are responsible for sensing light of different wavelengths. Generally, the cones respond to bright light and mediate high-resolution color vision, while the rods respond to dim light and mediate low-resolution night vision.

Except for rods and cones, a third class of photoreceptors, which use melanopsin as the photopigment, have been discovered in the mammalian retina (Hattar et al., 2002). They are intrinsic photosensitive retinal ganglion cells (ipRGC), which mediate non-imaging vision and support a variety of physiological functions, including synchronization of circadian rhythms, modulation of melatonin release, and regulation of pupil size (Berson et al., 2002; Panda et al., 2002). Most recently, intrinsic light response has also been found in teleost retinal HCs. In situ hybridization studies indicate that melanopsin is present in fish retinal HCs. Whole-cell recordings in dissociate retinal HCs from catfish and goldfish further demonstrate that intrinsic light response can be observed at least in some vertebrate HCs (Cheng et al., 2009).

In addition to these different photoreceptors, there are also regional differences in the retinal neuron organization from the center to the periphery. The peripheral retina has a higher ratio of rods to cones, making it more sensitive to light. Thus, the peripheral retina is able to detect weak signals in dark conditions. The center region of the retina, however, is specialized for high-resolution vision and known as the “fovea”, which contains only cones for maximal visual acuity.

Downstream of the visual signal transmission, ganglion cells output the processed information from the retina to the rest of the brain. Ganglion cells respond to stimulations with action potentials instead of graded potential changes. The long and large axons of ganglion cells are bound together to form optic nerves, which carry the image signal and project it to the rest of the central nervous system.

Therefore, the vertebrate retina forms a complex neuronal circuit and an elaborate structural network to refine and process the visual information at the first stage of vision.

A

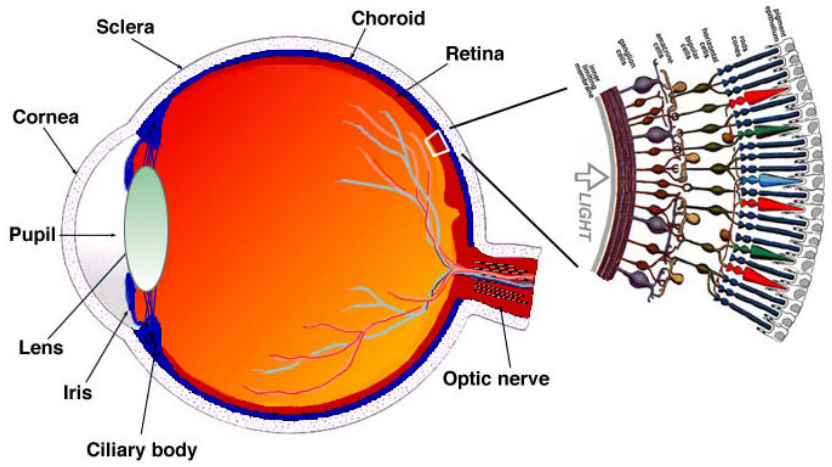

B

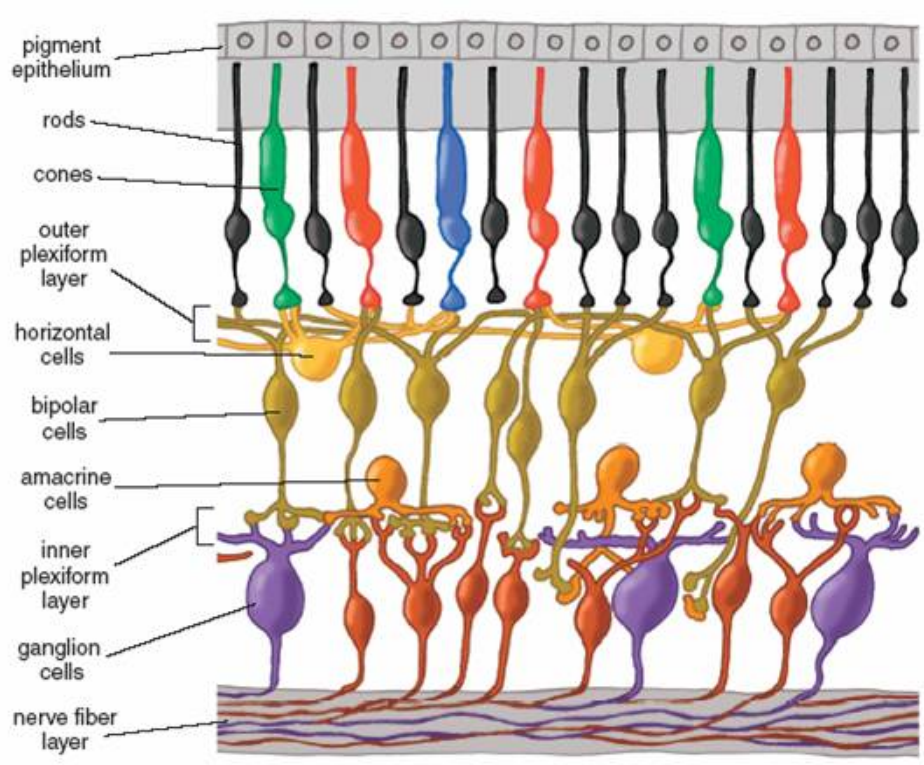

Figure 1-1. Schematic of the vertebrate eye and the retina.

Figure 1-1. Schematic of the vertebrate eye and the retina (Modified from Webvision).

(A) Vertical sagittal section of the vertebrate eye. There are three layers in the eye. The external layer is formed by the sclera and the cornea. The intermediate layer is divided into two parts, the anterior chamber (the iris and the ciliary body) and the posterior chamber (the choroid). The internal layer is the retina, which is also known as the sensory component of the eye.

(B) Cellular organization of the vertebrate retina. All vertebrate retinas are composed of three layers of neurons and two layers of synapses. The outer nuclear layer contains cell bodies of rods and cones, the inner nuclear layer contains cell bodies of bipolar cells, horizontal cells and amacrine cells and the ganglion cell layer contains cell bodies of ganglion cells and displaced amacrine cells. Separating these neuron layers are the outer and the inner plexiform layers where synaptic contacts occur.

Section 1.2: Neural circuitry and synaptic plasticity of the retina

Since multiple synaptic communications exist among retinal neurons and retinal neurons form highly selective synapses to transfer distinct synaptic signals, the vertebrate retina has long served as a model system to study neural circuitry and synaptic plasticity under light/dark conditions.

In the 1950s, Stephen Kuffler discovered that each ganglion cell only responds to the stimulation from a small circular patch of the retina, which is defined as the cell's receptive field. Two classes of ganglion cells are distinguished: the ON-center ganglion cells and the OFF-center ganglion cells. The ON-center ganglion cell increases its discharge rate in response to increased luminance, whereas the OFF-center ganglion cell increases its discharge rate following decreased luminance. This mechanism ensures that ganglion cells always convey increased action potentials to the brain whenever the light intensity increases or decreases. It is also found that each ganglion cell possesses a receptive field consisting of two parts: the center area and the surround area. The light response of ganglion cells in the center receptive field is opposite to that in the surround receptive field, which is known as the center-surround antagonistic organization. This allows the retina to be sensitive to the luminance contrast instead of absolute light intensity.

In the retina, the ON- and OFF-center pathways and the center-surround organization of retinal neurons are initiated at the photoreceptor terminals in the outer plexiform layer, where photoreceptors, bipolar cells and HCs are synaptically contacted. The ON- and

OFF-center ganglion cells selectively synapse with the terminals of the ON- and OFF-center bipolar cells in separate strata of the inner plexiform layer. In the dark, photoreceptors are depolarized. Like most other neurons, photoreceptors release the neurotransmitter glutamate during depolarization, and the glutamate release rate is reduced during light-induced hyperpolarization. The major visual signal is transmitted from photoreceptors to the optic nerve along a direct three-neuron chain: photoreceptors to bipolar cells to ganglion cells. As mentioned in section 1.1, there are two types of photoreceptors in the retina: rods and cones. Since rods and cones are presynaptic to different bipolar cells, their signals are segregated into parallel streams. In the cone pathway, two classes of cone bipolar cells are defined based on the glutamate response. One is the ON-center cone bipolar cell containing a G-protein-coupled metabotropic glutamate receptor (mGluR6), which responds to glutamate by hyperpolarization, and the other is the OFF-center cone bipolar cell containing ionotropic glutamate receptors (α-amino-3-hydroxy-5-methyl-4-isoxazolepropionic acid (AMPA) receptor and kainate receptor), responding to glutamate by depolarization. Cone bipolar cells relay direct signals from cone photoreceptors to ganglion cells, and this center-surround organization continues to ganglion cells via the synaptic connections in the inner plexiform layer. Compared to cone bipolar cells, in mammals, only one type of rod bipolar cell (the ON-center rod bipolar cell) is found. Rod bipolar cells do not contact ganglion cells directly. The rod signal is transmitted to rod bipolar cells and subsequently to AII amacrine cells in the inner retina. AII amacrine cells then make electrical synapses with

the ON-center cone bipolar cells and glycinergic chemical synapses with the OFF-center cone bipolar cells. In turn, the ON- and OFF-center cone bipolar cells pass the rod signal onto the ON- and OFF-center ganglion cells, respectively. In addition, the rod signal transmits from rods to cones through the electrical synapses in the outer retina and then it is relayed to ganglion cells via cone bipolar cells.

HCs and amacrine cells, known as the interneurons in the retina, mediate the lateral interaction and feedback loops in different plexiform layers. In the outer plexiform layer, HCs are laterally synaptic with photoreceptors, receiving the excitatory input from photoreceptors and sending the inhibitory signal back to photoreceptors. This process is known as the feedback pathway, which adjusts the gain of the photoreceptor output and in turn affects the activity of bipolar cells and ganglion cells. In the inner plexiform layer, amacrine cells are synaptically contacted with bipolar cells, modulating and integrating the visual signal for ganglion cells. The lateral signal transmitted by HCs and amacrine cells is modulated by various excitatory and inhibitory stimuli, such as amino acids, catecholamines, peptides, and nitric oxide.

Vertebrate vision depends on the contrast between the object and the background to perceive an image, and the center-surround organization of the retina plays a vital role in maintaining the normal visual function. The retinal neuronal circuit is critical to generate the center-surround receptive field. In addition, retinal HCs play an important role in providing the negative feedback to photoreceptors, and therefore contribute to the formation of the center-surround receptive field (Wu, 1992).

Section 1.3: Horizontal cells and the negative feedback pathway at the first visual synapse

HCs were first described in the fish retina as brick-like structures located mostly at the inner nuclear layer (Yamada and Ishikawa, 1965). In all vertebrates, neighboring HCs of the same physiological type are connected to each other through gap junctions at their dendrites, allowing lateral flow of small molecules and ions within the HC network. The conductance of the gap junctions between HCs is influenced by many intracellular and extracellular chemicals such as dopamine, retinoic acid, nitric oxide, and hydrogen ions that are released by other retinal neurons (Baldridge et al., 1987; McMahon and Brown, 1994; Zhang and McMahon, 2000; Bloomfield and Volgyi, 2009). The gap junctions between HCs result in large receptive fields spreading to other retinal regions, which are beyond their immediate dendritic fields (Naka and Rushton, 1967; Kaneko, 1971).

Based on the morphology difference, there are several subtypes of HCs identified in the vertebrate retina. For example, in zebrafish retina, two major types of HCs were identified as H_A type HCs and H_B type HCs (McMahon, 1994; Connaughton et al., 2004). As shown in **Figure 1-2**, H_A type HCs possess round somal bodies with many small processes projecting into the outer plexiform layer to contact cone pedicles. H_A type HCs can be further divided into two subgroups, H_A-1 HCs and H_A-2 HCs, with the major difference that the latter have axons while the former do not. Compared to H_A type HCs, H_B type HCs are more elongated in the somal body with shorter and thicker processes. Both H_A and H_B type HCs are cone-driven HCs.

A

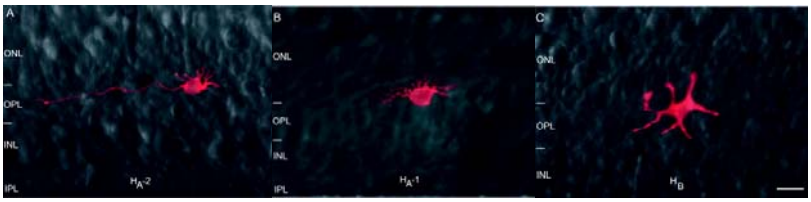

B

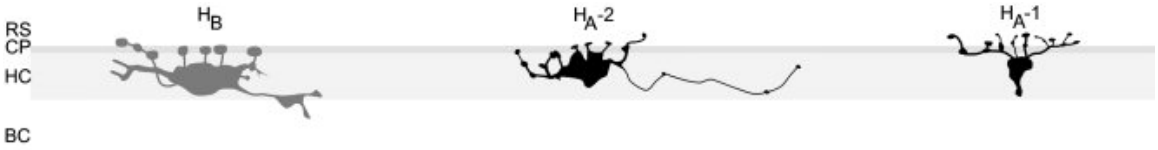

Figure 1-2. Two major types of horizontal cells (HCs) identified in the zebrafish retina (Modified from Connaughton et al., 2004).

(A) H_A type (stellate cells) and H_B type (laminar cells) HCs identified by DiOlistic staining. H_A type HCs have small and rounded cell bodies, whereas H_B type HCs usually have long somata. H_A type HCs are divided into two subclasses: cells with axons (H_A-2) and cells without axons (H_A-1). Both H_A and H_B type HCs are cone-driven HCs. Scale bar = 10 μm.

(B) Morphological comparison of different types of HCs from the zebrafish retina.

As the second-order neurons in the retina, HCs receive the direct glutamatergic input from, and provide a negative feedback to, photoreceptors, and contribute to the formation of the surround receptive field of bipolar cells and ganglion cells. HCs also influence the dynamic range, spatial properties, and color opponency of visual messages in bipolar cells, and subsequently the neurons in the inner retina. During visual information processing, the first signal relay occurs at the cone synapse. The morphology of the cone synaptic terminal is unique and conserved in all vertebrate species. In this synapse, HCs are postsynaptic to photoreceptors in a lateral position, while bipolar cells connect to photoreceptors in a central position. The processes of HCs deeply invaginate into the synaptic terminal of photoreceptors and are close to the synaptic ribbon.

In the dark, HCs depolarize to around -40 mV, since glutamate is continuously released from cones to HCs. Upon light stimulation, photoreceptors hyperpolarize due to the photopigment-induced reaction cascade, which leads to a decreased glutamate release and in turn hyperpolarizes HCs. The negative membrane potential change of HCs generates a feedback signal to cones and eventually induces an increased glutamate release from cones to HCs. This process is known as the negative feedback pathway from HCs to cones.

The negative feedback signal from HCs to cones is critical to support the normal retina function. The physiological importance of this pathway is mostly appreciated in three aspects.

First, the negative feedback pathway supports the center-surround antagonistic

receptive field organization (Stone and Witkovsky, 1987). Along the visual pathway, bipolar cells are the first neurons that exhibit the center-surround antagonistic receptive field organization. The center input is mediated by the photoreceptor-to-bipolar cell synapse, while the surround input is predominantly mediated by the feedback pathway from HCs to cones and then to bipolar cells. As a result of the negative feedback inhibition, HCs obtain excitatory chemical inputs from the center receptive field of photoreceptors and convert it into inhibitory feedback signals for cones in the surrounding zone, thereby shunting their responses. This antagonism is proposed to have an important role in establishing the receptive field for bipolar cells and ganglion cells, which can be dynamically regulated in response to different light conditions, thus encoding spatial information and contrast.

Second, the negative feedback pathway makes a significant contribution to the process of light adaptation (Burkhardt, 1993). Light adaptation refers to the decreased sensitivity of photoreceptors in the presence of steady light illumination. Under this condition, the negative feedback pathway enables HCs to impose a depolarized effect on the membrane potential of photoreceptors in the center receptive field, which decreases the light-evoked response in photoreceptors and consequently modifies the output of photoreceptors. As a result, the firing rate of the center receptive field of ganglion cells decreases. In this way, the negative feedback pathway can adjust the light sensitivity of cones. Since the electrical response of photoreceptors only spans a 30-mV range, while the environmental light intensity is very broad, the decreased sensitivity of retinal neurons

allows the limited responsive range to cover a much wider range of light intensities from the environment.

Last, the negative feedback pathway mediates the color opponency of retinal neurons (Stell and Lightfoot, 1975; Burkhardt, 1993; Twig et al., 2003). Color opponency begins at the second-order neurons in the retina. Retinal neurons can distinguish colors because light of different wavelengths can elicit responses with different polarities. In other words, light of some wavelengths induces depolarization, whereas others induce hyperpolarization. In fish, a network of excitatory feedforward and inhibitory feedback pathways between cones and HCs is widely acknowledged to explain the generation of color opponency. In this model, each type of HC receives the major excitatory input from only one spectral type of cone: the L-cone (red) to the monophasic HC (MHC or H1), the M-cone (green) to the biphasic HC (BHC or HC2), and the S-cone (blue) to the triphasic HC (THC or H3). On the other hand, feedback pathways mediate inhibitory inputs from the MHC to all types of cones, from the BHC to the S-cone, and none from THC. The final integrated output of the feedforward and feedback signals results in different response polarities in three spectral types of HCs (Stell and Lightfoot, 1975). This model was further modified, but the basic principle remains (Kamermans et al., 1991; Kraaij et al., 1998).

Section 1.4: Hypotheses of the negative feedback pathway

The physiological importance of the feedback inhibition has been well established.

However, the mechanism of HC negative feedback to cones is still not fully understood. There are three prevalent hypotheses developed in the past several decades to explain the underlying mechanism. They are gamma-aminobutyric acid (GABA)-based feedback model, proton-based feedback model, and ephaptic feedback model.

Over two decades ago, GABA was suggested to be the neurotransmitter mediating the feedback pathway between HCs and cones. Research indicates that GABA is contained in some HCs and GABA receptors are located at cone synaptic terminals (Lam et al., 1978; Tachibana and Kaneko, 1984). However, several later studies show that the application of GABA agonist or antagonist has no effect on the feedback signal in some species (Thoreson and Burkhardt, 1990; Burkhardt, 1993; Verweij et al., 1996), and the conventional presynaptic vesicles containing GABA can not be observed in HCs. Therefore, it is generally accepted that the negative feedback is a GABA-independent pathway.

Further experiments demonstrate that the negative feedback from HCs to cones is mediated through the modulation of the L-type Ca^{2+} channel in cones. In a voltage clamp recording experiment, the negative feedback from HCs to cones results in a left shift of the Ca^{2+} current-voltage curve, which induces an increased Ca^{2+} flow into cones (Kamermans et al., 2001a). Since the glutamate release in cones is a Ca^{2+}-dependent process, the increased Ca^{2+} influx leads to an increase in glutamate release from cones to HCs, and also depolarizes cones. In this way, the negative feedback effect is generated. Although the cause of the Ca^{2+} current negative shift is still unclear, two

models have been proposed to explain it.

One model is proton based. In this model, the light stimulus leads to an alkalization of the synaptic cleft, which affects the properties of the Ca^{2+} channel and results in an increased Ca^{2+} flux into the cone (Hirasawa and Kaneko, 2003; Vessey et al., 2005). Considerable evidence supports that the hyperpolarization of HCs is accompanied by an increase of extracellular pH, which is known to modulate the activation function of Ca^{2+} channels (Barnes et al., 1993). It has been proposed that the pH change in the synaptic invagination is caused by proton exchange or transport into HCs. This data suggests that the extracellular proton concentration is a likely candidate for the negative feedback mediator. However, the mechanism by which HCs modulate the extracellular pH is still not determined. Since the proton flux takes place in an extremely small place, there is still no way to measure the extracellular, intra-invagination pH change. Also, there are several reports that argue against the proton hypothesis (Fahrenfort et al., 2009). For example, in goldfish, healthy feedback responses can still be observed in the presence of 10 mM HEPES (Mangel et al., 1985).

The other model is the electric ephaptic model, which was first proposed by Byzov and Shura-Bura (Byzov and Shura-Bura, 1986) and later modified and experimentally tested by Kamermans and co-workers (Kamermans et al., 2001b). Here, the word “ephaptic” describes the communication between neurons through the modulation of the extracellular potential. Since the neurons are anatomically and electrically proximate, the electric field generated by one neuron can alter the excitability of neighboring neurons. In

this model, HGJ channels expressed at the tips of HC dendrites are proposed to modulate the activity of the Ca^{2+} channel by producing a continuous current sink within the synaptic cleft. As shown in **Figure 1-3** (Goodenough and Paul, 2003), the processes of laterally positioned HCs invaginate deeply into the cone pedicle. The HGJ channels located at the HC dendrite tips are opposed to the voltage-dependent Ca^{2+} channels and the glutamate containing vesicles along the synaptic ribbon. Centrally positioned processes from bipolar cells also synapse with cones in the cone pedicle. They may also interact with HC processes. This unique invaginating structure of the cone pedicle provides the structural basis for the ephaptic model.

In the dark, cones are depolarized and continuously release glutamate, which keeps HCs depolarized at around -40 mV. Upon light stimulation, a reduced glutamate release from cones hyperpolarizes HCs to around -80 mV, which leads to an increased current flow into HCs mediated by hemichannels. Since the small inward hemichannel current flows through the high resistance of the intersynaptic space, the extracellular potential near these hemichannels (located at the tips of the HC dendrites) will become negative. Locally, the potential difference over the cone membrane will become smaller. Thus, the Ca^{2+} channels in the cone pedicle will sense a depolarized membrane potential, resulting in an increased Ca^{2+} influx and the subsequent increase of glutamate release. In this way, HGJ channels expressed at the tips of the HC dendrites could mediate a negative feedback from HCs to cones. Studies show that the negative feedback can be blocked by gap junction inhibitors (Kamermans et al., 2001b), intracellular acidification (Fahrenfort et

al., 2009), or 100 μM Co^{2+} (Fahrenfort et al., 2004), implicating that hemichannels are likely the major source producing the current sink. However, the validity of the ephaptic hypothesis is still under debate since some key questions are yet to be answered. For example, one of the most important questions is: will these special hemichannels remain open under physiological conditions? This project will bring answers to some of these questions and shed light on the underlying mechanism for the negative feedback pathway.

Taken together, the proton hypothesis and the ephaptic hypothesis are currently two major models proposed for the negative feedback pathway. Both hypotheses receive considerable experimental support as well as contradictory evidence, and a lot of questions need to be further addressed and clarified. It is interesting to note that hemichannels could potentially modulate the extracellular pH, which may be a key component that possibly unites the ephaptic model and the proton model in a modified hypothesis.

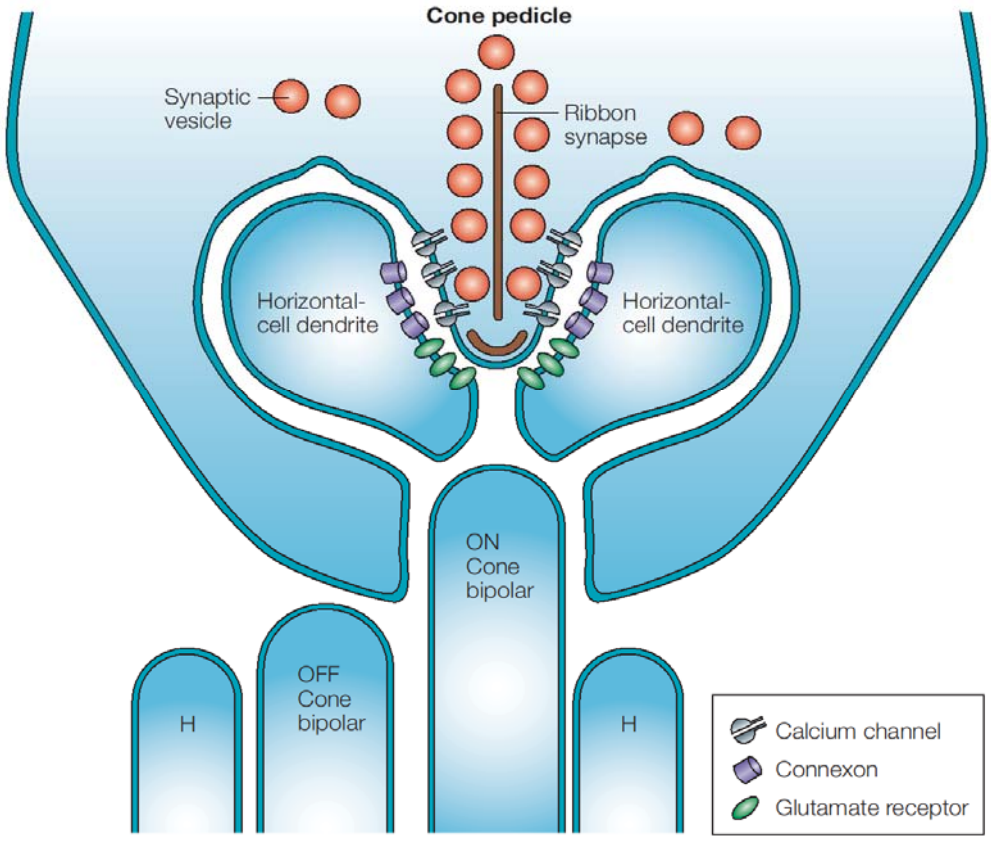

Figure 1-3. Schematic of a cone pedicle with an invaginating synapse, which provides the structural basis of the ephaptic feedback model (Modified from Goodenough and Paul 2003).

At the cone synapse, horizontal cells (HCs) and bipolar cells are postsynaptic with the cone, in a lateral and central position, respectively. The dendrites of HCs are deeply embedded in the cone pedicle, which is characterized by its unique ribbon synapse and associated synaptic vesicles. The hemi-gap-junction (HGJ) channels expressed at the tip of HC dendrites are apposed to the L-type Ca^{2+} channels in the cone. In the ephaptic feedback model, these HGJ channels are proposed to cause a negative extracellular potential change within the intersynaptic space upon light stimulation, which activates the Ca^{2+} channels and leads to an increased glutamate release.

Section 1.5: Molecular organization and biophysical properties of HGJ channels

As mentioned in section 1.3, HCs are extensively coupled to each other by gap junctions, which greatly enhance their receptive fields. Gap junctions are intercellular channels that connect adjacent cells. As shown in **Figure 1-4** (Bloomfield and Volgyi, 2009), a complete gap junction channel is composed of two HGJ channels (also known as hemichannels or connexons) from apposed plasma membranes (Verselis et al., 2000), and each HGJ channel is made of six connexin (Cx) subunits. There are two steps to assemble Cx proteins into a gap junction channel. First, six Cx subunits oligomerize into a HGJ channel in the plasma membrane of an individual cell. Second, two HGJ channels from adjacent cells align and dock to form a gap junction channel (Saez et al., 2005).

It is generally assumed that HGJ channels are closed during most physiological conditions to prevent loss of cytoplasmic molecules or entry of extracellular ions. For a long time, HGJ channels have only been considered as the structural precursor of gap junction channels. Recent studies, however, demonstrate that the HGJ channel activity is present in some single cells. The HGJ channel is found to be responsible for the large ionic conductance and high permeability of individual cells and its opening is modulated by various physiological and pathological conditions (Plotkin and Bellido, 2001; Contreras et al., 2004; Thompson et al., 2006; Zhang et al., 2008). Although the *in vivo* function of HGJ channels is still under debate, they have been shown to be involved in many physiological and pathological processes (Paul et al., 1991; DeVries and Schwartz, 1992; Beahm and Hall, 2002; Stout et al., 2002; Contreras et al., 2004; Thompson et al., 2006).

In addition, *in situ* hemichannel activities have been documented in the HCs isolated from fish retinas (DeVries and Schwartz, 1992; Malchow et al., 1993). The presence of HGJ channels in solitary native cells and transfected cell lines is well established, which lays the ground for studying the biophysical properties and potential physiological roles of these channels. Studies show that HGJ channels have similar gating and permeability properties to the gap junction channels that they form (Ebihara et al., 1995; Zhang and McMahon, 2000). Other studies on retinal neurons have shown that the cultured teleost HCs can elicit large voltage-sensitive hemichannel currents, which are sensitive to extracellular Ca^{2+}, intracellular pH, carbenoxolone, dopamine, and retinoic acid (DeVries and Schwartz, 1992; Trexler et al., 1996; Zhang and McMahon, 2001; Ripps et al., 2002, , 2004). In addition to the research on the HGJ channels in fish retinal HCs, studies on other tissues suggest that HGJ channels may also play roles in ATP release and Ca^{2+}-wave propagation in astrocytes (Stout et al., 2002), as well as in bone growth and bone remodeling (Plotkin and Bellido, 2001; Plotkin et al., 2002). These data indicate that unapposed hemichannels are responsible for the cell membrane conductance and may have significant biological functions.

The HGJ channel is composed of six Cx subunits, which belong to a family of highly homologous proteins. If all Cx subunits are of the same type, the formed HGJ channel is homomeric. Otherwise, a heteromeric HGJ channel is formed. Different Cx subunits contribute different properties of conductance and modulation to the hemichannels that they form. Although different hemichannels may exhibit different properties in gating and

modulation, most of them share two common properties. First, the majority of hemichannels are voltage-gating channels. In other words, they open upon depolarization of the membrane potential, but close upon hyperpolarization. Second, HGJ channels are Ca^{2+}-gating channels. They are open in response to low concentrations of extracellular Ca^{2+}, but are closed when the extracellular Ca^{2+} concentration is high (e.g. 1.5 to 2.5 mM). These common properties of HGJ channels bring up the key question again: are HGJ channels, which are hypothesized to mediate the feedback pathway in the retinal HCs, able to open at physiological Ca^{2+} concentrations and membrane potentials?

It is also noteworthy that some exceptions do exist. For example, Cx26 hemichannels expressed in *Xenopus* oocytes exhibit voltage-independent properties, and are open at both positive and negative membrane potentials (Ripps et al., 2004). Furthermore, hemichannels in the skate rod-driven HCs are found to be open even at 4 mM Ca^{2+} (Malchow et al., 1993). Therefore, it appears that the gating properties of hemichannels depend strongly on the Cx subunits. It is very possible that certain Cx proteins compose these unique HGJ channels in the retinal HCs, which are open under physiological conditions and generate the current sink for an ephaptic communication between HCs and cones.

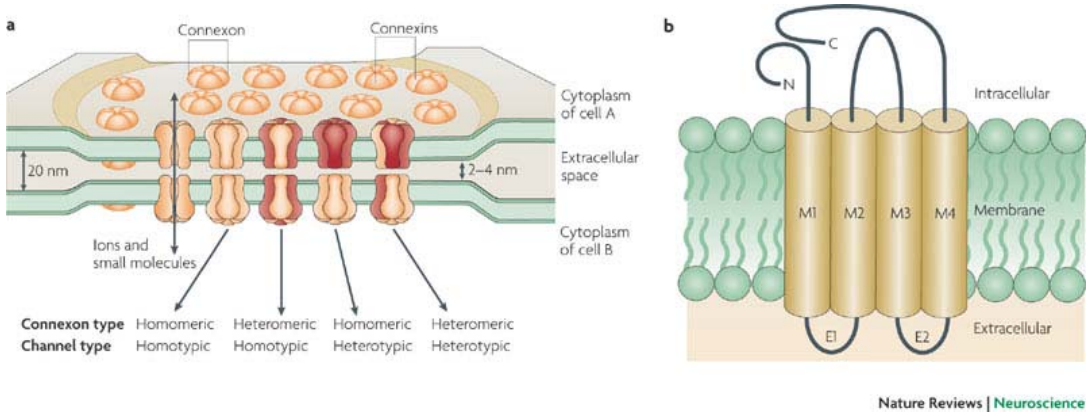

Figure 1-4. Structure and molecular organization of gap junctions and hemi-gap-junction (HGJ) channels (Modified from Bloomfield and Volgyi 2009).

(A) Gap junctions are formed by two HGJ channels between the opposing membranes of neighboring cells. Each HGJ channel (also known as hemichannel or connexon) is comprised of 6 connexin (Cx) subunits that are oriented perpendicular to the cells' membranes to form a central pore. HGJ channels may contain only one type of Cx subunit (homomeric hemichannels) or a mixture of different Cx subunits (heteromeric hemichannels).

(B) Connexin subunits are proteins that have four transmembrane domains, two extracellular loops (E1 and E2) and one intracellular loop, as well as cytosolic carboxyl and amino termini. The four transmembrane domains (M1–M4) share a conservative sequence that is important for docking in the cellular membrane. The cytoplasmic domains vary in length and amino acid sequence. Regulation of the three-dimensional structure of Cx proteins underlies the opening and closing of Cx channels, which is mediated at the cytoplasmic regions.

Section 1.6: Connexin family

Vertebrates encode two families of proteins as the molecular subunits for gap junctions and HGJ channels, known as the connexin (Cx) family and the pannexin (Panx) family. The latter is related to the invertebrate innexin (Inx) family and shares no sequence homology with Cx proteins. As the primary molecular subunits of gap junctions and HGJ channels, Cx proteins are membrane proteins with four conserved transmembrane domains, two conserved extracellular loops important for docking, one variable cytoplasmic loop, and cytoplasmic N- and C-termini (**Figure 1-4B**). Regulation of the conformation of Cx proteins underlies the opening and closing of Cx channels. A hemichannel consists of six Cx subunits and can be made of the same type of Cx protein (homomeric) or different types of Cx proteins (heteromeric). Interestingly, only certain combinations of Cx proteins will form functional hemichannels. In addition, a gap junction channel can be composed of two hemichannels with the same composition (homotypic) or different compositions (heterotypic). The different compositions of Cx channels lead to their differences in pore size and gating properties (Elfgang et al., 1995; Bevans et al., 1998).

In the late 1980s, the *cx* genes (*cxs*) were cloned, first among which were the human and the rat *cx32* (Kumar and Gilula, 1986; Paul, 1986). Then *cx30* (Gimlich et al., 1988) and *cx38* (Ebihara et al., 1989) from the frog *Xenopus laevis* are the first identified from nonmammalian vertebrates. They are soon followed by many other *cx* genes cloned from chicken, fish, croaker and other organisms. There are now 20 *cx* genes being identified in

human and 19 in the mouse, revealing a significant diversity in gap junctions and HGJ channels (Sohl and Willecke, 2004).

Studies on the phylogenesis and evolution of *cx* genes show that most *cx* genes can be found in most vertebrate species. A comparison of the *cx* family between human and zebrafish reveals an expanded family of 37 *cx* genes in zebrafish, almost twice as many as in human. Among them, 23 *cx* genes are recognized as homologs of 16 mammalian *cx* genes and the other 14 appear to be unique to zebrafish (Eastman et al., 2006; Cruciani and Mikalsen, 2007). These studies indicate a particular complexity of *cx* genes in zebrafish, which is mostly due to the genome duplication that happened in fish 200-million years ago (Taylor et al., 2001; Taylor et al., 2003).

Therefore, it is not surprising that a high molecular diversity of *cx* genes in the zebrafish retina has been observed. Since the first three *cx* genes were cloned and reported in zebrafish retina (Dermietzel et al., 2000), there are now more than 10 Cx proteins being reported to express in different retinal neurons. Among them, Cx52.6 and Cx55.5 are shown to specifically express in retinal HCs with hemichannel-forming properties (Dermietzel et al., 2000; Zoidl et al., 2004; Shields et al., 2007). Furthermore, they are reported to express only in H_A type HCs with distinct distribution patterns (Shields et al., 2007). Recently, another two *cx* genes, *cx52.7* and *cx52.9* were cloned from the zebrafish retina, which show high levels of protein sequence similarity to *cx52.6* and *cx55.5*, respectively (Zoidl et al., 2008). In a most recent study, Panx1 was also reported to express in the zebrafish retinal HCs, especially at their invaginating dendrites close to

synaptic ribbons (Prochnow et al., 2009). The molecular diversity of Cx proteins with various expression patterns in the zebrafish retina suggest that some Cx proteins may perform specialized roles *in vivo*, whereas others may serve more general functions.

Section 1.7: Zebrafish, a model animal for vision study

The zebrafish (*Danio rerio*) is a small tropical fish that naturally lives in Indian rivers. As a model organism, zebrafish has many advantages. First, zebrafish are easy to keep and breed. They are relatively small (the adult zebrafish usually does not exceed 5-6 cm), very fertile (an average of 100 offsprings per week per pair), and live in groups naturally (large numbers can be kept in a confined space). Second, zebrafish embryos are transparent and externally fertilized. They develop very rapidly, making zebrafish an ideal model organism to study the vertebrate development. Only 24 hours after fertilization, all major organs are recognizable. Within three days, the larva is hatched and starts swimming. Three months later, the zebrafish is sexually mature and capable of producing offspring. Lastly, the zebrafish has great potential for genetic analysis. The genetic property of zebrafish was first studied by George Streisinger and co-workers at the University of Oregon. Many techniques have been developed to introduce mutations in zebrafish. A large number of interesting mutants were recovered by several large-scale screens and some smaller mutagenesis studies (Baier et al., 1996; Fadool et al., 1997; Golling et al., 2002). So far, more than 1,300 mutant zebrafish lines have been generated using forward genetic screen methods, among which approximately 300 have retinal

phenotypes and 20 have lens phenotypes (Glass and Dahm, 2004). Following mutagenesis screens, candidate studying and positional cloning strategies have been successfully applied to characterize the regulators of eye development from the molecular level. Recently, a large reverse genetic screen that focuses on zebrafish retinal neurogenesis was performed by Pujic and colleagues, which complements the forward genetic mutagenesis (Pujic et al., 2006).

In addition to the favorable embryologic features and genetic advantages, the zebrafish is also a highly visually orientated species with large eyes, showing light response after only three days of development (Easter and Nicola, 1996). The zebrafish eye appears at about 12 hours post fertilization (hpf). By 24 hpf, the eyecups are well developed. Ganglion cells can be found at around 30 hpf, and the retinal layers become apparent at 50 hpf (Bilotta and Saszik, 2001). The adult zebrafish is tetrachromatic, possessing ultraviolet-sensitive cones as well as red, green, and blue-sensitive cones (Robinson et al., 1993). Zebrafish also have abundant rods. Like in other fishes, the zebrafish retina continues to grow throughout their lives. The morphology of the zebrafish retina and lens shows high degrees of similarity with that of other vertebrates, including humans. Several genetic behavioral tests such as the larval optokinetic and optomotor responses and vision mediated escape response of adult zebrafish, and electroretinography (ERG) have been successfully employed to screen mutant strains with visual defects (Neuhauss, 2003). A number of eye mutants have been generated with chemical mutagens, and the phenotypes include reduced eye size, disorganized retina, loss of photoreceptors, and

reduced ganglion cells (Malicki et al., 1996; Fadool et al., 1997).

Taken together, the unique embryonic features, great potential for genetic manipulation, and available visual research tools make zebrafish an attractive model to study the visual system, including its development, function, and disease.

Section 1.8: Morpholino-based gene knockdown in zebrafish

Compared to other model organisms such as the fly (*Drosophila melanogaster*) or the mouse (*Mus musculus*), a major drawback of zebrafish in the past was the lack of genetic tools. In recent years, however, both forward and reverse genetic methods have been greatly expanded. Although the knockout and knockin techniques are not yet available for zebrafish, a powerful alternative technique has been developed to functionally abolish any given gene product. The technique is known as morpholino-based gene knockdown.

Morpholinos are synthetic antisense RNA-like molecules based on the natural nucleic acid structure. In contrast to naturally occurring nucleic acids, morpholinos have the standard A, T, G and C bases attached to the morpholine ring instead of the deoxyribose ring and are linked through the phosphorodiamidate group instead of phosphate (**Figure 1-5A**) (Summerton and Weller, 1997). The replacement of anionic phosphates with uncharged phosphorodiamidate groups eliminates ionization in the physiological pH range, making morpholinos neutral in cells. The backbone of morpholinos endows them with resistance to nucleases, better solubility in water, and higher binding affinity.

Typically, morpholinos are designed as oligomers of 25 morpholine bases, complementary to the target RNA by standard nucleic acid base-pairing. Two types of morpholino interference are generally used, which are known as translational blocking and splicing blocking. Customized morpholinos are designed to complementarily bind to the 5' untranslated region (5' UTR) or cover the translational start codon (ATG) of mRNA sequence (**Figure 1-5B**) or a critical splicing site of the pre-mRNA. Unlike many other antisense structures (e.g. phosphorothioates and siRNA), morpholinos do not cause degradation of their target RNA molecules. Instead, morpholinos act by "steric blocking". They bind to a target sequence, hinder its translation into protein and thus result in a loss-of-function (or null) phenotype of the target gene. By blocking splicing sites in pre-mRNA, morpholinos can be used to modify and control normal splicing events (Summerton and Weller, 1997). Since morpholinos are nontoxic, it allows application of large amounts and high concentrations.

Morpholinos must be actively delivered into organisms or cells. In zebrafish, morpholinos are usually injected into the egg's yolk shortly after fertilization (1-8 cell staged embryos). Since the early embryonic cells are cytoplasmically connected, the hydrophilic morpholinos can rapidly diffuse throughout the embryo and immediately exert their effects *in vivo*. Most morpholino phenotypes are observed within 3 days of development, and may persist for up to 5 days. One big advantage of embryonic injection of morpholinos is that the desired phenotypes are quickly available for analysis in a short time from a few hours to several days. The disadvantage, however, is also apparent for

this approach. Since the morpholino effects will gradually diminish due to the progressive dilution of morpholinos by newly synthesized RNA, this method limits studies to the larval stage. So, to take advantage of morpholinos when studying a subject in the adult zebrafish, different approaches for morpholino introduction are explored.

In the current project, various Cx proteins in adult zebrafish retina HCs are expected to be selectively knocked-down by morpholinos against corresponding *cx* genes. A variety of methods, including scrape-loading, osmotic delivery, Endo-porter based delivery, EPEI based delivery, and microinjection, have been developed to introduce morpholinos into cultured cells (Gene Tools). However, because of the toxicity and relatively low delivery efficacy, most of these methods are only suitable for cell line cultures with high cell density and there is little success with primary cell culture. To circumvent this, a new method utilizing intraocular injection and electroporation to introduce morpholinos into adult zebrafish retinas was developed in the laboratory of David Hyde at Notre Dame University (Details will be described in Chapter III). Via this method, the expression of any protein in adult zebrafish retina can be selectively inhibited (Thummel et al., 2008). As mentioned above, the protein kinetics, especially the protein turnover rate, may affect the effectiveness of morpholinos. Although the half-lives of most plasma membrane proteins are longer than 24 hours, experiments have determined that Cx proteins have relatively short half-lives, even after they are incorporated into gap junction plaques. For example, in cultured cells, most Cx proteins, such as Cx43, Cx26, Cx32 and Cx45, show half-lives of 1.5 to 4 hours. Other studies suggest that the turnover of Cx proteins is also rapid *in*

vivo (Berthoud et al., 2004). Therefore, morpholino-mediated gene knockdown is an effective tool to study specific Cx proteins in the adult zebrafish retina.

A

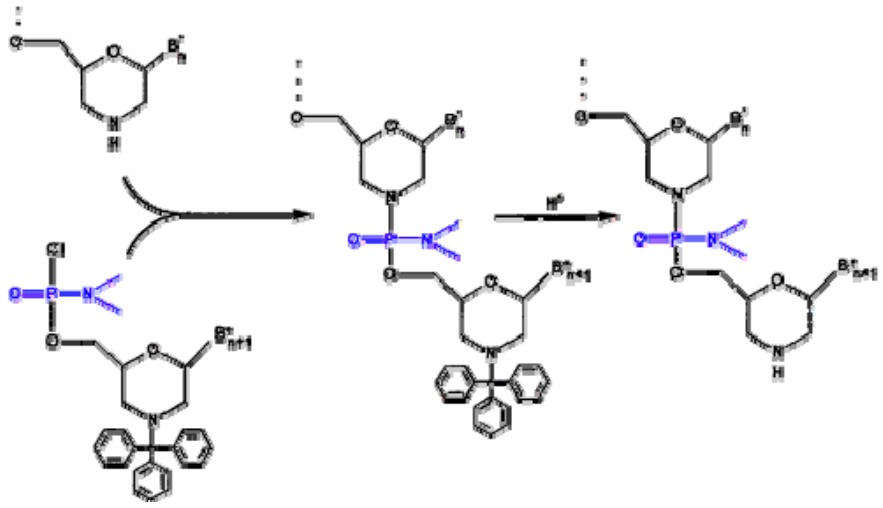

B

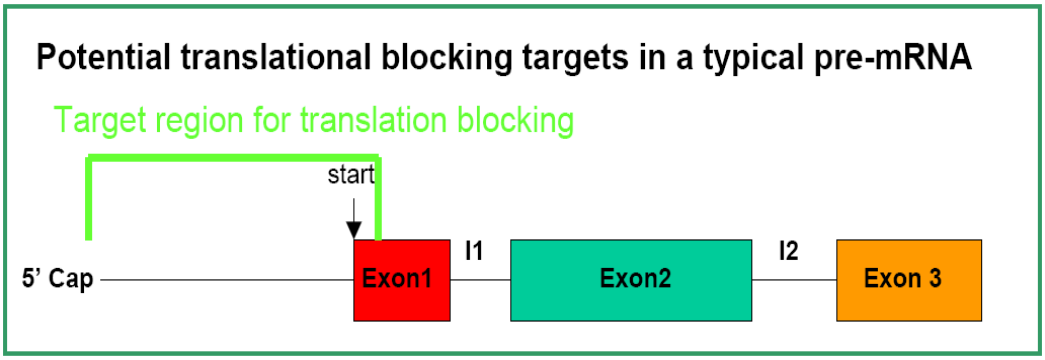

Figure 1-5. Structure of morpholinos and principles of morpholino-based gene knockdown (Modified from Gene Tools).

(A) Chemical structure of morpholinos. Compared to naturally occurring nucleic acids, morpholinos contain morpholine ring in stead of ribose or deoxyribose ring. The linkage between subunits is accomplished by non-ionic phosphorodiamidate linkages instead of anionic phosphates.

(B) A 25-base region near the 5' untranslated region or the translational start codon (ATG) is a simple and generally effective target to block the translation of interesting gene (acting via a steric block mechanism).

Section 1.9: Zinc, a neuromodulator in the retina

As an endogenous trace metal ion, zinc is widely distributed in the vertebrate retina, suggesting its pivotal role in this tissue. Many lines of evidence suggest that the deficiency of zinc may result in various visual dysfunctions and structural defects, including night blindness (McClain et al., 1979), abnormal dark adaptation (Morrison et al., 1978), age-related macular degeneration (Mares-Perlman et al., 1996), photoreceptor dysfunction (Keeling et al., 1982), and distortion of pigment epithelia (Leure-duPree and McClain, 1982).

Although zinc is present throughout the retina, intracellular zinc is primarily concentrated at the photoreceptor synaptic terminals. Modified Neo-Timm staining of the tiger salamander retina reveals that intracellular zinc is highly restricted to the outer nuclear layer, where the photoreceptor cell bodies reside (Wu et al., 1993). Ultrastructure studies in rat retina further show that endogenous zinc is co-localized with glutamate vesicles in neural processes at the outer plexiform layer (Akagi et al., 2001). In addition, the zebrafish retina stained with a fluorescent zinc indicator, Newport Green, shows that intracellular zinc discharges from the terminals of photoreceptors upon depolarization, when glutamate is also released at high levels (Redenti et al., 2007). Although the concentration of zinc in the synaptic cleft of the retina is yet to be determined, the zinc concentration in the synaptic cleft in hippocampus is estimated to reach 300 μM during strong stimulations (Assaf and Chung, 1984).

Many functions have been suggested for zinc that is released into the synaptic cleft.

The most important one is that zinc acts as a neuromodulator, which regulates the activities of ligand-gated and/or voltage-gated channels. Several lines of evidence demonstrate that zinc meets the criteria to be a neuromodulator (Kay and Toth, 2008), as zinc is presynaptically localized, is released upon stimulation, its effects can be blocked by zinc chelator, and it produces many postsynaptic effects. For example, at cone synaptic terminals, zinc is shown to modulate various excitatory and inhibitory receptors and channels in postsynaptic HCs, including the AMPA receptor (Shen and Yang, 1999; Zhang et al., 2002), the GABA receptor (Feigenspan and Weiler, 2004), and the A-type potassium channel (Zhang et al., 2006). Furthermore, zinc is also reported to modulate the HGJ channels expressed in *Xenopus* oocytes (Chappell et al., 2003). Direct studies of zinc's effect on the native HGJ channels in retinal HCs and its role in visual signal processing, however, are still lacking, which will be addressed in the current thesis project using the patch-clamp electrophysiological approach.

Section 1.10: Patch-clamp electrophysiology

Electrophysiology is a method to study the electrical properties of biological materials such as cells and tissues. It can measure the voltage change or electrical current flow in a wide range of scales, from whole cell level to single channel level.

There are two working models of the patch-clamp technique: voltage clamp and current clamp. The voltage clamp technique allows to clamp the cell at a chosen potential, which makes it possible to measure the ionic current crossing a cell membrane at any given

voltage. This is important because most ion channels (e.g. HGJ channels) are voltage-gated channels. Understanding how they work at different voltages helps to understand how the neurons process visual signals *in vivo*. In the current thesis project, the voltage clamp is widely used to study the native HGJ channels in retinal HCs. The other mode, the current clamp, allows measurement of the transmembrane voltage by injecting current into a cell through the recording electrode. Unlike the voltage clamp, the membrane potential varies in the current clamp, which is used to measure synaptic potentials. This mode is not used in the current project.

Generally, there are four recoding modes of patch-clamp (**Figure 1-6**). 1) The cell-attached mode. The recording pipette is placed against the target cell membrane, and a gentle suction is applied through the microelectrode to draw a piece of the cell membrane (patch) into the pipette tip. The glass tip of the pipette forms a high resistance "seal" with the cell membrane. Ion channel activities in the tiny patch of membrane surrounded by the pipette tip can be measured. Therefore, it is a single channel configuration. The advantages of this mode are that it is the simplest configuration and is easy to obtain, leaving the cell and cytosolic side intact. The disadvantage is that it is not easy to manipulate the media on either side of the cell, since the cell is still intact. 2) The whole cell mode. After the cell-attached mode is formed, if a stronger suction is applied, the patch of the membrane under the tip will be ruptured, leaving the electrode sealed with the rest of the cell membrane. The advantage of this mode is that it allows measurement of channel activities from the whole cell level. The macro-current recorded

under this mode is the sum of all the channels in the cell membrane. The disadvantage is that the cytosolic factors are washed out by pipette filling solution. So generally, the recording pipette is filled with a solution that has a similar ionic composition to the cytosol (high potassium ions, low sodium ions). 3) The outside-out mode. This mode is obtained by pulling away the recording pipette from a whole cell mode. The patch membrane will break away from the cell and reseal on itself to leave the extracellular side facing the bath solution. The pipette solution resembles the intracellular ionic environment. The advantage of this mode is that the extracellular side can be superfused to study the effects of extracellular factors on the channels. The disadvantage is that the cytosolic factors are washed out. 4) The inside-out mode. The inside-out mode is obtained from the cell-attached mode by pulling away the pipette from the cell until it is out of the bath solution and exposes the tip in the air. The vesicle attached to the tip will break and be destroyed by exposure to the air, which leaves the intracellular side facing the bath solution. The advantage of this mode is that it is ideal for studying the effects of cytosolic factors on the channel. But the disadvantage is that it is difficult to form.

In the current thesis study, different recording modes of the patch-clamp technique are utilized to fulfill the requirements of different tests.

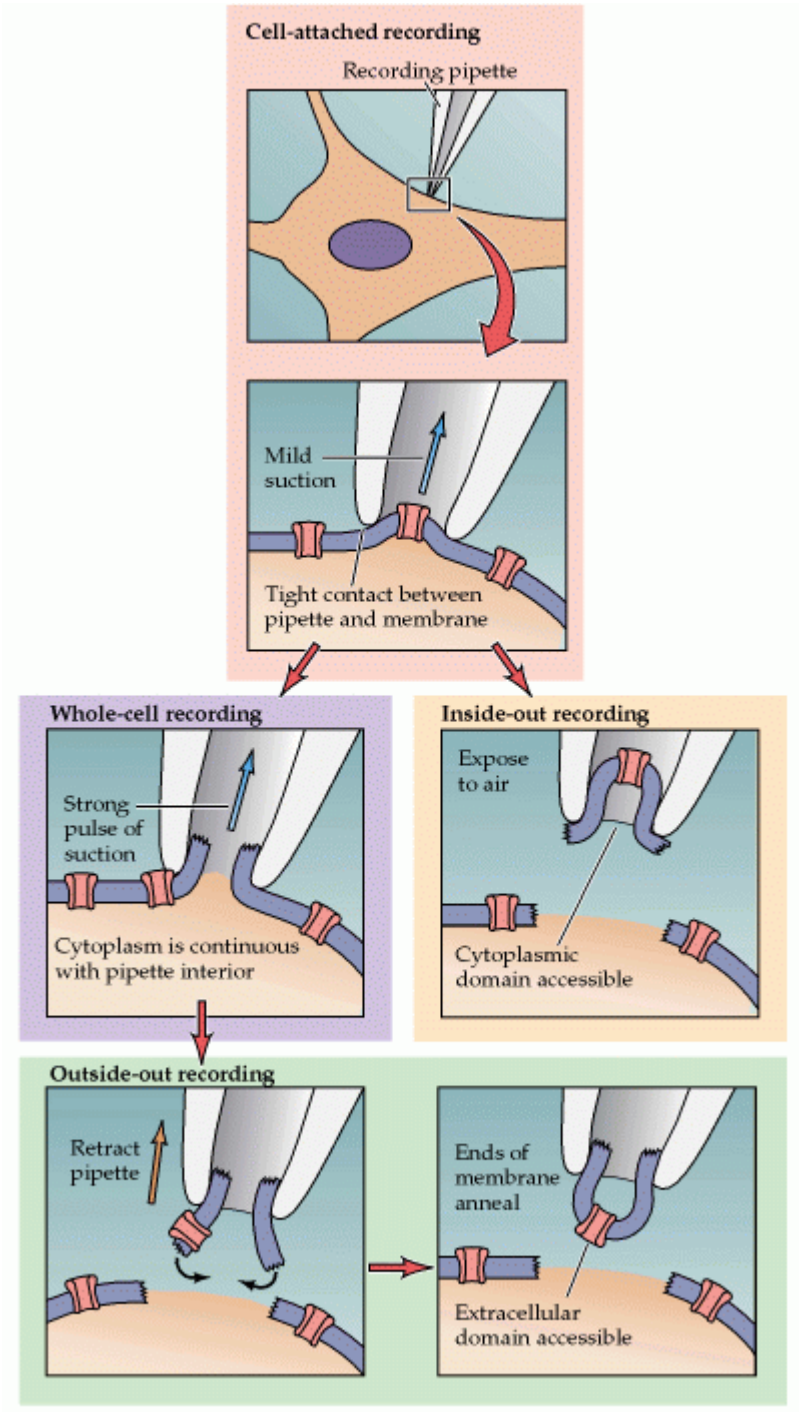

Figure 1-6. Four configurations (recording modes) of patch-clamp recording.

Figure 1-6. Four configurations (recording modes) of patch-clamp recording (Modified from the Internet).

There are four different recoding modes of patch-clamp.

1) The cell-attached mode. The recording pipette is placed against the target cell membrane, and a gentle suction is applied through the microelectrode to draw a piece of the cell membrane (patch) into the pipette tip. The glass tip of the pipette forms a high resistance “seal” with the cell membrane. Ion channel activities in the tiny patch of membrane surrounded by the pipette tip can be measured. This is a single channel configuration.

2) The whole cell mode. After the cell-attached mode is formed, if a stronger suction is applied, the patch of the membrane under the tip will be ruptured, leaving the electrode sealed with the rest of the cell membrane. The macro-current recorded under this mode is the sum of all the channels in the cell membrane.

3) The outside-out mode. This mode is obtained by pulling away the recording pipette from a whole cell mode. The patch membrane will break away from the cell and reseal on itself to leave the extracellular side facing the bath solution. This is a single channel configuration.

4) The inside-out mode. The inside-out mode is obtained from the cell-attached mode by pulling away the pipette from the cell until it is out of the bath solution and exposes the tip in the air. The vesicle attached to the tip will break and be destroyed by exposure to the air, which leaves the intracellular side facing the bath solution. This is a single channel configuration.

Section 1.11: Objectives of the current study

As the second-order neurons in the vertebrate retina, HCs receive excitatory synaptic input from photoreceptors and mediate the feedback inhibition in the outer retina. The negative feedback from HCs to cones has been shown to play important roles in neuronal network adaptation and the center-surround organization in the retina. According to the ephaptic hypothesis proposed by Kamermans *et al*, the key component in this pathway is the HGJ channel or hemichannel, which mediates the negative feedback through producing a continuous current sink to regulate the neurotransmitter release from photoreceptors. Although several lines of evidence support this model, many questions still need to be further addressed, since the lack of a specific blocker of HGJ channels prevented demonstration of a more direct evidence (Goodenough and Paul, 2003).

The overall objective of the current study is to test whether HGJ channels in zebrafish HCs could serve their putative roles in the feedback pathway at the first visual synapse and how neurotransmitters modulate the hemichannel currents. In this work, I focused on characterizing the biophysical properties of HGJ channels as well as their modulation by the neuromodulator zinc using electrophysiological methods. In addition, to uncover the molecular mechanism of the HGJ channels in zebrafish retinal HCs, I studied the function and properties of various Cx proteins that are expressed in zebrafish retinal HCs using morpholino-based gene knockdown and a *cx55.5* mutant zebrafish.

In Chapter II of this dissertation, I examined the gating and pharmacological properties of HGJ channels in zebrafish retinal HCs using the whole cell and single channel

patch-clamp methods. In the ephaptic feedback model, it is necessary for hemichannels to form a current sink by which the extrasynaptic potential could be modulated. In this view, HGJ channels located at the HC dendrites should remain open in the physiological range of membrane potentials and calcium concentrations. By characterizing the native HGJ channels in zebrafish HCs, it helps to understand the properties of HGJ channels and further determine whether HGJ channels could serve their proposed roles in the negative feedback pathway in the outer retina.

In Chapter III of the dissertation, I studied the expression and contribution of various Cx proteins to functional HGJ channels using immunocytochemical (ICC) staining, patch-clamp recording, *cx* mutant zebrafish and morpholino-based gene knockdown. Cx proteins are the molecular subunits of HGJ channels and zebrafish expresses many types of Cx protein in the retina, which accounts for the different properties of different HGJ channel currents. By studying the molecular formation of functional HGJ channels in zebrafish HCs, it helps to understand the molecular mechanism of HGJ channels, especially the relationship between the composition and the function.

In Chapter IV of this dissertation, I tested the effect of zinc on HGJ channels in isolated bass retinal HCs, as well as the mechanism of zinc regulation on HGJ channels. The properties of HCs are regulated by a variety of neurotransmitters released by retinal neurons during the light illumination. Among them, zinc is one of the most intriguing due to its multiple physiological functions in the retina as well as in the brain. By studying the modulation of zinc on HGJ channel currents, it helps to understand how zinc performs its

regulatory role in HGJ channels and what mechanism is underlying its regulation.

Overall, completion of these objectives will expand our understanding in the property and function of HGJ channels and the mechanism underlying the neuronal network adaptation in the retinal circuitry.

CHAPTER II

FUNCTIONAL CHARACTERIZATION OF HEMI-GAP-JUNCTION CHANNELS IN ZEBRAFISH RETINAL HORIZONTAL CELLS

Section 2.1: Summary abstract

Functional hemi-gap-junction (HGJ) channels are present in fish retinal horizontal cells (HCs) and may play important roles in shaping initial visual signals at the first visual synapse. The opening of HGJ channels is triggered by various experimental stimuli (e.g. membrane potential and Ca^{2+} concentration) and some HGJ channels have low open probability under physiological conditions. In this study I examined the gating mechanism of native HGJ channels in zebrafish retinal HCs. In Ca^{2+}-free solution, outward hemichannel currents elicited by depolarization to +60 mV averaged 182 ± 21 pA, while inward hemichannel currents induced by hyperpolarization to -60 mV averaged 40 ± 5 pA. Currents of both polarities were blocked by reducing extracellular pH. Increasing the external [Ca^{2+}] suppressed the outward and inward hemichannel currents with different sensitivities. Substantial inward hemichannel currents persisted at physiological concentrations near 1 mM [Ca^{2+}], a concentration at which outward hemichannel currents were largely blocked. Application of 200 μM quinine enhanced outward hemichannel currents without affecting inward hemichannel currents, and 200 μM carbenoxolone selectively suppressed outward hemichannel currents with little effect on inward

hemichannel currents. On the other hand, 100 μM Co^{2+} significantly inhibited both outward and inward hemichannel currents. Single-channel recordings from outside-out patches showed that the unitary conductance of hemichannels was 70 ± 5 pS at a holding potential of +20 mV, whereas it was 47 ± 4 pS at -20 mV. There are significant differences of the unitary conductance and the total open probability between outward and inward single channel hemichannel currents. Taken together, these data demonstrate that functional HGJ channels are expressed in zebrafish retinal HCs. Outward and inward hemichannel currents are induced at positive and negative potentials, respectively, which show different properties in voltage gating, calcium sensitivity, pharmacological regulation and single channel events. The different properties of outward and inward hemichannel currents suggest that their channels may be composed of different connexin (Cx) proteins. The inward hemichannel currents largely persist under physiological conditions, which is consistent with their proposed role in the ephaptic feedback model in the outer retina.

Section 2.2: Introduction

Horizontal cells (HCs), second-order neurons in the vertebrate retina, receive excitatory synaptic inputs from, and make an inhibitory feedback to, photoreceptors at the first visual synapse (Burkhardt, 1977; Stone and Witkovsky, 1987). In the outer retina, HCs are electrically coupled to each other via gap junction channels, which are critical in mediating lateral signal transmission and processing. Other than being the precursor of gap junction channels, hemi-gap-junction (HGJ) channels are also independent

functional ion channels existing in various fish retinal HCs. It is generally thought that HGJ channels are normally closed in individual cells under physiological conditions to prevent loss of cytoplasmic molecules and entry of extracellular ions. However, in certain cells some HGJ channels are open under either physiological or pathological conditions and may play important roles *in vivo* (Paul et al., 1991; Malchow et al., 1993; Ebihara et al., 1995; Zhang and McMahon, 2000; Beahm and Hall, 2002; Thompson et al., 2006).

Functional HGJ channels present in fish retinal HCs are suggested to play a role in modifying initial visual signals at the first visual synapse. Studies of retinal HCs demonstrate that prolonged depolarization of the cell membrane induces HGJ channel currents, which are sensitive to membrane potential, extracellular Ca^{2+}, pH, and many neurotransmitters (DeVries and Schwartz, 1989; Ebihara and Steiner, 1993; Zhang and McMahon, 2001; Goodenough and Paul, 2003). Recent studies further suggest that HGJ channels, which are located at the dendrites of HCs, may keep open and regulate the release of transmitters from photoreceptors in the intact retina, affect synaptic communication and mediate the negative feedback pathway in the first visual synapse (Janssen-Bienhold et al., 2001; Kamermans et al., 2001b; Kamermans and Fahrenfort, 2004). These results suggest that HGJ channels not only serve as the structural precursors of gap junction channels, but also play a physiological role in the visual information process.

The zebrafish is a highly visual animal that has large eyes and responds to light only three days after fertilization (Easter and Nicola, 1996). It is not only an ideal model for

genetic and developmental studies, but also a good model to investigate the visual function from the molecular level. Numerous mutants have been developed and used to examine the genetic basis of visual development and function. In addition, several connexin (*cx*) genes have been cloned and identified from the zebrafish retina (Dermietzel et al., 2000; McLachlan et al., 2003; Valiunas et al., 2004; Zoidl et al., 2004; Zoidl et al., 2008). Among them, *cx52.6* and *cx55.5* are specifically expressed in HCs (Shields et al., 2007), and form functional HGJ channels in heterologous expression systems (Zoidl et al., 2004; Shields et al., 2007).

Our laboratory has previously described conductance, gating characteristics and modulation of gap junction channels in zebrafish HCs (McMahon, 1994; McMahon and Brown, 1994). Given that HGJ channels may be open *in vivo* and may play important roles in processing visual signals, in this study I sought to determine whether functional HGJ channels are expressed in zebrafish retinal HCs, and to examine their electrophysiological, biophysical and pharmacological properties in a cultured condition.

Section 2.3: Materials and methods

Retinal primary cell culture

Wild type adult zebrafish (*Danio rerio*) were kept in a 14:10 (light/dark) cycle and euthanized in accordance with the National Institutes of Health guidelines for animal use. Zebrafish were dark-adapted overnight prior to experiments. Eyes were enucleated and hemisected along the anterior pole under dim red light. Retinas were removed and then

incubated in 90% L-15 medium (GIBCO) containing 20 U/ml papain (Worthington) activated with 0.3 mg/ml cysteine. The L-15 medium was diluted with deionized water. Penicillin/Streptomycin (1:100, Sigma) was routinely added to the medium to prevent contamination. Retinas were incubated in 90% L-15/papain solution for 10 minutes followed by six changes of fresh 90% L-15 medium, and then dissociated by repeated passage through a trimmed 1 ml pipette tip. Cultures were maintained at 20°C and cells were recorded either at 2 hours after dissociation or on the following day.

Solutions and chemicals

The normal Ca^{2+} bath solution contained (in mM): 137 NaCl, 2.5 KCl, 2.5 $MgCl_2$, 2.5 $CaCl_2$, 10 HEPES, 10 glucose and 1mg/ml BSA (Sigma, Fraction VII), and pH was adjusted to 7.5 using NaOH. The Ca^{2+}-free bath solution contained (in mM): 114.5 NaCl, 2.5 KCl, 1 $MgCl_2$, 10 HEPES, 30 CsCl, 1 Na-pyruvate, 10 glucose and 1mg/ml BSA, and pH was adjusted to 7.5 with NaOH. Both whole cell and outside-out single channel recordings used the same pipette solution. In order to block potassium channels, K^+ in the normal pipette solution was replaced by Cs^+ and tetraethylammonium chloride (TEA) was added to the pipette solution. The pipette solution contained (in mM): 124 CsCl, 1 $CaCl_2$, 11 EGTA, 10 HEPES, 1 Mg-ATP, 0.1 Na-GTP, and 10 TEA, pH to 7.5 with CsOH.

A 10 mM stock solution of quinine (Sigma) was prepared by dissolving the drug in water. 200 μM carbenoxolone (Sigma) was always freshly prepared prior to experiments. To test the external pH effect, the pH of the Ca^{2+}-free bath solution was adjusted to desired

values with either NaOH or HCl. The switch of external solution surrounding the target cell was completed within 30 seconds using a perfusion system.

Patch-clamp recording

Recordings from solitary HCs were performed using the conventional whole-cell patch-clamp configuration. Patch pipettes were pulled from Corning 7052 glass (AM Systems) and fire-polished to a resistance of 6-10 MΩ. The pipette series resistance and capacitance were compensated by 80%. The offset potential between the pipette and the bath solution was zeroed prior to seal formation.

For outside-out single channel recording, recording pipettes were fire-polished to resistance of 10-20 MΩ and were coated with silicone elastomer to reduce pipette capacitance and noise. Single channel currents were filtered at 2 kHz (-3 dB Bessel filter) and digitally sampled at 20 kHz. Currents were recorded using Axopatch 1-D amplifier (Axon Instruments) in voltage clamp mode. Voltage commands and data analysis were performed using pCLAMP 9.0 software.

Data analysis

The amplitude of macroscopic hemichannel currents referred to in this work was read as steady-state currents in the last 10 ms of the voltage steps. Single channel currents were analyzed using pCLAMP 9.0 software. All recordings were further digitally filtered at 500 Hz (lowpass 8 pole Bessel) in the analysis software. Single channel amplitudes were

binned and displayed as all-point amplitude histograms and fit by the sum of two Gaussian functions. The distributions of open and shut duration were plotted as a histogram fit by single exponential curves. The single channel open probability was determined by the ratio of the time in the open state to the duration of recording T: NPo = $(t_1 + t_2 + t_3 \ldots t_n)/T$, where t is the amount of time that N channels are open and N is the number of channels observed in the patch.

The results were presented as mean ± SE. *P* values stated were calculated using either the *t* or the paired *t* test. Curve fitting and statistical analyses were performed using either Origin 7.0 or Sigmaplot 10.0 software.

Section 2.4: Results

Morphology of zebrafish HCs in primary cell culture

Solitary HCs were readily identified in culture by their relatively large cell bodies with multiple processes (**Figure 2-1A**, left panel). After 24 hours of culture, the morphology of cells changed as some of the original processes retracted and new smaller processes formed (**Figure 2-1A**, right panel). Consistent with previous studies, two major types of HCs were found in the primary cell culture, H_A and H_B (McMahon, 1994; Connaughton and Dowling, 1998; Connaughton et al., 2004). The majority of HCs in the culture were putative H_A type HCs, which resemble cone-driven H_1-HCs in other teleosts (Stell and Lightfoot, 1975). All patch-clamp recordings in this study were performed on H_A type HCs.

Outward and inward hemichannel currents in zebrafish retinal HCs elicited in Ca^{2+}-free medium

Previous studies show that HGJ channels in some teleost retinal HCs are activated by reducing the extracellular Ca^{2+} concentration (DeVries and Schwartz, 1992; Zhang and McMahon, 2001). To test if this also applies to the HGJ channels in zebrafish retinal HCs, I examined HGJ channel currents at various extracellular Ca^{2+} concentrations. To eliminate contamination from K^+ channels, I blocked K^+ channels in HCs by replacing intracellular K^+ with Cs^+, and also included the K^+ channel blocker TEA in the pipette solution. As shown in **Figure 2-1B** (left panel), in the bath solution containing 2.5 mM Ca^{2+}, a 23 pA outward current and a 9 pA inward current were induced by stepping the membrane potential from a holding potential of 0 mV to +60 mV and -60 mV, respectively. When the cell was switched from 2.5 mM Ca^{2+} medium to Ca^{2+}-free medium, increased outward currents and inward currents were evoked during prolonged depolarization and hyperpolarization. The outward current was increased to 247 pA at +60 mV, whereas the inward current was increased to 54 pA at -60 mV (**Figure 2-1B**, right panel). The effect was reversible upon returning to 2.5 mM Ca^{2+} medium. Similar results were obtained with 39 additional HCs. On average, the outward current was 182 ± 21 pA at +60 mV (n = 40) and the inward current was 40 ± 5 pA at -60 mV (n = 40) in Ca^{2+}-free medium.

To confirm that HGJ channels mediated the low Ca^{2+}-evoked currents, I tested if pH modulates these currents. **Figure 2-1C** shows representative current traces from HCs superfused with bath solutions of varying pH values. In Ca^{2+}-free medium at pH 7.5,

outward and inward currents were evoked at +60 mV and -60 mV, respectively. When the extracellular pH was decreased to 5.5, the outward current was suppressed from 198 pA to 31 pA, while the inward current was reduced from 48 pA to 11 pA. The suppression produced by lowering external pH was reversible. These data are summarized in **Figure 2-1D**. Upon switching extracellular pH from 7.5 to 5.5, outward currents were reduced to 10 ± 2% of control ($P < 0.001$, n = 5), and inward currents were reduced to 28 ± 5% of control ($P < 0.001$, n = 5).

Taken together, these data demonstrate that outward and inward currents are elicited in Ca^{2+}-free medium in zebrafish retinal HCs, and that these currents are sensitive to changes in extracellular Ca^{2+} and pH, further supporting the hypothesis that low Ca^{2+}-induced HC currents are mediated by HGJ channels.

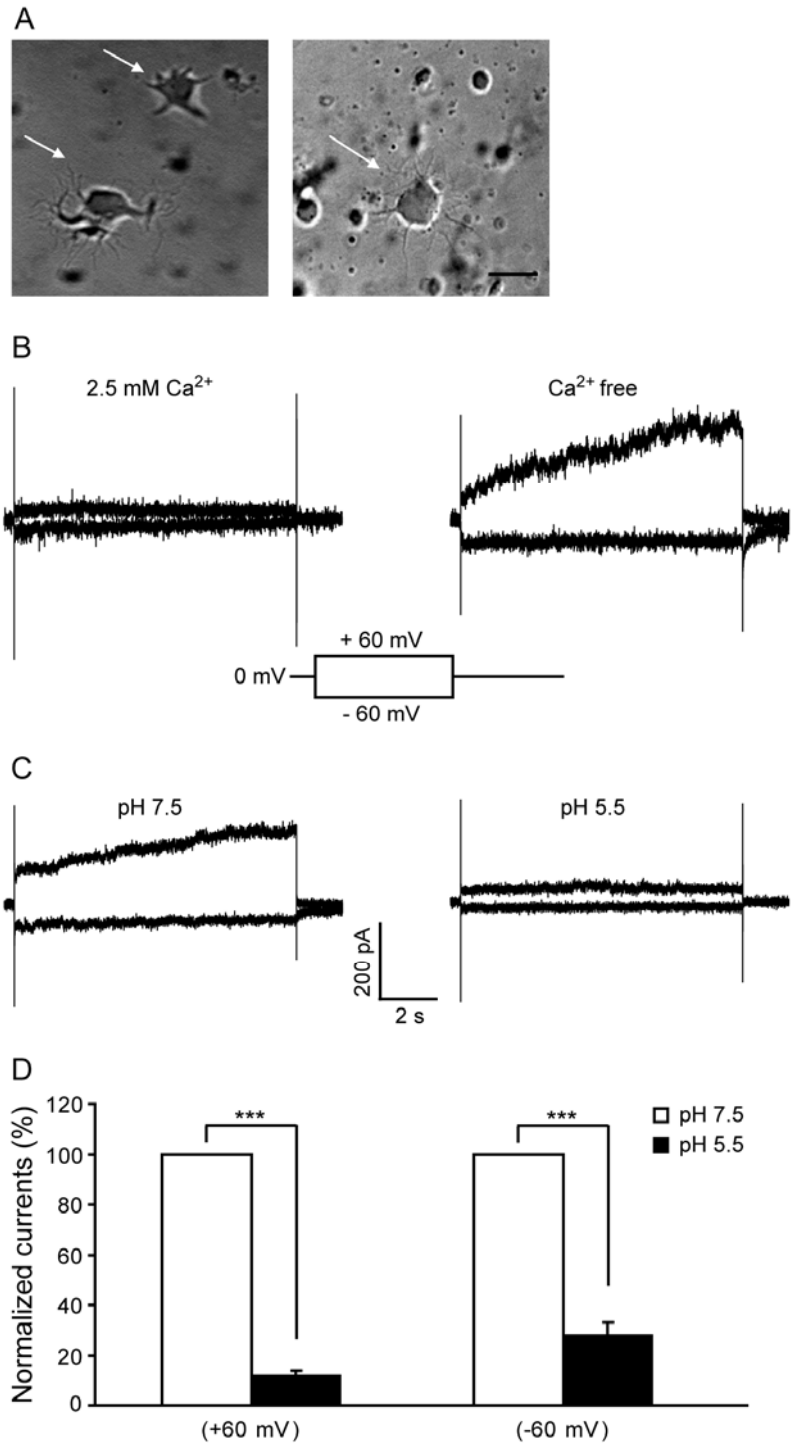

Figure 2-1. Low Ca^{2+}-evoked HGJ channel currents in cultured zebrafish HCs are sensitive to extracellular pH.

Figure 2-1. Low Ca^{2+}-evoked HGJ channel currents in cultured zebrafish HCs are sensitive to extracellular pH.

(A) Photomicrographs of solitary HCs in primary cell culture (indicated by arrows) immediately after isolation (left) and after one day in culture (right), Scale bar = 10 μm.

(B) Both outward and inward currents were substantially blocked in 2.5 mM Ca^{2+} medium (left), while they were greatly increased after perfusion with Ca^{2+}-free medium (right). Voltage protocol shown as inset: currents were induced by 10s voltage steps from a holding potential of 0 mV to +60 mV and -60 mV, respectively. Time and amplitude are indicated on the scale bar.

(C) Representative current traces recorded in pH 7.5 Ca^{2+}-free medium (left) and the same cell in pH 5.5 Ca^{2+}-free medium (right).

(D) Normalized currents obtained in Ca^{2+}-free medium with different pH values (pH 7.5, open bar and pH 5.5, closed bar). Outward and inward currents were normalized to the value induced in pH 7.5 Ca^{2+}-free medium under +60 mV and -60 mV, respectively (n=5, mean ± SE). Asterisks indicate values significantly different between two groups, *** $P < 0.001$.

Voltage and Ca^{2+} gating of outward and inward hemichannel currents in zebrafish retinal HCs

To study the voltage-gating properties of HGJ channels in zebrafish HCs, 10s voltage steps (from -90 mV to +90 mV with a 15-mV increment) were applied from a holding potential of 0 mV. In steady state, both outward and inward HGJ channel currents increased proportionally with positive and negative voltages, while increasing the extracellular Ca^{2+} from 0 mM to 2.5 mM reduced the amplitudes of both outward and inward HGJ channel currents. The averaged current-voltage relation of HGJ channel currents is shown in **Figure 2-2A**. Net currents mediated by HGJ channels were calculated as the "difference" currents, obtained by subtracting the currents recorded in 2.5 mM Ca^{2+} medium from corresponding traces recorded in Ca^{2+}-free medium. There was no significant difference between the currents induced in Ca^{2+}-free medium and the calculated net currents at the holding potential of ±60 mV ($P > 0.05$, n = 5). Therefore, in the following study, macroscopic HGJ channel currents reported are the currents evoked in Ca^{2+}-free medium at the holding potential of ±60 mV.

To test the activity of HGJ channels at different concentrations of extracellular Ca^{2+}, I studied the dose-response of Ca^{2+} for both outward and inward HGJ channel currents. **Figure 2-2B** shows the dose inhibition plot of normalized currents vs. $[Ca^{2+}]$ on a logarithmic scale. The outward and inward HGJ channel currents exhibited different sensitivities to the extracellular $[Ca^{2+}]$, especially in the range of 1 to 1.5 mM, which is similar to the physiological Ca^{2+} concentration. In this $[Ca^{2+}]$ range, outward hemichannel

currents were suppressed, but a substantial proportion of the inward currents remained. The data were fit by the Hill equation, which yielded a half-maximal inhibitory concentration (IC_{50}) of 0.69 mM for outward HGJ channel currents and 1.58 mM for inward HGJ channel currents.

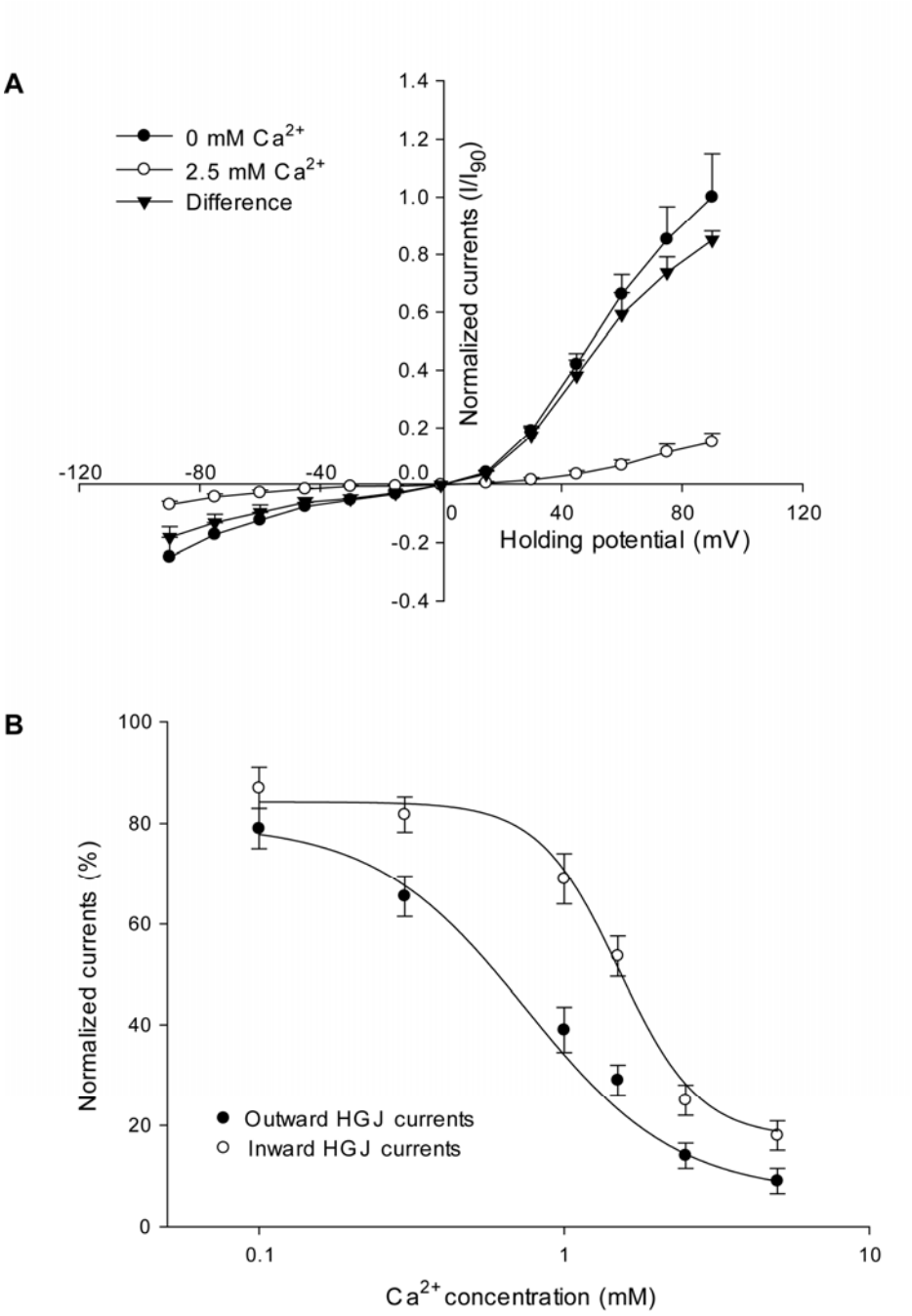

Figure 2-2. Voltage-gating and Ca^{2+}-sensitive properties of HGJ channel currents in zebrafish HCs.

Figure 2-2. Voltage-gating and Ca^{2+}-sensitive properties of HGJ channel currents in zebrafish HCs.

(A) Normalized I-V curve in Ca^{2+}-free medium (closed circles) and in the medium containing 2.5 mM Ca^{2+} (open circles). Net currents mediated by HGJ channels are shown as the difference (closed triangles), which was obtained by subtracting the current traces recorded in 2.5 mM Ca^{2+} medium from corresponding traces recorded in Ca^{2+}-free medium. Currents were induced by 10s voltage steps from -90 mV to +90 mV in 15 mV increments from a holding potential of 0 mV and were normalized to the value elicited under +90 mV in Ca^{2+}-free medium (n=5, mean ± SE).

(B) Dose inhibition plots for normalized outward and inward HGJ channel currents vs. Ca^{2+} concentration on a logarithmic scale. Currents were normalized to the initial response obtained in Ca^{2+}-free medium. Each point was averaged from 4 to 6 cells and the data was fitted with Hill equation. The half maximal inhibitory concentration (IC_{50}) is 0.69 mM for outward HGJ currents and 1.58 mM for inward HGJ currents.

Differential effects of quinine on hemichannel currents in zebrafish retinal HCs

To understand the pharmacological properties of HGJ channel currents in zebrafish HCs, external quinine was applied. Previous studies show that quinine has distinct effects on HGJ channels composed of variable Cx proteins. Quinine enhances certain HGJ channel currents in cultured HCs (Malchow et al., 1994; Dixon et al., 1996) and in some heterologous expression systems (White et al., 1999; Al-Ubaidi et al., 2000), but has little effect on the currents of HGJ channels composed of Cx26 (Ripps et al., 2004).

Using the same voltage protocol as shown in **Figure 2-1B**, I tested the effect of 200 μM quinine on HGJ channel currents in zebrafish HCs. An example trace is shown in **Figure 2-3**. External application of 200 μM quinine resulted in a remarkable increase in outward HGJ channel currents from 206 pA to 510 pA (**Figure 2-3A**, left panel). However, quinine had little effect on inward HGJ channel currents, which were slightly changed from 80 pA to 91 pA (**Figure 2-3A**, right panel). As shown in **Figure 2-3B**, 200 μM quinine significantly enhanced the average outward currents to 294 ± 62% of control ($P < 0.05$, n = 5), leaving average inward currents unchanged at 105 ± 8% of control ($P > 0.05$, n = 5).

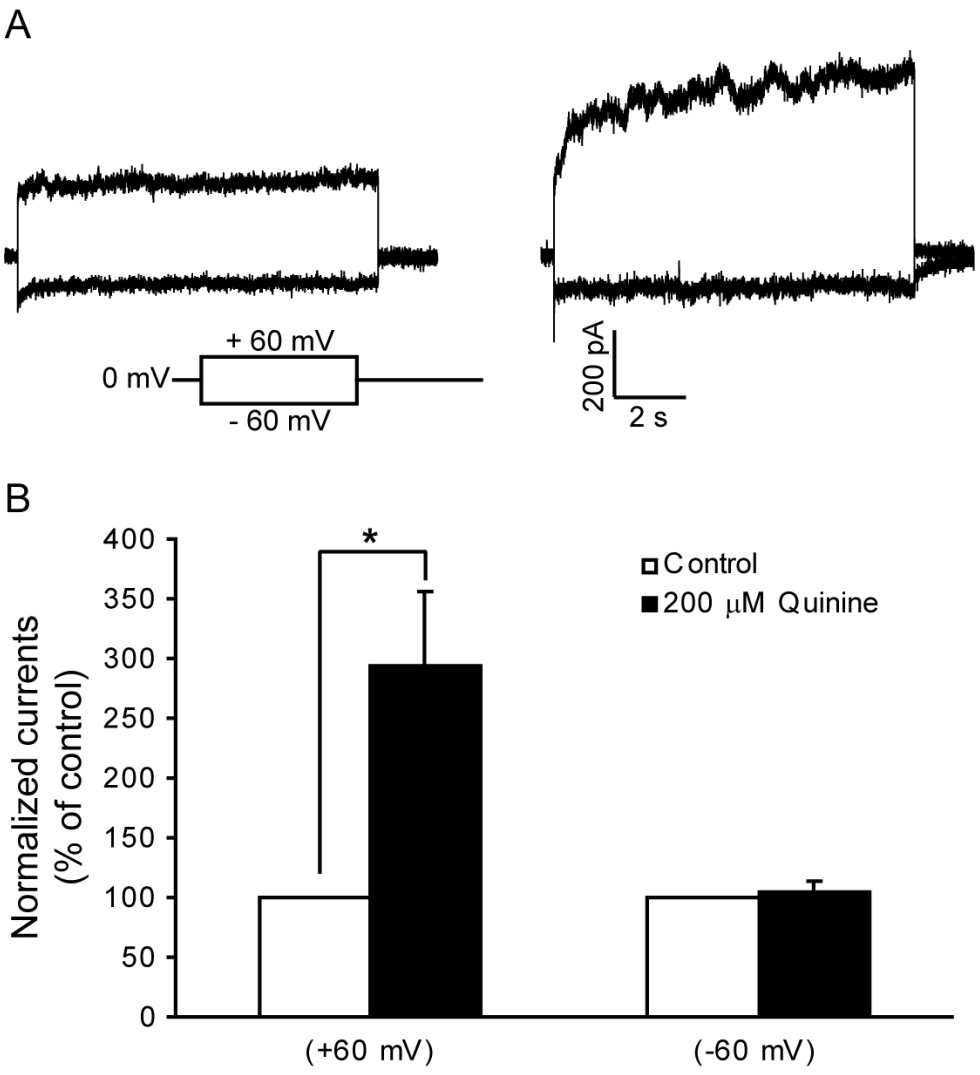

Figure 2-3. Effect of quinine on macroscopic hemichannel currents of isolated zebrafish HCs.

(A) Representative current trace elicited in Ca^{2+}-free medium (left), and the one from the same cell after superfusion by 200 μM quinine (right). The voltage protocol (inset) is the same as in Figure 2-1B. Time and amplitude are indicated as the scale bar.

(B) Normalized currents obtained in Ca^{2+}-free medium (open bar) and in medium containing 200 μM quinine (closed bar). Outward and inward hemichannel currents were normalized to the currents elicited in Ca^{2+}-free medium at +60 mV and -60 mV, respectively (n=5, mean ± SE). Asterisks indicate values significantly different between two groups, * $P < 0.05$.

Carbenoxolone selectively suppresses outward hemichannel currents

Carbenoxolone is a non-specific gap junction blocker (de Groot et al., 2003), which blocks Cx38 and Cx26 HGJ channel currents in heterologous expression systems (Ripps et al., 2002, , 2004), and has been used to test the ephaptic feedback hypothesis (Kamermans et al., 2001b).

To study the effect of carbenoxolone on zebrafish HC hemichannels, HGJ channel currents were recorded in the absence or presence of 200 μM carbenoxolone using the same voltage protocol described in **Figure 2-1B**. External application of 200 μM carbenoxolone suppressed the outward hemichannel current from 280 pA to 150 pA, while the inward hemichannel current slightly decreased from 41 pA to 30 pA (**Figure 2-4A**). Statistical analysis (**Figure 2-4B**) showed that 200 μM carbenoxolone inhibited outward hemichannel currents to 56 ± 5 % of control ($P < 0.05$, n=6), but had no significant effect on inward hemichannel currents (89 ± 18 %, $P > 0.05$, n=6). The different effects of carbenoxolone on outward and inward hemichannel currents are consistent with the idea that different HGJ channels in zebrafish HCs with distinct Cx protein composition may mediate the outward and inward currents.

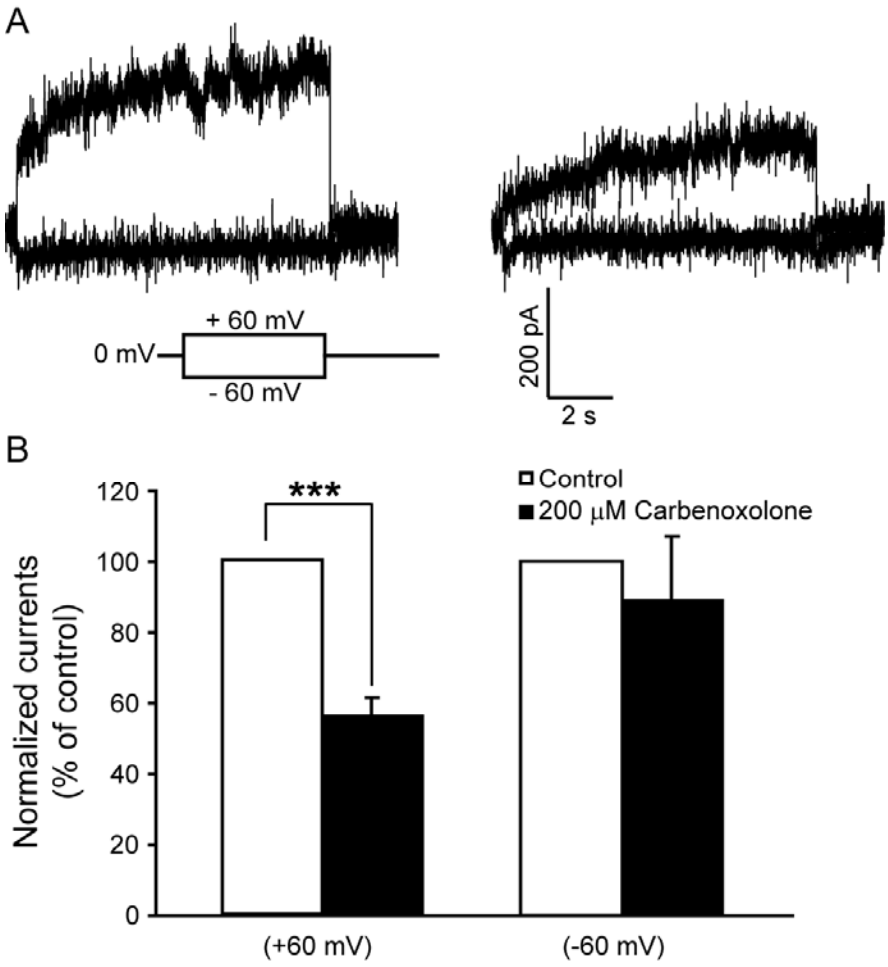

Figure 2-4. Effects of carbenoxolone on macroscopic hemichannel currents of isolated zebrafish HCs.

(A) Representative current trace elicited in Ca^{2+}-free medium before (left) and after application of 200 μM carbenoxolone (right). The voltage protocol (inset) is the same as in Figure 2-1B. Time and amplitude are indicated on the scale bar.

(B) Normalized currents obtained in Ca^{2+}-free medium (open bar) and in medium containing 200 μM carbenoxolone (closed bar). Outward and inward hemichannel currents were normalized to the currents elicited in Ca^{2+}-free medium at +60 mV and -60 mV, respectively (n=5, mean ± SE). Asterisks indicate values significantly different from the control, ***$P < 0.001$.

Co^{2+} inhibits both outward and inward hemichannel currents

The cobalt ion (Co^{2+}) has been shown to inhibit HGJ channels (Malchow et al., 1993; Fahrenfort et al., 2004), and low concentrations of Co^{2+} block Cx26 hemichannel currents at both positive and negative membrane potentials (Ripps et al., 2004). Furthermore, low concentrations of Co^{2+} have also been widely used to test the potential role of hemichannels in the feedback pathway (Fahrenfort et al., 2004).

To test the effect of Co^{2+} on zebrafish hemichannel currents, the HGJ channel currents were recorded with or without 100 μM Co^{2+} using the same protocol as **Figure 2-1B**. As shown in **Figure 2-5A** (left panel), 710 pA of outward hemichannel currents and 115 pA of inward hemichannel currents were elicited in Ca^{2+}-free medium. After external application of 100 μM Co^{2+}, the outward and inward hemichannel currents were reduced to 357 pA and 47 pA, respectively (**Figure 2-5A**, right panel). Statistical analysis (**Figure 2-5B**) showed that 100 μM Co^{2+} significantly blocked the outward currents to 46 ± 5% of control ($P < 0.001$, n = 6) and decreased the inward currents to 53 ± 6% of control ($P < 0.001$, n = 6).

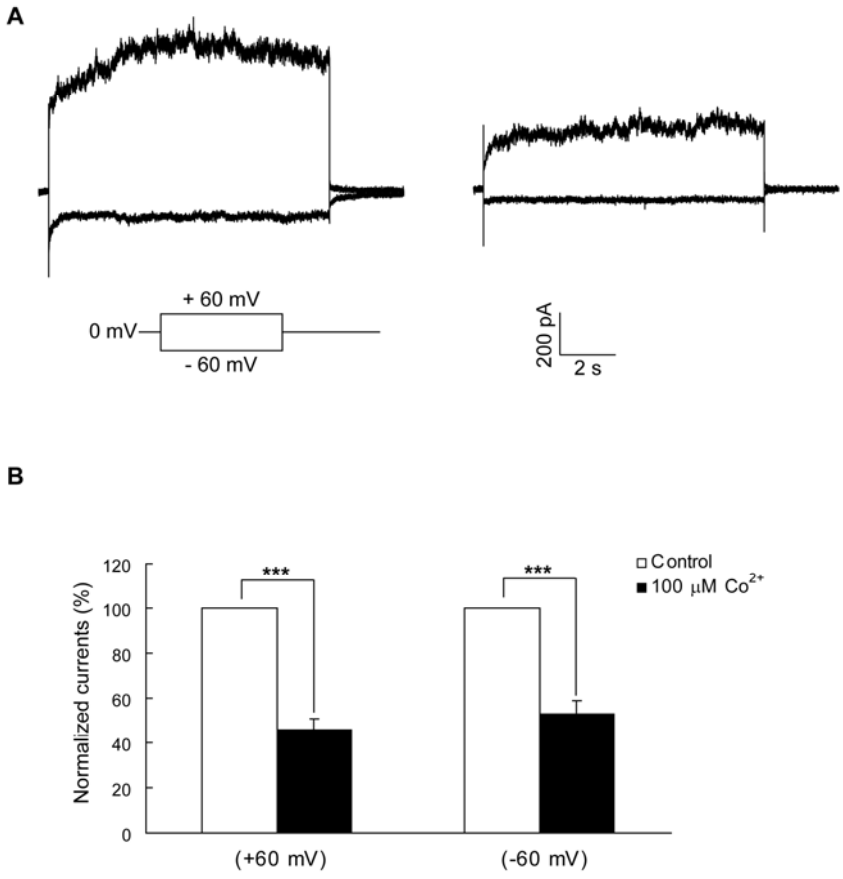

Figure 2-5: Effects of Co^{2+} on macroscopic hemichannel currents of isolated zebrafish HCs.

(A) Representative current trace elicited in Ca^{2+}-free medium before (left) and after application of 100 μM Co^{2+} (right). The voltage protocol (inset) is the same as in Figure 2-1B. Time and amplitude are indicated on the scale bar.

(B) Normalized currents obtained in Ca^{2+}-free medium (open bar) and in medium containing 100 μM Co^{2+} (closed bar). Outward and inward currents were normalized to the currents elicited in Ca^{2+}-free medium at +60 mV and -60 mV, respectively (n=5, mean ± SE). Asterisks indicate values significantly different from the control, ***$P < 0.001$.

Single-channel properties of HGJ channels in zebrafish HCs

The outside-out patch-clamp recording was utilized to further examine the properties of HGJ channels in zebrafish HCs from the single channel level. Representative current traces are illustrated in **Figure 2-6A** and the corresponding all-point histograms are shown in **Figure 2-6B**. Outward and inward single channel currents were elicited in Ca^{2+}-free medium by stepping the membrane potential from 0 mV to +20 mV and to -20 mV, respectively (**Figure 2-6A**). Consistent with the properties of macroscopic HGJ channel currents, both the outward and inward single channel currents were substantially blocked by external 2.5 mM Ca^{2+} (data not shown). All-points histograms (**Figure 2-6B**) of single channel currents showed an average unitary conductance of 70 ± 5 pS for outward currents and 47 ± 4 pS for inward currents, which are significantly different from each other ($P < 0.001$, n = 5, **Figure 2-6C**).

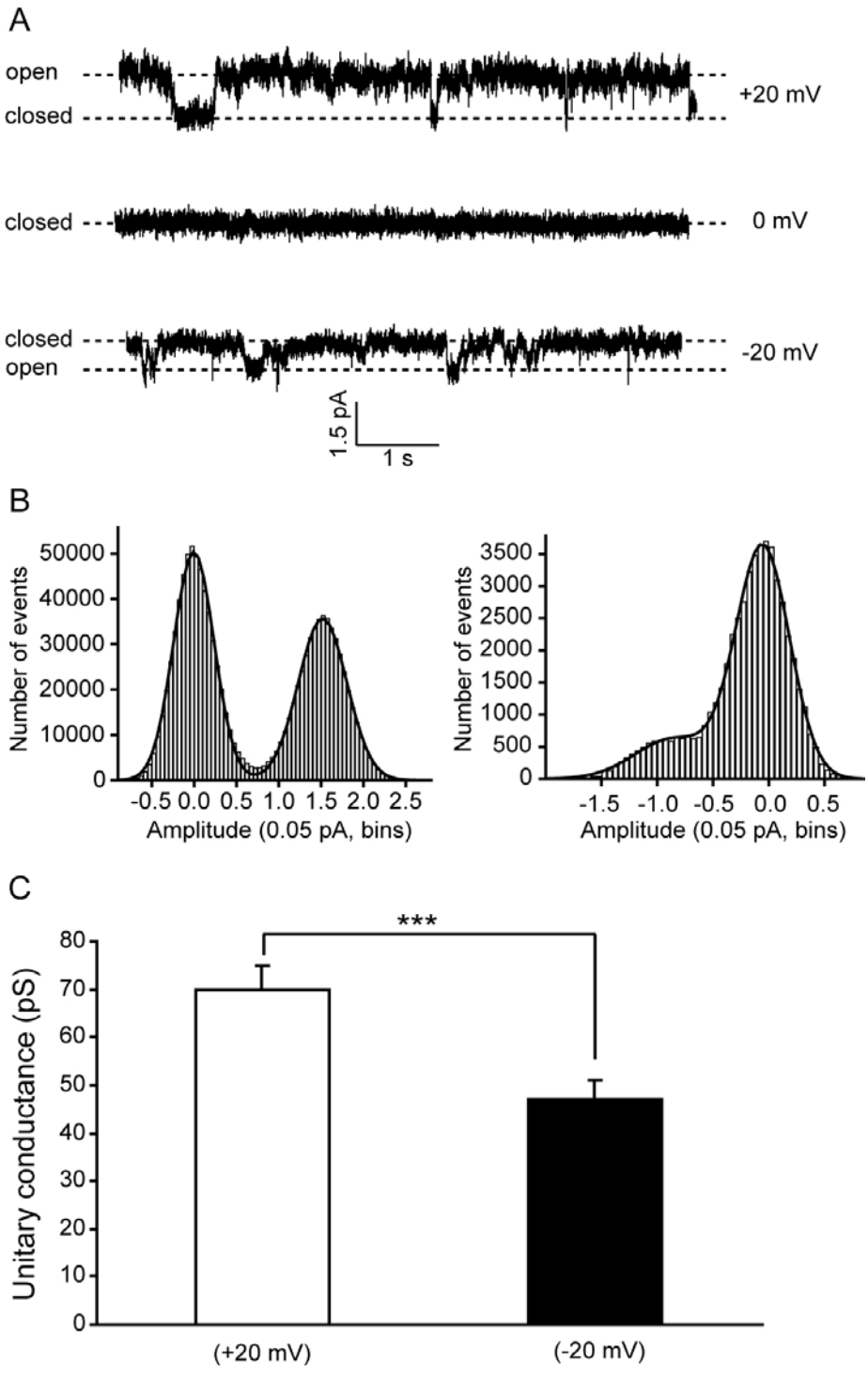

Figure 2-6. Single channel currents recorded from solitary zebrafish HCs.

Figure 2-6. Single channel currents recorded from solitary zebrafish HCs.

(A) Representative outward (top) and inward (bottom) currents elicited at holding potentials of 0 mV (middle), +20 mV (top) and -20 mV (bottom) in outside-out patch-clamp configuration. Time and amplitude are indicated on the scale bar.

(B) All-points histogram of outward and inward single channel currents shown in A. Distribution of the digitized currents was plotted as a histogram and data points were fit with Gaussian function. Peaks in the histogram indicate currents corresponding to open and closed channels.

(C) Unitary conductance of outward HGJ currents (70 ± 5 pS, open bar) and inward HGJ currents (47 ± 4 pS, closed bar). Asterisks indicate values significantly different between outward and inward single channel currents, *** $P < 0.001$ (n=5, mean ± SE).

To further understand the underlying kinetic process of channel gating properties, the closed and open dwell times of HGJ channels at ±20 mV were analyzed. The distributions of closed and open duration for outward (**Figure 2-7A**) and inward (**Figure 2-7B**) single channel currents were best fitted by a single exponential function. The closed durations of outward and inward currents were calculated to be 19.6 ± 3.0 ms and 23.9 ± 5.6 ms, respectively ($P > 0.05$, n = 5, data not shown), and the open durations were 9.5 ± 2.3 ms and 6.1 ± 0.5 ms ($P > 0.05$, n = 5, data not shown) for the outward and inward currents. However, the total channel open probability (NP_o), was 0.54 ± 0.08 for outward currents and 0.26 ± 0.06 for inward currents (**Figure 2-7C**, $P < 0.05$, n = 5).

Taken together, there are significant differences of unitary conductance and total channel open probability between the outward and the inward single HGJ channels in HCs.

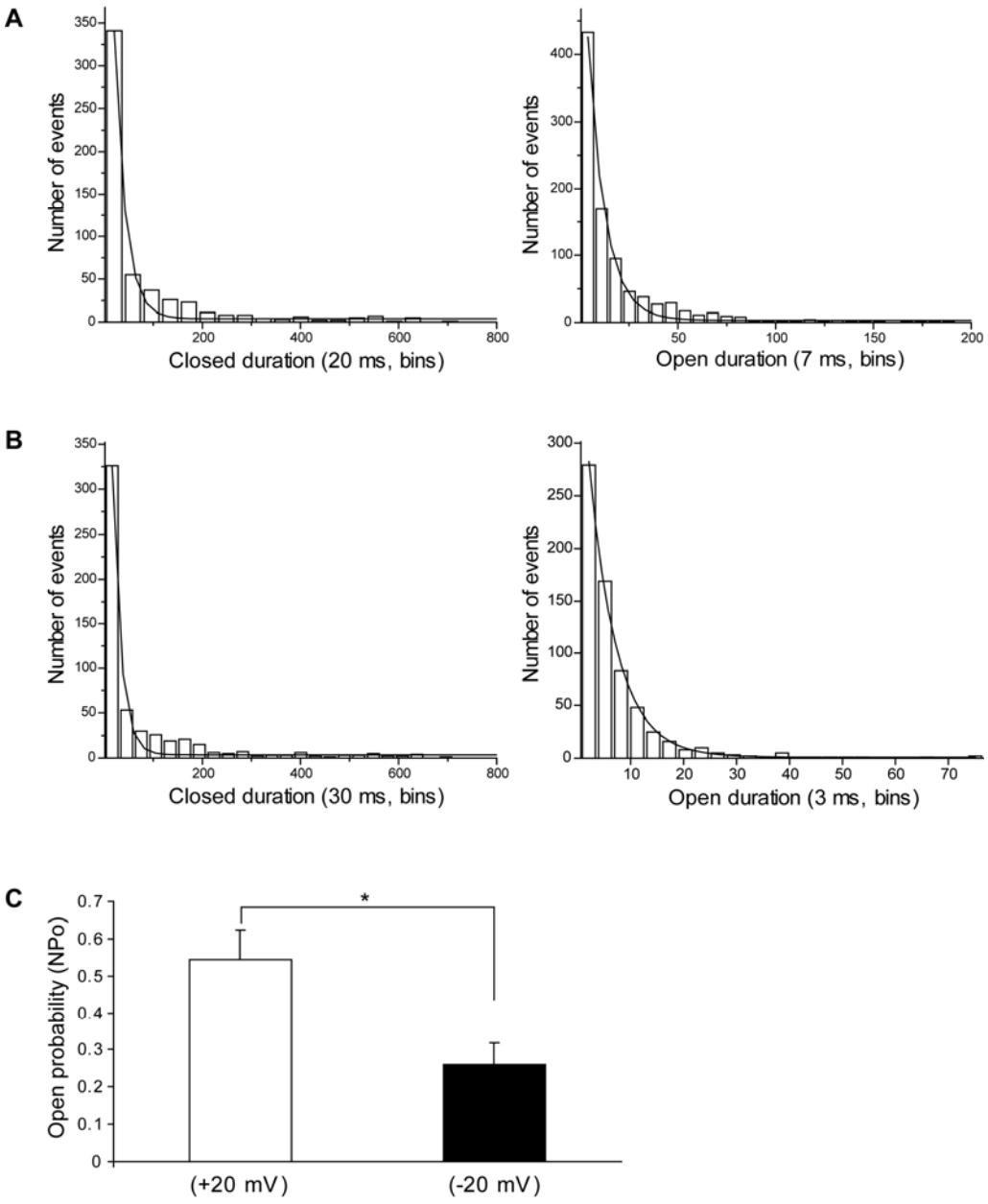

Figure 2-7. Dwell time and total channel open probability of the outward and the inward single HGJ channels at holding potential of +20 mV and -20 mV.

Figure 2-7. Dwell time and total channel open probability of the outward and the inward single HGJ channels at holding potentials of +20 mV and -20 mV.

(A) Histogram of closed (left) and open (right) durations in outward currents at +20 mV. The distribution of time was plotted as a histogram and the data points were fitted with the single decaying exponential function. The “τ” value obtained from the best fitting result reflects the dwell time. τ_c = 21.35 ms for closed time and τ_o = 8.8 ms for open time.

(B) Histogram of closed (left) and open (right) durations in inward currents at -20 mV. τ_c = 25.68 ms for closed time and τ_o = 5.24 ms for open time.

(C) Total channel open probability of outward HGJ channels (0.54 ± 0.08, open bar) and inward HGJ channels (0.26 ± 0.06, closed bar). Asterisks indicate values significantly different between outward and inward currents, * $P < 0.05$ (n=5, mean ± SE).

Section 2.5: Discussion

In the present study, I characterized the activity of HGJ channels in zebrafish retinal HCs from the whole cell and single cell level using whole cell and outside-out patch-clamp configurations, respectively. Both of these recording modes allow us to study the effect of extracellular factors on channels by superfusing the extracellular side. The major findings of this study are as follows. (1) Functional HGJ channels are expressed in zebrafish retinal HCs. Outward and inward HGJ channel currents can be elicited by depolarization and hyperpolarization, respectively. (2) The properties of outward hemichannel currents are consistent with those previously reported in other teleosts (DeVries and Schwartz, 1992; Zhang and McMahon, 2000, 2001), while the inward hemichannel currents have not yet been described. (3) The outward and inward hemichannel currents show different properties following pharmacological modulation. In addition, there are quantitative differences in unitary conductance and total channel open probability between the channels that mediate these two types of hemichannel currents. Interestingly, the inward hemichannel currents can be elicited in the physiological range of voltage and extracellular [Ca^{2+}], which may play important roles in shaping and processing visual signals at the first visual synapse.

Functional hemichannels in zebrafish HCs

Functional HGJ channels have been previously recorded from cultured teleost retinal HCs (DeVries and Schwartz, 1992; Zhang and McMahon, 2000, , 2001) and from some

expression systems expressing heterologous Cx proteins (Paul et al., 1991; Beahm and Hall, 2002; Contreras et al., 2003; Gomez-Hernandez et al., 2003; Ripps et al., 2004; Valiunas et al., 2004). Based on these studies, there are two properties shared by functional HGJ channels. First, extracellular [Ca^{2+}] at the millimolar level closes most HGJ channels. Second, almost all documented HGJ channels are activated by depolarizing potentials, but are closed by hyperpolarizing voltages. However, in this study, in addition to outward HGJ channel currents, inward HGJ channel currents were also elicited from solitary zebrafish HCs by hyperpolarization.

Although both outward and inward HGJ channel currents were largely suppressed by 2.5 mM Ca^{2+}, they exhibited different sensitivity to Ca^{2+} regulation, and showed different properties of pharmacological regulation. Compared with inward hemichannel currents, outward hemichannel currents showed higher sensitivity to external [Ca^{2+}], quinine, carbenoxolone and to lowering of extracellular pH. Single channel recordings from outside-out patches further demonstrated that there were significant differences in the properties of channels mediating outward and inward single hemichannel currents. Outward hemichannel currents exhibited a larger unitary conductance and a higher total channel open probability than those of inward hemichannel currents. These differences in pharmacology, conductance and gating properties suggest that the outward and inward hemichannel currents may be mediated by HGJ channels formed by different Cx proteins, and may also account for the larger amplitude of outward hemichannel currents at the whole cell level.

Potential physiological role of HGJ channels in zebrafish HCs

As a functional ion channel, the opening of HGJ channels under certain physiological or pathological conditions may affect membrane potential and cell volume of the local neuron, and may also facilitate intercellular communication through the release and entry of small signal molecules. In addition, HGJ channels, which are expressed in various teleost retinal HCs, may play important roles in regulating the visual information at the outer retina through their effect on local neurons and the neuronal network.

Recently, there is increasing interest in HGJ channels due to their proposed role in feedback inhibition between retinal HCs and cones (Kamermans et al., 2001b; Kamermans and Fahrenfort, 2004). According to this hypothesis, light-induced hyperpolarization of HCs leads to an increase in currents mediated by HGJ channels in HC dendrites, which generates a negative extracellular potential within the cone-HC synaptic cleft. Voltage-dependent Ca^{2+} channels in cone terminals sense the resultant depolarization at the cone synapse, which then leads to an increase in glutamate release. According to this view, HGJ channels located at the HC dendrites should remain open at the membrane potential in the physiological range from around -30 mV to -80 mV. In this study, the data show that HGJ channels in zebrafish HCs possess this property, since they remain open at negative membrane potentials up to -90 mV.

Another prerequisite for HGJ channels to participate in ephaptic feedback is that they must remain open at physiological Ca^{2+} concentrations (1-2 mM), which usually close most HGJ channels. Indeed, in zebrafish retinal HCs, substantial inward HGJ currents

were recorded in this study at negative potentials in the presence of 1 mM Ca^{2+}, whereas outward currents were mostly blocked.

Low concentrations of Co^{2+} are shown to block the feedback-mediated response in the retina of different species (Thoreson and Burkhardt, 1990; Verweij et al., 2003; Fahrenfort et al., 2004) . In goldfish, 50 ~ 100 μM Co^{2+} diminishes the negative feedback by interfering with the HGJ channel activity in a GABA-independent way without significantly affecting Ca^{2+} currents of cones (Fahrenfort et al., 2004). In this study, 100 μM Co^{2+} significantly blocked both outward and inward hemichannel currents, which further indicates that HGJ channels may be involved in the cone-HC feedback pathway.

The light-induced alkalinization and neurotransmitter-modulated proton changes have been shown within cone synapses (Barnes et al., 1993; DeVries, 2001; Molina et al., 2004). Interestingly, both outward and inward HGJ currents are insensitive to increased pH (data not shown), indicating that the light-induced alkalinization has little effect on HGJ channel activity. These data suggest that the inward HGJ channels remain functional in the physiological range of extracellular pH. Thus, inward hemichannel currents in zebrafish HCs satisfy the voltage, Ca^{2+} and pH requirements to participate in an ephaptic feedback mechanism.

By establishing that native HGJ channels are present in zebrafish HCs and that HGJ channels have characteristics consistent with their proposed role in an ephaptic negative feedback mechanism, the current study extends the plausibility of the ephaptic mechanism but does not exclude the contributions of other mechanisms. In fact, both

GABA-dependent (Wu, 1992; Schwartz, 2002) and pH-dependent (Vessey et al., 2005) negative feedback mechanisms have also been proposed to function at the first visual synapse and have considerable experimental support. By defining the physiological and pharmacological properties of native hemichannels, this work provides a basis for further studies investigating the potential role of HGJ channels in the negative feedback pathway in HCs.

CHAPTER III

MOLECULAR DISSECTION OF HEMI-GAP-JUNCTION CHANNEL CURRENTS IN ZEBRAFISH RETINAL HORIZONTAL CELLS

Section 3.1: Summary abstract

As the molecular subunit of gap junctions and hemi-gap-junction (HGJ) channels, *connexin* (*cx*) is a multigene family. Previous studies demonstrate that zebrafish retina exhibits a high diversity of *cx* expression, among which Cx55.5 and Cx52.6 are specifically expressed in retinal horizontal cells (HCs). The study in Chapter II demonstrated that outward and inward hemichannel currents elicited from zebrafish isolated HCs exhibited distinct properties, suggesting that functional HGJ channels exhibit a complex composition of Cxs. To elucidate the molecular basis of these outward and inward hemichannel currents, *cx55.5* mutant zebrafish and morpholino-based gene knockdown technique combined with patch-clamp electrophysiological recording were utilized in this study. It was found that cultured HCs from wild type (WT) zebrafish were immunoreactive to both Cx55.5 and Cx52.6 antibodies with punctate staining on cell bodies and dendritic processes. In contrast, Cx55.5 and Cx52.6 immunostaining were almost eliminated in HCs isolated from *cx55.5* mutant zebrafish. Additionally, HCs from *cx55.5* mutant zebrafish exhibited decreased inward hemichannel currents evoked at negative potentials but increased outward hemichannel currents induced at positive

potentials. These results indicate that the absence of Cx55.5 affected Cx52.6 expression, and suggest that a third Cx protein may be up-regulated to compensate for the loss of Cx55.5 function during the development. To circumvent any unexpected developmental compensation/interruption of Cx expression, *cx* gene knockdown by antisense morpholinos was used as an alternative approach to study specific Cx proteins. Using intraocular injection and electroporation, various morpholinos were introduced into adult zebrafish retinal neurons to block the translation of specific Cx proteins in HCs. Immunocytochemical data showed that the protein level of Cx55.5 was significantly decreased four days after introduction of anti-Cx55.5 morpholino, while the Cx52.6 protein level was mostly unaffected. Interestingly, under this condition, both outward and inward hemichannel currents were significantly reduced. In the meantime, anti-Cx52.6 morpholino selectively blocked the expression of Cx52.6, and resulted in a significant decrease of outward hemichannel currents only. The control morpholino showed no effect on either the Cx expression or hemichannel currents. Taken together, these data demonstrate that both Cx55.5 and Cx52.6 are expressed in the isolated WT zebrafish retinal HCs. The expression of Cx55.5 and Cx52.6 in adult zebrafish HCs can be specifically blocked by using Cx55.5-directed or Cx52.6-directed morpholinos, respectively. These data also suggest that inward hemichannel currents are solely dependent on Cx55.5, while outward hemichannel currents are affected by both Cx55.5 and Cx52.6.

Section 3.2: Introduction

The zebrafish, an important vertebrate model, is widely used for visual study due to its highly developed visual system and fast generation time (Bilotta and Saszik, 2001; Glass and Dahm, 2004). More importantly, both forward and reverse genetic approaches have been well established (Muto et al., 2005; Pujic et al., 2006) and the resultant understanding between physiological functions and specific genes allows investigation of visual functions at the molecular level (Neuhauss, 2003).

Previous studies show that zebrafish retina exhibits a high diversity of connexin (Cx) expression. Many *cx* genes have been identified and cloned from the zebrafish retina, including *cx43* (Wagner et al., 1998), *cx27.5*, *cx 44.1*, *cx55.5* (Dermietzel et al., 2000), *cx52.6* (Zoidl et al., 2004) and *cx35* (McLachlan et al., 2003). Among them, Cx52.6 and Cx55.5 are specifically expressed in horizontal cells (HCs) with distinct distribution patterns (Shields et al., 2007), and are able to form functional hemi-gap-junction (HGJ) channels in heterologous expression systems (Zoidl et al., 2004; Shields et al., 2007). Recently, novel *cx* genes have been identified and cloned in the adult zebrafish retina, among which *cx52.7* and *cx52.9* were shown to be highly related to *cx52.6* and *cx55.5*, respectively (Zoidl et al., 2008). In addition to the *cx* gene family, expression of some pannexin (*panx*) genes have also been reported in zebrafish retina (Zoidl et al., 2008). These studies demonstrate a particular complexity of Cx expression in zebrafish retina. Thus, it is not surprising to find different types of gap junctions and HGJ channels present in zebrafish retina.

Different Cx proteins are known to confer different properties to the channels that they form. Studies in Chapter II demonstrated that inward hemichannel currents induced at negative voltages are physiologically and pharmacologically distinct from outward hemichannel currents elicited at positive potentials, suggesting the possibility that different molecular compositions of HGJ channels mediate the outward and inward hemichannel currents.

In this study, *cx55.5* mutant zebrafish and morpholino-targeted Cx knockdown combined with patch-clamp techniques were applied to dissect the molecular composition of functional HGJ channels in HCs. Reduced Cx55.5 expression resulted in a decrease of both outward and inward hemichannel currents, whereas reduced Cx52.6 expression caused a decrease of outward currents only. These data suggest that inward hemichannel currents are likely mediated by homomeric Cx55.5 HGJ channels, while the outward hemichannel currents may be carried by heteromeric Cx55.5/Cx52.6 HGJ channels.

Section 3.3: Materials and methods

Retinal primary cell culture

Wild type zebrafish and *cx55.5* mutant adult zebrafish (*Danio rerio*) were kept in 14L:10D light-dark cycle and euthanized in accordance with the National Institutes of Health guidelines for animal use. Zebrafish were dark-adapted overnight prior to experiments. Retinal primary cell culture used the same protocol as described in Chapter

II. Cell cultures were maintained at 20°C and cells were recorded on the following day.

Solutions and chemicals

The normal Ca^{2+} bath solution contained (in mM): 137 NaCl, 2.5 KCl, 2.5 $MgCl_2$, 2.5 $CaCl_2$, 10 HEPES, 10 glucose and 1mg/ml BSA (Sigma, Fraction VII), and pH was adjusted to 7.5 using NaOH. The Ca^{2+}-free bath solution contained (in mM): 114.5 NaCl, 2.5 KCl, 1 $MgCl_2$, 10 HEPES, 30 CsCl, 1 Na-pyruvate, 10 glucose and 1mg/ml BSA, and pH was adjusted to 7.5 with NaOH. In order to block K^+ channels, K^+ in the normal pipette solution was replaced by Cs^+ and tetraethylammonium chloride (TEA) was added in the pipette solution. The pipette solution contained (in mM): 124 CsCl, 1 $CaCl_2$, 11 EGTA, 10 HEPES, 1 Mg-ATP, 0.1 Na-GTP and 10 TEA, pH to 7.5 with CsOH.

Patch-clamp recording

Recordings from solitary HCs were performed using conventional whole-cell patch-clamp configuration. Patch pipettes were pulled from Corning 7052 glass (AM Systems) and fire-polished to a resistance of 6-10 MΩ. The pipette series resistance and capacitance were compensated by 80%. The offset potential between the pipette and bath solutions was zeroed prior to seal formation.

Data analysis

The amplitude of macroscopic hemichannel currents referred to in this work was read

as steady-state currents in the last 10 ms of the voltage steps. The results are presented as mean ± SE. *P* values stated were calculated using either a student's *t*- or a paired *t*-test. Curve fitting and statistical analyses were performed in Sigmaplot 10.0.

cx55.5 mutant zebrafish and genotyping

The *cx55.5* mutant zebrafish was generated using the TILLING technique developed by the Kamermans lab and was shared in collaboration. A nucleotide substitution of adenosine (A) for cytidine (C) was introduced to create a pre-mature stop codon at amino acid position 54 in the first extracellular loop of *cx55.5*. Since the truncated Cx55.5 cannot form functional channels, the *cx55.5* mutant zebrafish is a null strain (*cx55.5*$^{-/-}$).

To genotype the *cx55.5* mutant zebrafish, custom TaqMan assay (Applied Biosystems) was used. The TaqMan reagent contained a 40x stock solution with following ingredients:

Forward Primer: GTGGAATGATGAACAGGCTGACT;

Reverse primer: CACACATTGCGGCAACCA;

Mutant probe (VIC): CTCGGTGTTTCAGATAA;

Wild type probe (FAM): CGGTGTTGCAGATAA.

Both probes anneal to the sense strand. In each reaction, 1 ul of genomic DNA isolated from a tailclip was used in a total of 5 ul of reaction-mix. The assay was performed on an ABI Prism 7000 qPCR machine using the following protocols:

Stage 1: 50°C for 2 minutes (1 step);

Stage 2: 95°C for 10 minutes (1 step);

Stage 3: 95°C for 15 seconds, 64°C for 1 minute (40 steps).

Based on the different fluorescent signals (VIC for *cx55.5* mutant and FAM for WT) produced during the amplification of PCR products, the cx55.5 mutant zebrafish can be readily identified and confirmed.

Intraocular injection and electroporation of morpholinos in adult zebrafish retina

Morpholinos were delivered into adult zebrafish retina using a modified intraocular injection and electroporation protocol originally developed in the Hyde laboratory at Notre Dame University (Thummel et al., 2008). Dark-adapted WT adult zebrafish were anesthetized in 2-phenoxyethanol dilute solution (1:1000) for 35 ~ 45 seconds until the movement of gills slows down. The outer cornea layer was removed by grabbing the outer cornea near the optical fissure and pulling across the eye. A small incision was made in the cornea adjacent to the iris using a sapphire blade scalpel. As shown in **Figure 3-1A**, 0.25 µl ~ 0.5 µl of lissamine-tagged morpholino solution (3 mM) was injected into the vitreous space of the left eye through the incision using a Hamilton syringe, while the right eye was not injected and served as the control.

After the intraocular injection, the zebrafish was transferred to a Petri dish filled with anesthesia and was individually electroporated. A 3 mm-diameter platinum plate electrode (CUY 650-P3 Tweezers, Protech International Inc.) was used to direct morpholinos into the retina. Typically, the dorsal part of the retina was targeted by gently pressing the ventral half of the eye with the positive electrode. Since morpholinos are

lissamine-tagged, they are slightly positively charged. Thus, these morpholinos were easily introduced into the dorsal retina by the electric pulses, and visualized by red fluorescence (excitation peak is at 575.0 nm and emission peak is at 593.0 nm). As shown in **Figure 3-1B**, the red rectangle represents the dorsal retina targeted by lissamine-tagged morpholinos. Electroporation was performed using CUY 21 Edit Square Wave Electroporator (Protech International, Inc.) through 2 consecutive 50-msec pulses at 75 V with a 1-sec pause between pulses. The fish was then revived in fresh fish water. Four days after electroporation, the fish was killed and the retina isolated for further experiments.

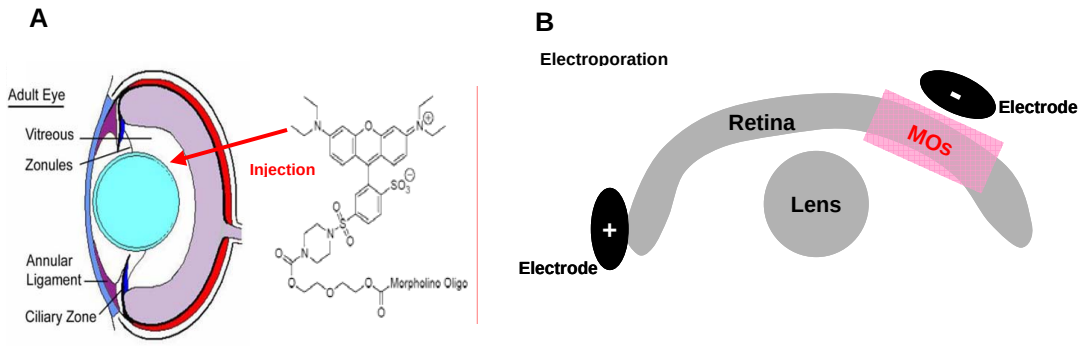

Figure 3-1. Intraocular injection and electroporation of lissamine-tagged morpholinos (MOs) into adult zebrafish retina.

(A) Diagram of 3'-Lissamine (red fluorescence)-labeled MOs, which are injected into the vitreous space of adult zebrafish eye (Modified from Gene Tools, and Soules and Link, 2005).

(B) Diagram of the electroporation technique. Lissamine-tagged MOs were introduced into the dorsal part of the retina (indicated as the red box) by electric pulses. The ventral half of the eye is gently pressed with the positive electrode, while the dorsal part of the eye is very close to the negative electrode without touching.

Morpholinos

Three lissamine-tagged morpholinos were used in this study (Gene Tools, Philomath, OR):

1) Anti-Cx55.5 morpholino (5'-CACCAAGAAAGTTCCAGTCTCCCAT-3'), which targets the *cx55.5* gene at the first 25 nucleotides of coding sequence and was designed to block the translation of *cx55.5* RNA into protein.

2) Anti-Cx52.6 morpholino (5'-TCACATGGCCTAAAACTGGAAGAGT-3'), which targets the *cx52.6* gene at 25 nucleotides within the 5' untranslated region (5'-UTR) and was designed to inhibit the translation of *cx52.6* RNA into protein.

3) Control morpholino (5'-CCTCTTACCTCAGTTACAATTTATA-3'), which is targeted to a splice site mutant of human beta-globin and has no complementary sequence in the zebrafish genome.

All morpholinos were resuspended in distilled water for a stock solution of 3 mM and were stored in 4 °C.

Immunocytochemistry

The anti-Cx52.6 and anti-Cx55.5 antibodies are kind gifts from the Kamermans lab. The carboxyl terminus is highly variable among Cx proteins. The anti-Cx52.6 antibody was generated against a 16 amino acid peptide (CKDFSEESDSVESGNY) in the carboxyl terminus of Cx52.6. The anti-Cx55.5 antibody was generated against a 15 amino acid peptide (SSRSDTKLSRPTSPD) in the carboxyl terminus of Cx55.5 (Shields et al., 2007).

Cultured isolated retinal neurons were first fixed with 4% paraformaldehyde in pH 6.5 phosphate buffer (0.1 M) for 10 minutes and then with 4% paraformaldehyde in pH 10.4 sodium carbonate buffer (0.1 M) for another 10 minutes at room temperature. After rinsing with 0.1 M pH 7.4 phosphate buffered saline (PBS) 4×10 minutes, samples were blocked at room temperature with 2% normal goat serum (NGS; Jackson Immunoresearch, West Grove, PA) in 0.1 M pH 7.4 PBS for 1 hour, followed by primary antibody incubation for 2 hours at room temperature first and then overnight at 4°C. Primary antibodies were dissolved in 0.1 M pH 7.4 PBS containing 0.3% triton X-100, 0.02% sodium azide, and 5% NGS. The primary antibodies used were rabbit anti-Cx52.6 (1:800) and rabbit anti-Cx55.5 (1: 4000). After rinsing, samples were incubated with Alexa Fluor 488 goat anti-rabbit IgG (Molecular Probes, Eugene, OR) secondary antibodies (1:500) for 2 hours at room temperature.

Confocal imaging

Specimens were visualized using Zeiss LSM5 PASCAL confocal microscopy (Carl Zeiss, Thornwood, NY) at excitation wavelength of 488 nm for Alexa Fluor 488. Lissamine-tagged morpholinos were visualized via 543 nm laser excitation and a 560 nm long pass emission filter in confocal microscopy. HCs were z-scanned at a thickness of 0.8 μm per slice, digitized and projected using software from the LSM5. The contrast and brightness of sampled images were adjusted using either confocal software or Adobe Photoshop. All settings were the same for each set of experiments.

Section 3.4: Results

Immunocytochemistry for Cx52.6 and Cx55.5 in cultured wild type zebrafish HCs

Previous immunohistochemistry shows that Cx52.6 and Cx55.5 are specifically expressed in HCs from zebrafish retinal cryosections. In addition, immuno-electron microscopy (EM) experiments further show that Cx52.6 and Cx55.5 are involved in the formation of gap junctions between HCs and that both Cx52.6 and Cx55.5 are present in unpaired HGJ channels. Cx55.5, in particular, is shown to be abundant in the dendrites of HCs within the cone synaptic terminals (Shields et al., 2007).

In this study, immunocytochemistry was used to ensure that Cx52.6 and Cx55.5 are expressed in cultured zebrafish HCs. Cultured retinal HCs isolated from WT zebrafish were treated with antibodies against Cx52.6 (**Figure 3-2**, left panel) or Cx55.5 (**Figure 3-2**, right panel). Both Cx proteins were stained with bright puncta surrounding the cell body and dendrites of HCs. These data demonstrated that both Cx55.5 and Cx52.6 are expressed in cultured HCs isolated from WT zebrafish.

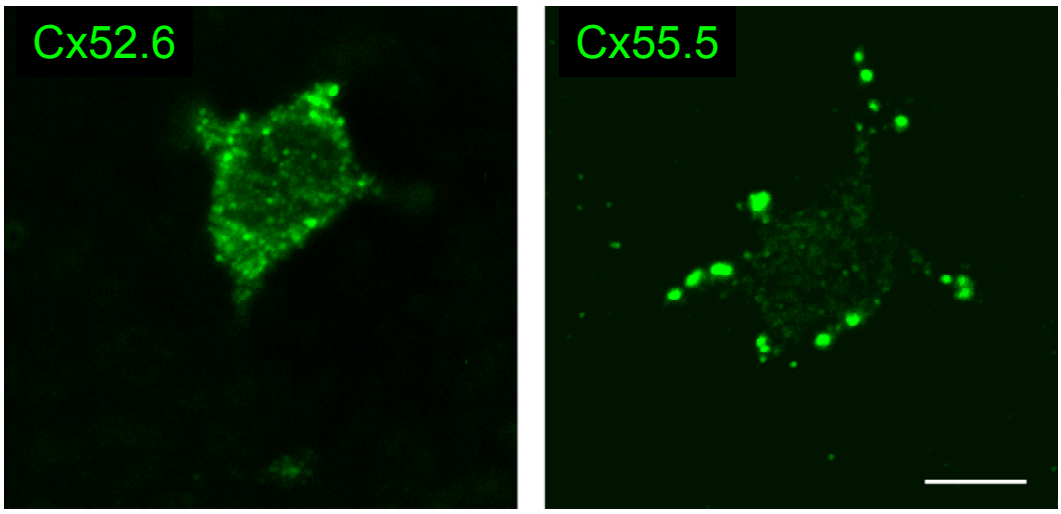

Figure 3-2. Immunocytochemistry of Cx52.6 and Cx55.5 in cultured WT zebrafish solitary HCs. Cx52.6 (left panel) and Cx55.5 (right panel) antibodies produce intense punctate staining on the soma and dendrites of cultured HCs. Scale bar = 5 μm.

HCs from *cx55.5* mutant zebrafish exhibit significant decreased inward hemichannel currents but increased outward hemichannel currents

As mentioned in Chapter II, the outward and inward hemichannel currents showed different properties. Inward hemichannel currents exhibited a distinct Ca^{+}-sensitivity, voltage-gating, pharmacological regulation and unitary conductance from those of outward hemichannel currents, which suggested that the outward and inward currents are mediated by different Cx channels. To examine the contribution of Cx55.5 to the native HGJ channel currents, whole-cell patch-clamp recording technique was utilized to study the properties of hemichannel currents in *cx55.5* mutant zebrafish HCs. As shown in **Figure 3-3A**, a 10s voltage protocol stepping from 0 mV to 60 mV and from 0 mV to -60 mV was used to induce the outward and inward hemichannel currents, respectively. In Ca^{2+}-free medium, a 310 pA outward hemichannel current and a 48 pA inward hemichannel current was elicited from the WT zebrafish HCs (**Figure 3-3A**, left panel). In contrast, under the same condition, a 528 pA outward hemichannel current and a 10 pA inward hemichannel current were induced from the *cx55.5* mutant zebrafish HCs (**Figure 3-3A**, right panel). Compared to WT zebrafish HCs, the inward hemichannel currents of *cx55.5* mutant zebrafish HCs decreased significantly, while the outward hemichannel currents increased. Consistent results were obtained from additional recordings (**Figure 3-3B**). The outward hemichannel currents averaged 182 ± 21 pA (n=40) in WT zebrafish and 334 ± 38 pA (n=8) in *cx55.5* mutant zebrafish. On the other hand, the inward hemichannel currents averaged 11 ± 2 pA (n=8) in *cx55.5* mutant zebrafish, which is

significantly lower than that in WT zebrafish (40 ± 5 pA, n=40).

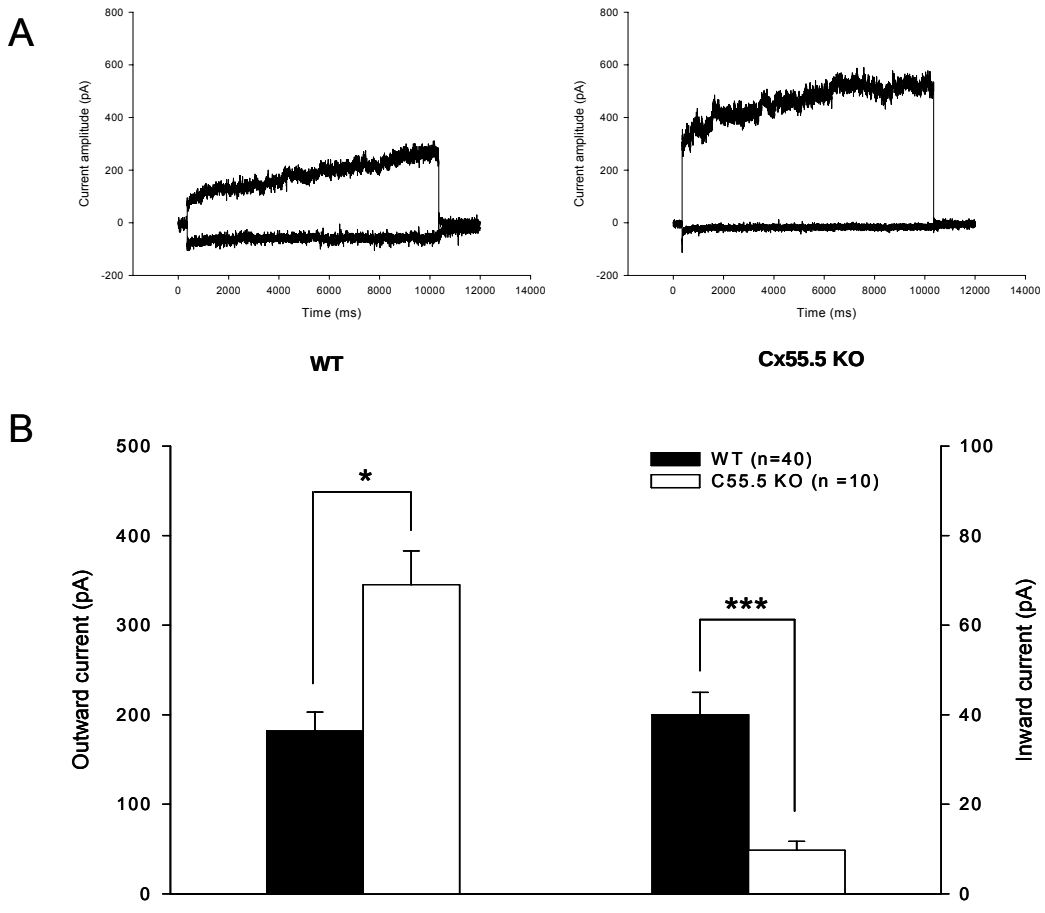

Figure 3-3. Hemichannel currents elicited from wild type and *cx55.5* mutant zebrafish retinal horizontal cells (HCs).

(A) Representative outward and inward hemichannel currents elicited in Ca^{2+}-free medium from wild type (left) and *cx55.5* mutant (right) zebrafish retinal HCs. The voltage protocol used is the same as that in Figure 2-1B.

(B) Outward and inward hemichannel currents obtained in wild type (n=40, closed bar) and *cx55.5* mutant (n=8, open bar) zebrafish HCs. Outward (left) and inward (right) hemichannel currents were elicited at +60 mV and -60 mV membrane potential, respectively (mean ± SE). Asterisks indicate values significantly different between wild type and *cx55.5* mutant zebrafish, **P* < 0.05, ****P*< 0.001.

Immunocytochemistry was performed to examine the expression of Cx55.5 and 52.6 in *cx55.5* mutant zebrafish HCs. Compared to cultured HCs from WT zebrafish, which were immunoreactive to Cx55.5 (**Figure 3-4**, Upper Panel, left) and Cx52.6 (**Figure 3-4**, Upper Panel, right) antibodies with punctate staining on the cell body and dendritic processes, the immunostaining of Cx55.5 (**Figure 3-4**, bottom panel, left) and Cx52.6 (**Figure 3-4**, bottom panel, right) were not observed in the HCs isolated from *cx55.5* mutant zebrafish. These data are consistent with the quantitative PCR results, which showed that the mRNA levels of both *cx55.5* and *cx52.6* decreased significantly in *cx55.5* mutant zebrafish (Unpublished data from Dr. Kamermans).

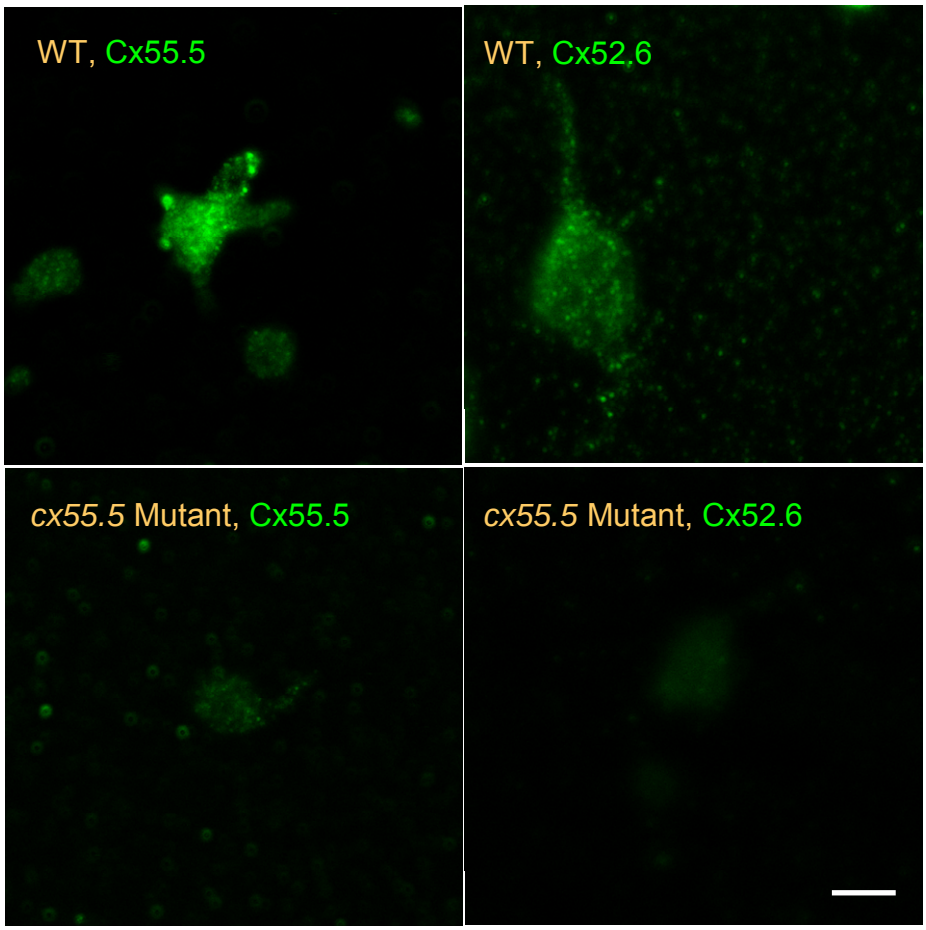

Figure 3-4. Immunocytochemistry for Cx55.5 (left) and Cx52.6 (right) proteins in cultured solitary HCs from wild type (upper panel) and *cx55.5* mutant zebrafish (bottom panel). Cx55.5 and Cx52.6 were positively stained with bright puncta on the cell body and dendrites of wild type HCs, which were not observed in *cx55.5* mutant zebrafish HCs. Scale bar = 5 μm.

Anti-Cx55.5 morpholino reduces Cx55.5 expression in the *in vivo* retina

To circumvent any potential unexpected influence of Cx55.5 deficiency on other Cx expression during the development, the expression of Cx55.5 in WT adult zebrafish retina was transiently and specifically blocked by the anti-Cx55.5 morpholino.

Lissamine-tagged anti-Cx55.5 morpholino was injected into the vitreous space of the adult zebrafish eye, followed by the electroporation (see methods). Four days after electroporation, retinas were dissected and cryosectioned. As shown in **Figure 3-5A** (left panel), the differential interference contrast (DIC) image of the zebrafish eyeball section showed that the morphology of the retina laminar structure was not significantly altered after electroporation. The lissamine-tagged morpholino was successfully introduced into the dorsal part of the retina and persisted for four days after morpholino treatment (**Figure 3-5A**, right panel, indicated as the white box). In a zoom-in view of the retina section (**Figure 3-5B**), retinal neurons were successfully targeted by the morpholino in multiple layers (individual HCs are indicated by arrows). Furthermore, as shown in **Figure 3-5C**, isolated HCs were also labeled with the red fluorescent morpholino in primary cell culture.

A

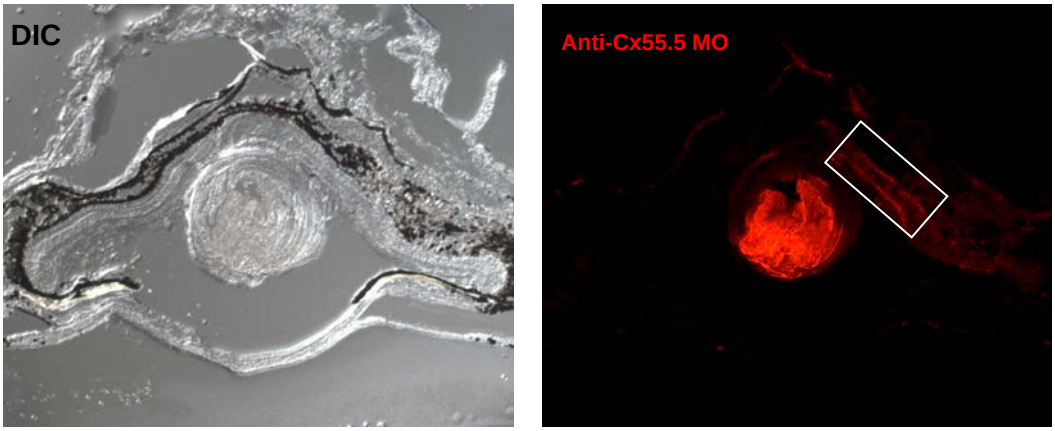

B

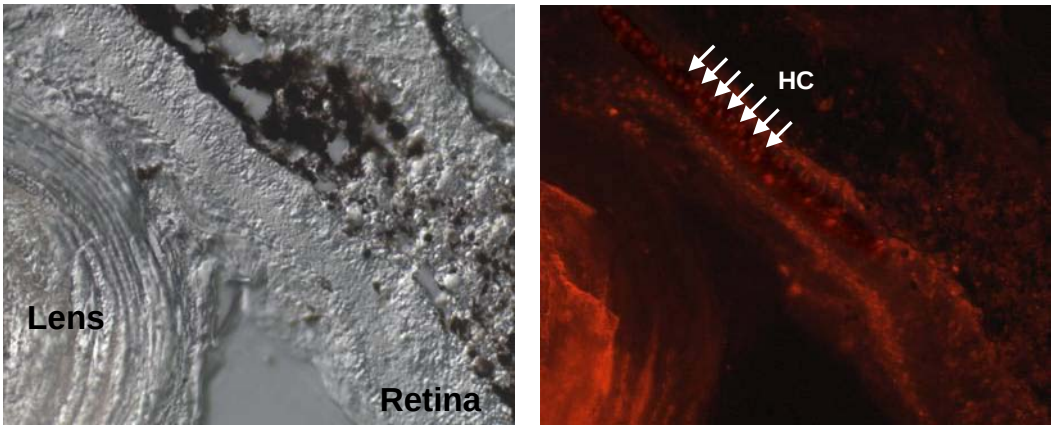

C

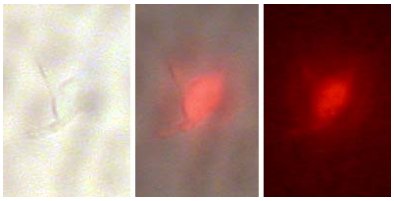

Figure 3-5. Anti-Cx55.5 morpholino (MO) targeted HCs in retinal vertical slices and in retinal primary cell culture.

Figure 3-5. Anti-Cx55.5 morpholino (MO) targeted HCs in retinal vertical slices and in retinal primary cell culture.

(A) DIC image of zebrafish eyeball slice showed normal morphology of the retina (left panel). The lissamine-tagged MO was successfully introduced into the dorsal part of the retina (right panel, white box).

(B) Zoom-in view of (A). DIC image showed laminar structure of the retina (left panel). Lissamine-tagged MO was targeted to different neuron layers of the dorsal retina (right panel). Arrows indicate individual HCs labeled with lissamine-tagged anti-Cx55.5 MO confined to the distal inner nuclear layer and proximal outer plexiform layer.

(C) Solitary HCs in primary cell culture isolated from retinas treated with lissamine-tagged anti-Cx55.5 MO.

To test the knockdown efficacy of anti-Cx55.5 morpholino, immunocytochemistry was performed on retinal slices to examine the protein level of Cx55.5 four days after electroporation. As shown in **Figure 3-6A**, immunostaining of Cx55.5 (green fluorescence) showed that the expression is restricted to the HC layer (indicated by arrows). Anti-Cx55.5 morpholino was successfully introduced into HCs (**Figure 3-6B**, indicated by arrows) shown as red fluorescence. In the merge view, the HC layer that was positively labeled with lissamine-tagged anti-Cx55.5 morpholino showed reduced Cx55.5 antibody staining (**Figure 3-6C**). The DIC image indicated that the morphology of the retina remained intact (**Figure 3-6D**). These data suggest that anti-Cx55.5 morpholino can be successfully introduced into adult zebrafish HCs by intraocular injection and electroporation, and that the suppression of Cx55.5 expression can be achieved four days after transfection.

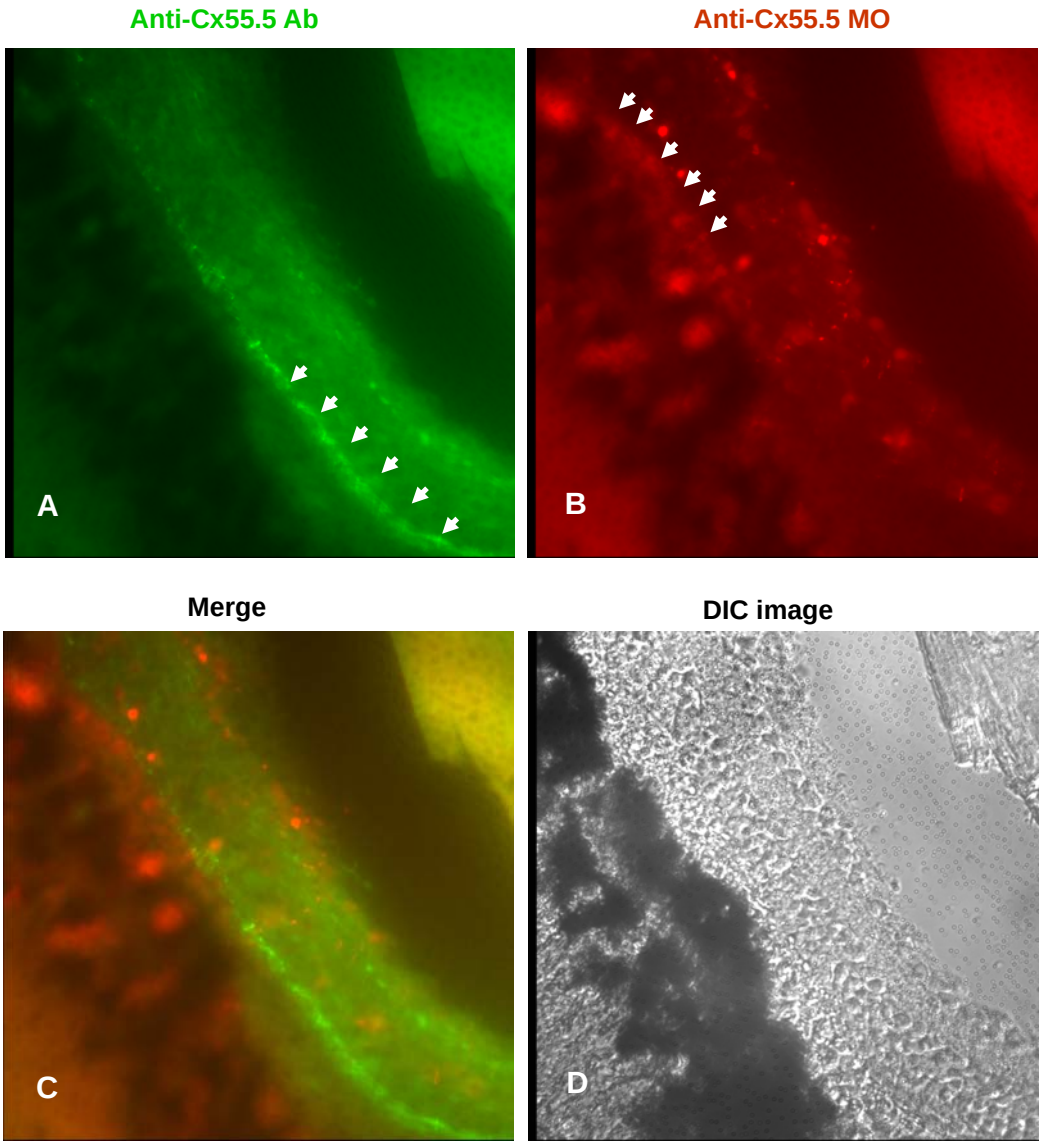

Figure 3-6. Immunocytochemistry of Cx55.5 in retinal vertical slices 4 days after electroporation with anti-Cx55.5 morpholino (MO).
(A) The expression of Cx55.5 (green fluorescence) in retinal vertical slice. Immuno-labeled HCs were indicated by arrows.

(B) Anti-Cx55.5 MO-targeted neurons (red fluorescence) in retinal vertical slice. Anti-Cx55.5 MO-targeted HCs were indicated by arrows.

(C) Superimposed view of (A) and (B).

(D) DIC image of the retinal vertical slice.

Anti-Cx55.5 morpholino suppresses both outward and inward hemichannel currents, while anti-Cx52.6 morpholino selectively inhibits outward hemichannel currents

To further study the molecular mechanism of hemichannel currents in zebrafish retinal HCs, anti-Cx55.5 morpholino and anti-Cx52.6 morpholino were designed to inhibit protein expression of Cx55.5 and Cx52.6 in adult zebrafish retinal HCs. Whole cell patch-clamp recording was used to characterize the hemichannel currents in untreated HCs and morpholino-treated HCs 4 days post-transfection. Representative current traces are illustrated in **Figure 3-7** and the averaged data are shown in **Figure 3-8**.

As shown in **Figure 3-7A**, in Ca^{2+}-free medium, a 374 pA outward hemichannel current was elicited in the untreated HC when membrane potential stepping from 0 mV to 60 mV (left panel, black trace), while a 40 pA outward hemichannel current was induced in the HC treated with anti-Cx55.5 morpholino (grey trace). On the other hand, when membrane potential stepping from 0 mV to -60 mV, a 9 pA inward hemichannel current was induced in the HC treated with anti-Cx55.5 morpholino (grey trace) compared to a 38 pA inward hemichannel current recorded in the untreated HC (black trace). As shown in **Figure 3-8A**, after anti-Cx55.5 morpholino treatment, outward hemichannel currents in HCs were reduced from 221 ± 30 pA (left panel, closed bar) to 20 ± 3 pA (left panel, open bar), while inward hemichannel currents decreased from 39 ± 5 pA (right panel, closed bar) to 10 ± 2 pA (right panel, open bar). These data demonstrate that both outward and inward hemichannel currents decreased significantly after anti-Cx55.5 morpholino treatment (P<0.001, n=5).

Using the same voltage protocol, I further tested the effect of anti-Cx52.6 morpholino on hemichannel currents. As shown in **Figure 3-7B** (left panel), upon depolarization, a 180 pA and a 42 pA outward hemichannel current was elicited from untreated (black trace) and morpholino-treated HCs (grey trace), respectively. In contrast, upon hyperpolarization, a 39 pA and a 29 pA inward hemichannel currents were induced from untreated (**Figure 3-7B**, right panel, black trace) and morpholino-treated HCs (**Figure 3-7B**, right panel, grey trace), respectively. On average, after anti-Cx52.6 morpholino treatment, outward hemichannel currents reduced significantly from 334 ± 90 pA to 91 ± 33 pA (**Figure 3-8B**, left panel, $P<0.05$, n=5). Interestingly, for inward hemichannel currents (**Figure 3-8B**, right panel), there is no significant difference between the untreated group (37 ± 5 pA) and morpholino-treated group (27 ± 6 pA, $P>0.05$, n=5). These data demonstrate that outward hemichannel currents, but not inward hemichannel currents, were significantly inhibited in the HCs treated with anti-Cx52.6 morpholino.

To confirm that the observed effect of anti-Cx morpholinos was not due to non-specific targeting of morpholinos or the process of injection and electroporation, a control morpholino with no sequence complementarity to the zebrafish genome was introduced into HCs using the same transfection protocol. As shown in **Figure 3-7C**, 212 pA outward (left panel, black trace) and 50 pA inward (right panel, black trace) hemichannel currents were elicited in the untreated HC. On the other hand, 295 pA outward (left panel, grey trace) and 52 pA inward (right panel, grey trace) hemichannel currents were recorded in control morpholino-treated HC. Statistical analysis showed that the control morpholino did

not significantly affect either outward or inward hemichannel currents (**Figure 3-8C**), which confirms that the change of hemichannel currents in morpholino-treated HCs is caused by specific targeting of morpholinos.

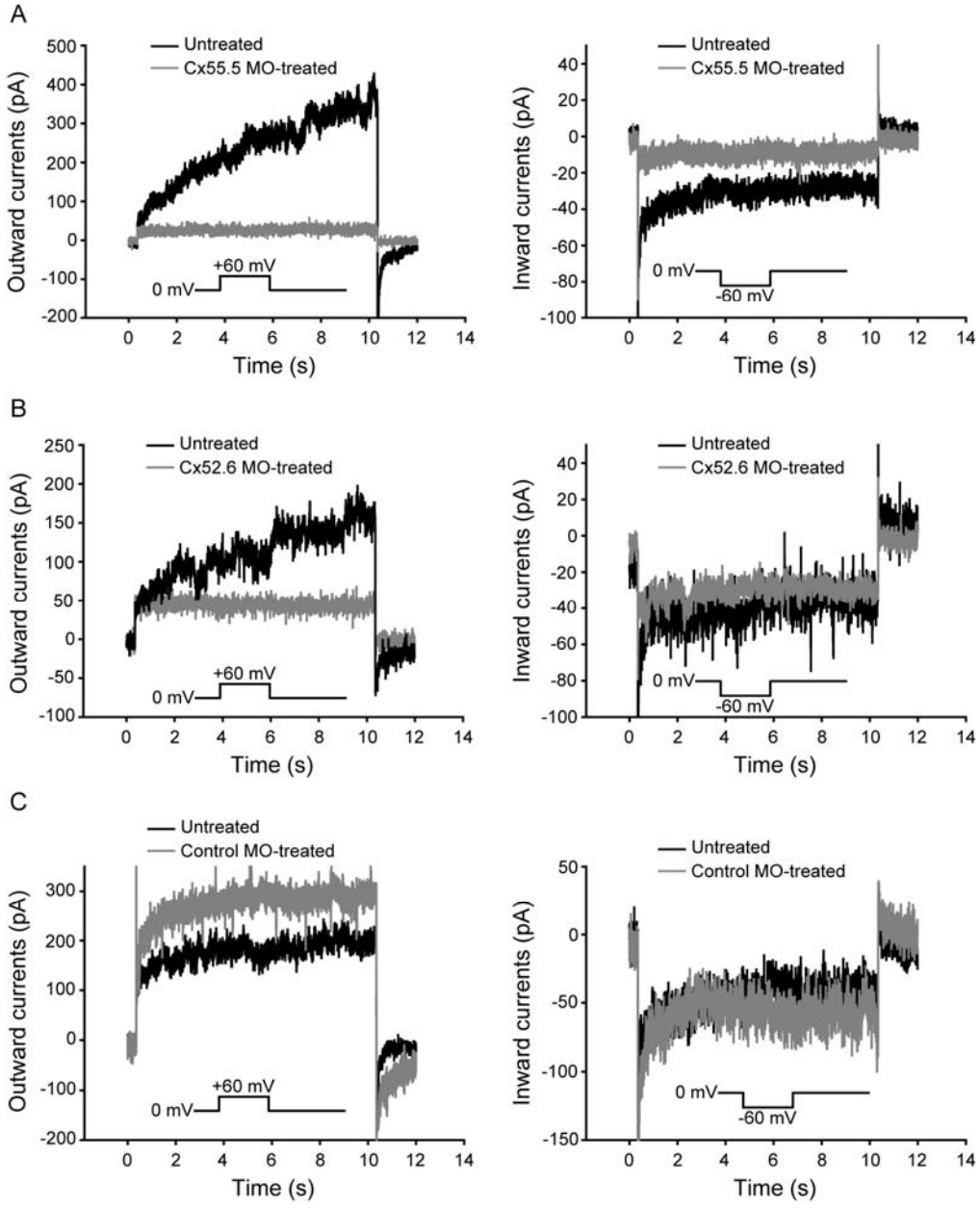

Figure 3-7. Anti-Cx55.5 morpholino (MO) inhibited both outward and inward hemichannel currents, while anti-Cx52.6 MO selectively inhibited outward hemichannel currents only.

Figure 3-7. Anti-Cx55.5 morpholino (MO) inhibited both outward and inward hemichannel currents, while anti-Cx52.6 MO selectively inhibited outward hemichannel currents only. In Ca^{2+}-free medium, 10s depolarized voltage stepping from 0 to 60 mV was used to elicit outward hemichannel currents, while hyperpolarized voltage stepping from 0 to -60 mV was used to induce the inward hemichannel currents.

(A) Compared to untreated HCs (black trace), both outward (left panel) and inward (right panel) hemichannel currents were substantially decreased in Cx55.5 MO-treated HCs (grey trace).

(B) Compared to untreated HCs (black trace), the outward hemichannel currents (left panel) were substantially decreased in Cx52.6 MO-treated HCs (grey trace), while inward currents were sustained (right panel).

(C) Compared to untreated HCs (black trace), both outward (left panel) and inward (right panel) hemichannel currents were sustained in control MO-treated HCs (grey trace).

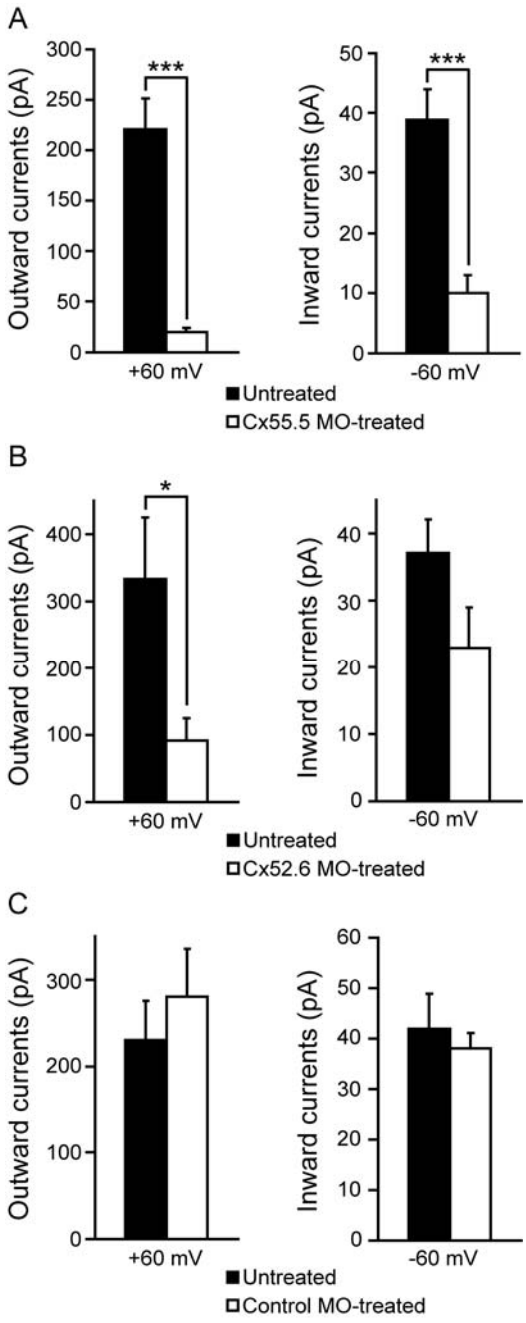

Figure 3-8. Outward and inward hemichannel currents between untreated and different morpholino (MO)-treated HCs.

Figure 3-8. Outward and inward hemichannel currents between untreated and different morpholino (MO)-treated HCs.

(A) Outward (left panel) and inward (right panel) hemichannel currents between untreated HCs (closed bar) and anti-Cx55.5 MO-treated HCs (open bar). Asterisks indicate significant difference, *** $P< 0.001$ (n=5).

(B) Outward (left panel) and inward (right panel) hemichannel currents between untreated HCs (closed bar) and anti-Cx52.6 MO-treated HCs (open bar). Asterisks indicate significant difference, * $P< 0.05$ (n=5).

(C) Outward (left panel) and inward (right panel) hemichannel currents between untreated HCs (closed bar) and control MO-treated HCs (open bar). There is no significant difference between the two groups for either current ($P>0.05$, n=5).

Anti-Cx55.5 morpholino and anti-Cx52.6 morpholino inhibit the protein expression of Cx55.5 and Cx52.6, respectively, in cultured HCs

To examine the knockdown efficiency and specificity of anti-Cx morpholinos, immunocytochemistry was performed on isolated HCs for Cx55.5 and Cx52.6 four days post morpholino transfection. As shown in **Figure 3-9A**, Cx55.5 immunofluorescence was imaged in isolated HCs treated with either anti-Cx55.5 morpholino or anti-Cx52.6 morpholino or control morpholino. Compared to anti-Cx55.5 morpholino-treated HCs, which showed a decrease in Cx55.5 expression, HCs treated with anti-Cx52.6 morpholino or control exhibited bright punctuate immunostaining of Cx55.5. Red fluorescence indicated successful introduction of lissamine-tagged morpholinos into HCs. These data demonstrate that the expression of Cx55.5 was effectively and specifically reduced by anti-Cx55.5 morpholino. On the other hand, anti-Cx52.6 morpholino specifically and substantially decreased Cx52.6 expression in isolated HCs (**Figure 3-9B**). Consistent with the electrophysiological data, the control morpholino did not affect either Cx55.5 or Cx52.6 expression (**Figure 3-9C**, A and B, bottom panel).

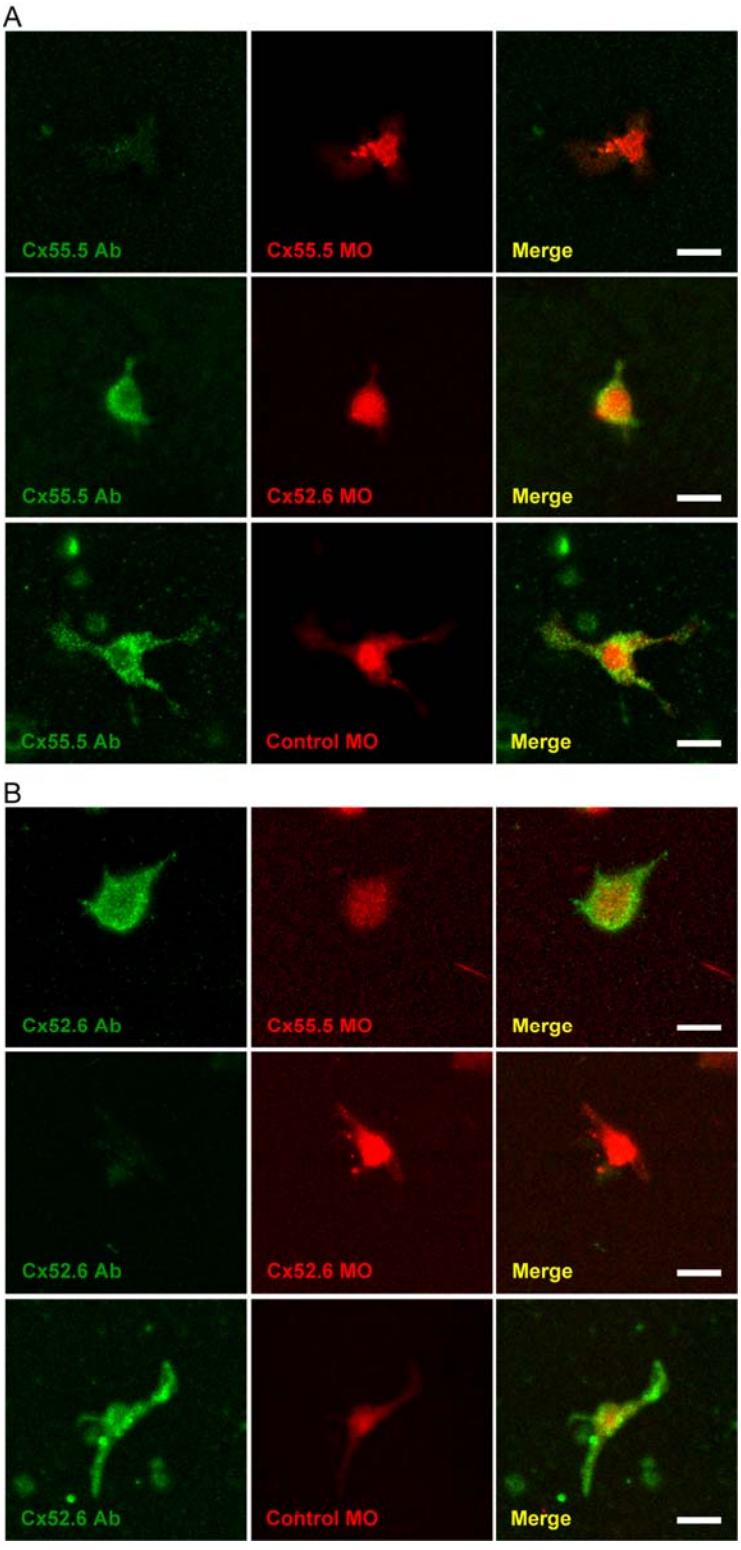

Figure 3-9. Anti-Cx55.5 morpholino (MO) and anti-Cx52.6 MO inhibited the protein expression of Cx55.5 and Cx52.6, respectively, in cultured HCs.

Figure 3-9. Anti-Cx55.5 morpholino (MO) and anti-Cx52.6 MO inhibited the protein expression of Cx55.5 and Cx52.6, respectively, in cultured HCs.

(A) Immunofluorescence of Cx55.5 (green) in HCs treated with anti-Cx55.5 MO (upper panel), anti-Cx52.6 MO (middle panel) and control MO (bottom panel). Lissamine-tagged MOs are visualized as the red fluorescence. Merged images indicate that the expression of Cx55.5 in HCs was suppressed 4 days after the introduction of anti-Cx55.5 MO. However, neither anti-Cx52.6 MO nor control MO had any significant effect on Cx55.5 expression. Scale bar = 10 μm.

(B) Immunofluorescence of Cx52.6 (green) in HCs treated with anti-Cx55.5 MO (upper panel), anti-Cx52.6 MO (middle panel) and control MO (bottom panel). Lissamine-tagged MOs are visualized as the red fluorescence. Merged images indicate that the expression of Cx52.6 in HCs was suppressed 4 days after the introduction of anti-Cx52.6 MO. However, neither anti-Cx55.5 MO nor control MO had any significant effect on Cx52.6 expression. Scale bar = 10 μm.

Section 3.5: Discussion

Cx proteins, the building blocks of gap junctions and HGJ channels, have a common topology with four transmembrane domains, two extracellular loops, one cytoplasmic loop and cytoplasmic N- and C-terminus. The transmembrane and extracellular domains are the most conserved regions, and functional diversity among Cxs is usually caused by variations within these conserved domains. Cx proteins are a complex family, and the high diversity of *cx* genes has been reported in the human, mouse and zebrafish genomes (Sohl and Willecke, 2004).

High diversity of connexin expression in zebrafish retina

In zebrafish (*Danio rerio*), a systematic study of genomic databases reveals a remarkable 37 putative *cx* genes, which compose the largest *cx* gene family in a single species yet reported (Eastman et al., 2006). Different Cx isoforms confer different properties to the functional Cx channels they form, such as channel pore size, charge specificities, gating properties and regulation (Elfgang et al., 1995; Bevans et al., 1998; Cao et al., 1998; Harris, 2001). The large number of *cx* genes in zebrafish is not only due to the genome duplication during evolution, but also likely due to the fitness that of diverse Cx proteins contributes *in vivo*.

The vertebrate retina contains multiple neurons, complex synaptic connections and a high degree of electrical coupling as well as expression of many *cx* genes. For example, the expression of more than 10 *cx* genes including *cx27.5*, *cx44.1*, *cx55.5*, *cx43*, *cx52.6*

and *cx35* are identified in zebrafish retina (Janssen-Bienhold et al., 1998; Dermietzel et al., 2000; McLachlan et al., 2003; Zoidl et al., 2004; Zoidl et al., 2008). They exhibit distinct expression patterns in the retina and most of them are shown to form the functional Cx channels in native cells or heterologous expression systems. Some Cx proteins exhibit a very restricted expression pattern, such as Cx52.6 and Cx55.5, which exclusively express in retinal HCs (Shields et al., 2007), indicating that they may contribute to highly specialized functions. Other Cx proteins show more wide-spread expression patterns, such as Cx27.5, which discretely localizes to the inner nuclear layer and the ganglion cell layer (Dermietzel et al., 2000), indicating that they may serve more general functions.

Studies in Chapter II on functional characterization of hemichannel currents in zebrafish retinal HCs demonstrated that outward and inward hemichannel currents displayed distinct properties in unitary conductance, voltage and calcium gating properties and pharmacological regulations, indicating different Cx proteins contributing to HGJ channels in native zebrafish HCs. In this study, I focused on examining the functional contribution of Cx52.6 and Cx55.5 to the native hemichannel currents in zebrafish retinal HCs.

Molecular composition of functional HGJ channels in zebrafish HCs

The expression pattern of Cx52.6 and Cx55.5 in the cultured isolated zebrafish HCs was examined, and both Cx52.6 and Cx55.5 were found in the cell body and dendritic

processes of wild type zebrafish HCs. To elucidate the potential role of specific Cx protein in native HGJ channel currents, I analyzed native hemichannel currents using electrophysiological recording combined with different gene manipulation techniques, which selectively block Cx55.5 or Cx52.6 expression in a permanent or transient way.

As for the *cx55.5* mutant zebrafish used in this study, functional Cx55.5 cannot be produced due to a nonsense mutation in the *cx55.5* gene. Compared to WT zebrafish HCs, inward hemichannel currents elicited at negative potentials were reduced substantially, while outward hemichannel currents induced at positive potentials increased in *cx55.5* mutant zebrafish HCs. In addition, the protein level of Cx52.6 and Cx55.5 also decreased dramatically in HCs from the *cx55.5* mutant zebrafish. These data indicate that Cx55.5 and Cx52.6 are not independent of each other during development. The deficiency of Cx55.5 expression resulted in decreased expression of Cx52.6. Therefore, the marked decrease of inward hemichannel currents in *cx55.5* mutant zebrafish HCs is most likely due to Cx55.5 deficiency, but the involvement of Cx52.6 can not be excluded. On the other hand, the increased outward hemichannel currents in *cx55.5* mutant zebrafish HCs may be caused by other Cx protein up-regulated during development to compensate for the loss of Cx55.5 and Cx52.6. Preliminary EM data from the Kamermans lab also supported this notion that other *cx* genes may be up-regulated in *cx55.5* mutant zebrafish (ARVO, 2008).

To overcome the developmental dependence and compensation effect in *cx55.5* mutant zebrafish and to better define the role of Cx proteins, Cx protein translation in

adult zebrafish HCs was specifically blocked using the morpholino-based gene knockdown technique. The immunocytochemistry data showed that anti-Cx55.5 morpholino and anti-Cx52.6 morpholino can transiently suppress the protein expression of Cx55.5 and Cx52.6, respectively, at four days post transfection. Interestingly, the suppression of Cx55.5 expression by anti-Cx55.5 morpholino resulted in a marked decrease of both inward and outward hemichannel currents, while the inhibition of Cx52.6 expression led to a significant decrease in outward hemichannel currents only. These data suggest that the Cx55.5 isoform is necessary for inward hemichannel currents, which may be mediated by homomeric Cx55.5 HGJ channels or heteromeric HGJ channels formed by Cx55.5 and other unidentified Cx isoforms. However, outward hemichannel currents require both Cx55.5 and Cx52.6, which may form Cx55.5/Cx52.6 heteromeric HGJ channels in native HCs.

Potential physiological roles of different connexin isoforms

So far, Cx channels are known or hypothesized to be involved in developmental, physiological and pathological processes, and exhibit great influence on intercellular communication between adjacent cells as well as unpaired cells. In the vertebrate retina, HCs are widely coupled to each other via gap junctions (Kaneko, 1971; McMahon et al., 1989) and HGJ channels located at the HC dendritic tips are proposed to mediate the negative feedback by an ephaptic mechanism (Kamermans et al., 2001b). The electrical coupling between HCs and the negative feedback generated by HCs to photoreceptors

are pivotal to the visual information processing and normal visual functions. However, some fundamental questions are yet to be answered. For example, what molecular mechanism underlies functional Cx channels? How is Cx channel function determined by channel composition? What Cx isoforms endow Cx channels with the ability to mediate the proposed feedback in HCs? Understanding the molecular composition of these functional Cx channels and physiological roles of different Cx isoforms will help to answer these questions.

In this study, the electrophysiological data for morpholino-treated HCs demonstrated that both Cx52.6 and Cx55.5 are necessary for outward hemichannel currents. Combined with the previously reported immuno-EM study, which shows that both Cx52.6 and Cx55.5 are abundant in the plasma membrane of apposing HCs (Shields et al., 2007), it suggests that Cx52.6 and Cx55.5 may form homomeric HGJ channels and then heterotypic gap junctions, or they may form heteromeric HGJ channels and then homotypic gap junctions, or both.

In addition, previous studies also show that Cx55.5, but not Cx52.6, is localized to the dendritic tips of HCs (Shields et al., 2007) and Cx55.5 can form functional channels with an unusual property of voltage-dependence (Dermietzel et al., 2000). Therefore, Cx55.5 has long been assumed as the candidate to mediate inward hemichannel currents, which are proposed to mediate the negative feedback signal. Consistently, in this study, data from *cx55.5* mutant zebrafish and morpholino-based Cx knockdown demonstrated that Cx55.5 is necessary for inward hemichannel currents, but not Cx52.6. In addition,

reduced feedback signals and altered visual behaviors have been recently shown in *cx55.5* mutant zebrafish by the Kamermans lab (ARVO, 2008). These data suggest that Cx55.5 formed hemichannels are responsible for the inward hemichannel currents. Alternatively, it is also possible that the inward hemichannel currents are mediated by heteromeric Cx channels composed of Cx55.5 and other unidentified Cx proteins. This question can be further addressed by identification of novel *cx* genes in HCs and functional characterization. The current study provides a good example for studying Cx proteins in retinal HCs.

CHAPTER IV

ZINC MODULATION OF HEMI-GAP-JUNCTION CHANNEL CURRENTS IN BASS RETINAL HORIZONTAL CELLS[†]

Section 4.1: Summary abstract

Hemi-gap-junction (HGJ) channels of retinal horizontal cells (HCs) function as transmembrane ion channels that are modulated by voltage and calcium. As an endogenous retinal neuromodulator, zinc, which is co-released with glutamate at photoreceptor synapses, plays an important role in shaping visual signals by acting on postsynaptic HCs *in vivo*. To understand more fully the regulation and function of HC HGJ channels, we examined the effect of Zn^{2+} on HGJ channel currents in bass retinal HCs. Hemichannel currents elicited by depolarization in Ca^{2+}-free medium and in 1 mM Ca^{2+} medium, were significantly inhibited by extracellular Zn^{2+}. The inhibition by Zn^{2+} of hemichannel currents was dose-dependent with a half-maximum inhibitory concentration of 37 μM. Compared with other divalent cations, Zn^{2+} exhibited higher inhibitory potency with the order being $Zn^{2+} > Cd^{2+} \approx Co^{2+} > Ca^{2+} > Ba^{2+} > Mg^{2+}$. Zn^{2+} and Ca^{2+} were found to modulate HGJ channels independently in additivity experiments. Modification of histidine residues with N-bromosuccinimide (N-BrSuc) suppressed the inhibitory action of Zn^{2+}, while modification of cysteine residues had no significant effect on Zn^{2+} inhibition. Taken together, these results suggest that zinc acts on HGJ channels in a calcium-independent

[†]This chapter was previously published in Journal of Neurophysiology (Sun et al., 2009).

way, that histidine residues on the extracellular domain of HGJ channels mediate the inhibitory action of zinc.

Section 4.2: Introduction

Horizontal cells (HCs) are second-order neurons in the vertebrate retina that receive excitatory synaptic input from, and provide inhibitory feedback to, photoreceptors (Baylor et al., 1971; Naka, 1972; Wu, 1992). HCs are extensively coupled via cell-to-cell gap junction channels (Witkovsky et al., 1983; Baldridge et al., 1987; McMahon et al., 1989; Zhang and McMahon, 2000, 2001), and also express unapposed hemi-gap-junction (HGJ) channels in their non-junctional membranes (DeVries and Schwartz, 1992; Malchow et al., 1993; Zhang and McMahon, 2001; Goodenough and Paul, 2003; Saez et al., 2005). HC HGJ channels function as transmembrane ion channels (DeVries and Schwartz, 1992; Malchow et al., 1993; Zhang and McMahon, 2001) and have been proposed to participate in ephaptic feedback from HCs to cones (Kamermans et al., 2001b; Kamermans and Fahrenfort, 2004). Previous studies have demonstrated that HGJ channels are modulated by transmembrane voltage, extracellular Ca^{2+} and light-adapting retinal neurotransmitters, such as dopamine, nitric oxide and retinoic acid (DeVries and Schwartz, 1992; Zhang and McMahon, 2000, , 2001; Ripps et al., 2002; Retamal et al., 2006; Zhang et al., 2008). In this study, I examined whether zinc modulates HGJ channels of HCs.

Zinc, a trace metal highly concentrated in the retina, plays a pivotal role in maintaining

normal visual function (Grahn et al., 2001; Ugarte and Osborne, 2001), while zinc deficiency results in a variety of ocular diseases (Huber and Gershoff, 1975; Morrison et al., 1978). Zinc is concentrated in photoreceptor cell bodies and synaptic terminals (Wu et al., 1993; Lee et al., 2008), and is released from photoreceptors onto HCs and bipolar cells (Akagi et al., 2001; Ugarte and Osborne, 2001; Zhang et al., 2002; Redenti et al., 2007). Convergent evidence indicates that zinc functions as a neuromodulator of synaptic transmission in the retina and in the rest of the brain by regulating a variety of voltage-gated and ligand-gated channels in postsynaptic neurons (Wu et al., 1993; Dong and Werblin, 1996; Huang, 1997; Han and Wu, 1999; Akagi et al., 2001; Zhang et al., 2002; Zhang et al., 2006). In the retina, zinc has been shown to modulate GABA receptors, glutamate receptors, and K^+ channels on HCs, glycine receptors on ganglion cells, and GABA receptors on bipolar cells (Wu et al., 1993; Dong and Werblin, 1996; Qian et al., 1997; Han and Wu, 1999; Zhang et al., 2002; Zhang et al., 2006).

In this study, the effects of extracellular Zn^{2+} on HGJ channels in isolated retinal HCs were investigated using whole-cell patch-clamp technique. The results demonstrate that micromolar Zn^{2+} partially suppresses HC HGJ channel currents, that HGJ channels are modulated by zinc at physiological concentrations of extracellular calcium, that zinc modulates HGJ channels in a Ca^{2+} independent way, and that the likely binding sites of Zn^{2+} are to extracellular histidine residues.

Section 4.3: Materials and methods

Cell culture

Dark-adapted adult hybrid striped bass (*Roccus* chrysops × *Roccus* saxitalis) were euthanized in accordance with National Institutes of Health guidelines for animal use. Retinas were removed under dim red light and then incubated in L-15 medium (GIBCO) containing 20 U/ml papain (Worthington) activated with 0.3 mg/ml cysteine. Penicillin/Streptomycin (1:100, Sigma) was routinely added to the medium to reduce contamination. The retinas were incubated in L-15/papain solution for 30 min followed by six changes of fresh L-15 medium, and then dissociated by repeated passage through a serological pipette. Isolated cells were plated onto plastic 35-mm dishes containing fresh L-15 medium. Cultures were maintained at 20 °C and cells were used following 1-4 days in culture.

Solutions and chemicals

The normal Ca^{2+} extracellular solution contained (in mM): 137 NaCl, 2.5 KCl, 2.5 $MgCl_2$, 2.5 $CaCl_2$, 10 HEPES, 10 glucose and 1mg/ml BSA (Sigma, Fraction VII); pH was adjusted to 7.4 using NaOH. The Ca^{2+}-free extracellular solution contained (in mM): 114.5 NaCl, 30 CsCl, 2.5 KCl, 1 $MgCl_2$, 10 HEPES, 1 Na-pyruvate, 10 glucose, and 1mg/ml BSA, and pH was adjusted to 7.4 with NaOH. To block potassium channels, K^+ in the normal pipette solution was replaced by Cs^+ and tetraethylammonium chloride (TEA) was added. The pipette solution contained (in mM): 124 CsCl, 1 $CaCl_2$, 11 EGTA, 10 HEPES, 1 Mg-ATP, 0.1 Na-GTP, and 10 TEA, pH to 7.4 with CsOH. Solution changes during

recording were performed with a perfusion system and were completed within 30 seconds. The histidine-modifying reagent, N-bromosuccinimide (N-BrSuc, MP Biomedicals) was dissolved in extracellular solution at 1 mM concentration. The membrane-impermeant cysteine modifier, 2-(trimethylammonium)ethyl methane thiosulfonate bromide (MTSET, Anatrace), was prepared as a 10 mM stock in extracellular solution, set on ice for up to 1h, then diluted to 1 mM working concentration in extracellular solution at room temperature immediately before incubation in cell culture. The non-charged membrane-permeant cysteine modifier, N-ethylmaleimide (NEM, Sigma-Aldrich) was prepared as a 100 mM stock in water and then diluted to 1 mM working concentration in extracellular solution.

Patch-clamp recording

Recordings from solitary HCs were performed using conventional whole-cell patch-clamp configuration. Patch pipettes were pulled from Corning 7052 glass (AM Systems) and fire-polished to 4-6 MΩ resistance. The pipette series resistance and capacitance were compensated by 80%. The offset potential between the pipette and bath solutions was zeroed prior to seal formation. Voltage commands and data analysis were performed by pCLAMP 9.0 software.

Data analysis

Dose inhibition curves were obtained by calculating the inhibition percentage of Zn^{2+} at

different concentrations and were fitted with Hill equation, $I_{mem} = I_{max} \cdot A^n / (IC_{50} + A^n)$, where I_{mem} is the cell membrane current elicited by a given antagonist concentration (A), IC_{50} is the antagonist concentration that elicits a half-maximal response, I_{max} is the measured maximal response, and n is the Hill coefficient; the normalized percent inhibition of zinc was calculated by the equation: $(I_{control} - I_{Zn})/I_{control} \times 100\%$. Here, the inhibition percentage was calculated by measuring the reduction of the current following application of Zn^{2+} (or other cations), and expressing this as a fraction of the peak current amplitude in the control medium without Zn^{2+} (or other cations).

The data are presented as mean ± SE. *P* values stated were calculated using either the *t*-test or the paired *t*-test. Statistical analyses were performed with Sigmaplot 10.0.

Section 4.4: Results

Zinc inhibits HGJ channel currents

To examine the effect of Zn^{2+} on HGJ channel currents, isolated solitary HCs were recorded using whole cell voltage clamp, and outward HGJ channel currents were elicited by superfusion with Ca^{2+}-free medium and cell membrane depolarization, while blocking K^+ channels with Cs^+, and TEA. As shown in **Figure 4-1A**, at a membrane potential of +40 mV, outward HGJ channel current was increased by switching the extracellular solution from 2.5 mM Ca^{2+} medium to Ca^{2+}-free medium. Application of 30 μM Zn^{2+} suppressed this hemi-channel current from 3040 pA to 1860 pA. The action of 30 μM Zn^{2+} on HGJ channel currents was reversible upon washout, and the following application of

100 μM Zn^{2+} decreased the current further to 390 pA. The dose inhibition curve for Zn^{2+} is shown in **Figure 4-1B**, and when fit with the Hill equation yielded a half-maximum inhibitory concentration (IC_{50}) of 37 μM. I also tested the effect of 5 μM Zn^{2+} on HGJ channel currents. No potentiation of currents was observed, suggesting that Zn^{2+} inhibits HGJ channel currents in a monophasic manner. In contrast, Ca^{2+}, another divalent cation modulator for HGJ channel currents (Zhang and McMahon, 2001), exhibited an IC_{50} value of 245 μM, which is ~ 7-fold higher than zinc (**Figure 4-1C**).

As shown in **Figure 4-1C**, approximately 10% of the hemichannel current remained at 1 mM Ca^{2+}, a concentration similar to that in the intact retina (Dearry and Burnside, 1984). To test whether Zn^{2+} inhibits HC hemichannel currents at physiological Ca^{2+} concentrations, we examined Zn^{2+} action on hemichannel currents in the presence of 1 mM Ca^{2+}. 10 μM Zn^{2+} significantly reduced the Ca^{2+}-resistant hemichannel current to 19 ± 4% of control ($P < 0.05$, n = 5). These data indicate that Zn^{2+} can modulate HGJ channel currents at physiological Ca^{2+} concentrations.

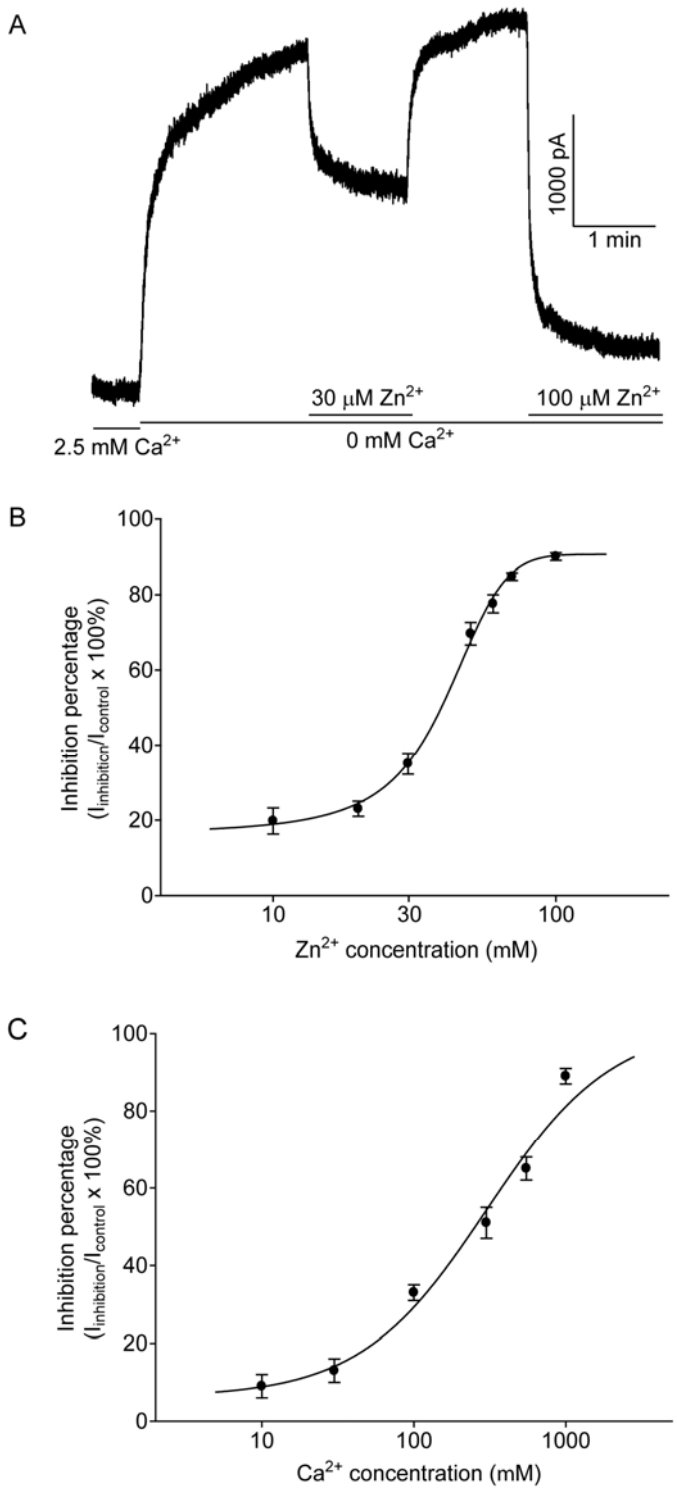

Figure 4-1. Zinc inhibits HGJ channel currents in bass HCs.

Figure 4-1. Zinc inhibits HGJ channel currents in bass HCs.

(A) At a holding potential of +40 mV, outward hemichannel currents were induced by switching the extracellular solution from 2.5 mM Ca^{2+} medium to Ca^{2+}-free medium. External application of 30 μM Zn^{2+} or 100 μM Zn^{2+} suppressed the currents to different degrees.

(B) Normalized dose inhibition relationships for Zn^{2+} in Ca^{2+}-free medium. The reduction of currents by Zn^{2+} was normalized to the initial response obtained in Ca^{2+}-free medium.

(C) Normalized dose inhibition relationships for Ca^{2+}. The reduction of currents by Ca^{2+} was normalized to the initial response obtained in Ca^{2+}-free medium. Each point is an average derived from 4 to 5 cells and dose-inhibition curves were fit with Hill equation.

Zinc is a potent modulator of HGJ channel currents

HGJ channels possess a high sensitivity to extracellular divalent cations, which is rarely observed on cell-cell gap junction channels (Spray et al., 2006; Srinivas et al., 2006). To compare the inhibitory potency of Zn^{2+} with other divalent cations, I added 100 μM of different cations to the Ca^{2+}-free medium and determined their inhibition of HGJ channel currents (**Figure 4-2A**). HGJ channel currents were induced under Ca^{2+}-free medium by stepping membrane potential for 10 s from 0 mV to +40 mV (**Figure 4-2A**, inset). The inhibitory potency of these cations was in the order of: $Zn^{2+} > Cd^{2+} \approx Co^{2+} > Ca^{2+} > Ba^{2+} > Mg^{2+}$ (**Figure 4-2B**).

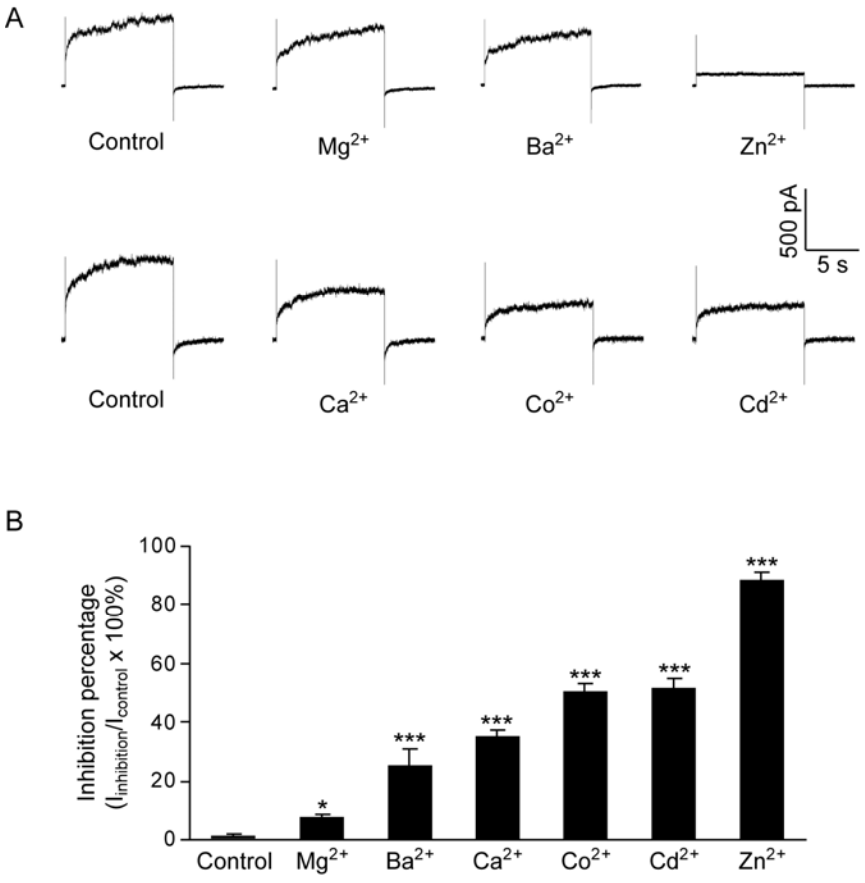

Figure 4-2. Inhibitory potencies of different divalent cations on HGJ currents.

(A) Representative current traces of the currents induced in control medium and in medium containing 100 μM Mg^{2+}, Ba^{2+}, Zn^{2+} (upper traces) or 100 μM Ca^{2+}, Co^{2+}, Cd^{2+} (bottom traces).

(B) Inhibition by the different divalent cations. Asterisks indicate values significantly different from control, paired *t* test, * $p < 0.05$ and *** $p < 0.001$ (n = 5).

Zinc modulation is independent of calcium

Ca^{2+} and retinoic acid interact in gating HGJ channels in bass retinal HCs (Zhang and McMahon, 2001), and Co^{2+} and Ni^{2+} share the same binding site with Ca^{2+} on connexin hemichannels (Srinivas et al., 2006). Next, we examined an interaction between Zn^{2+} and Ca^{2+} on HGJ channel currents.

If Zn^{2+} and Ca^{2+} act on HGJ channels independently, their inhibitory effects would be expected to be additive when both are present at low concentrations (individual inhibition percentage < 50%), provided that there are sufficient HGJ channel targets for both Zn^{2+} and Ca^{2+}. However, if there is overlap in the binding sites of Zn^{2+} and Ca^{2+}, one would expect a significantly lower total inhibition instead of simple addition in the presence of both cations. As shown in **Figure 4-3A**, HGJ channel currents were inhibited by 24% (from 705 pA to 537 pA) by application of 20 μM Zn^{2+} alone, while application of 100 μM Ca^{2+} alone reduced the current by 40% (from 790 pA to 471 pA). The co-application of 20 μM Zn^{2+} and 100 μM Ca^{2+} (Ca^{2+} added before Zn^{2+}) produced a total reduction of 62% (from 790 pA to 490 pA), which is close to the sum of their separate inhibitory effects (64%). Statistical analyses (**Figure 4-3B**) show that there is no significant difference between the inhibition by co-application (58 ± 3%) vs the sum (60 ± 4%) of separate inhibitions (*t* test, $P > 0.05$, n = 4). Similar results were also obtained when Zn^{2+} was added before Ca^{2+} during co-application experiments (data not shown). These data suggested that Zn^{2+} and Ca^{2+} modulate HGJ channel currents independently, at least at low concentrations.

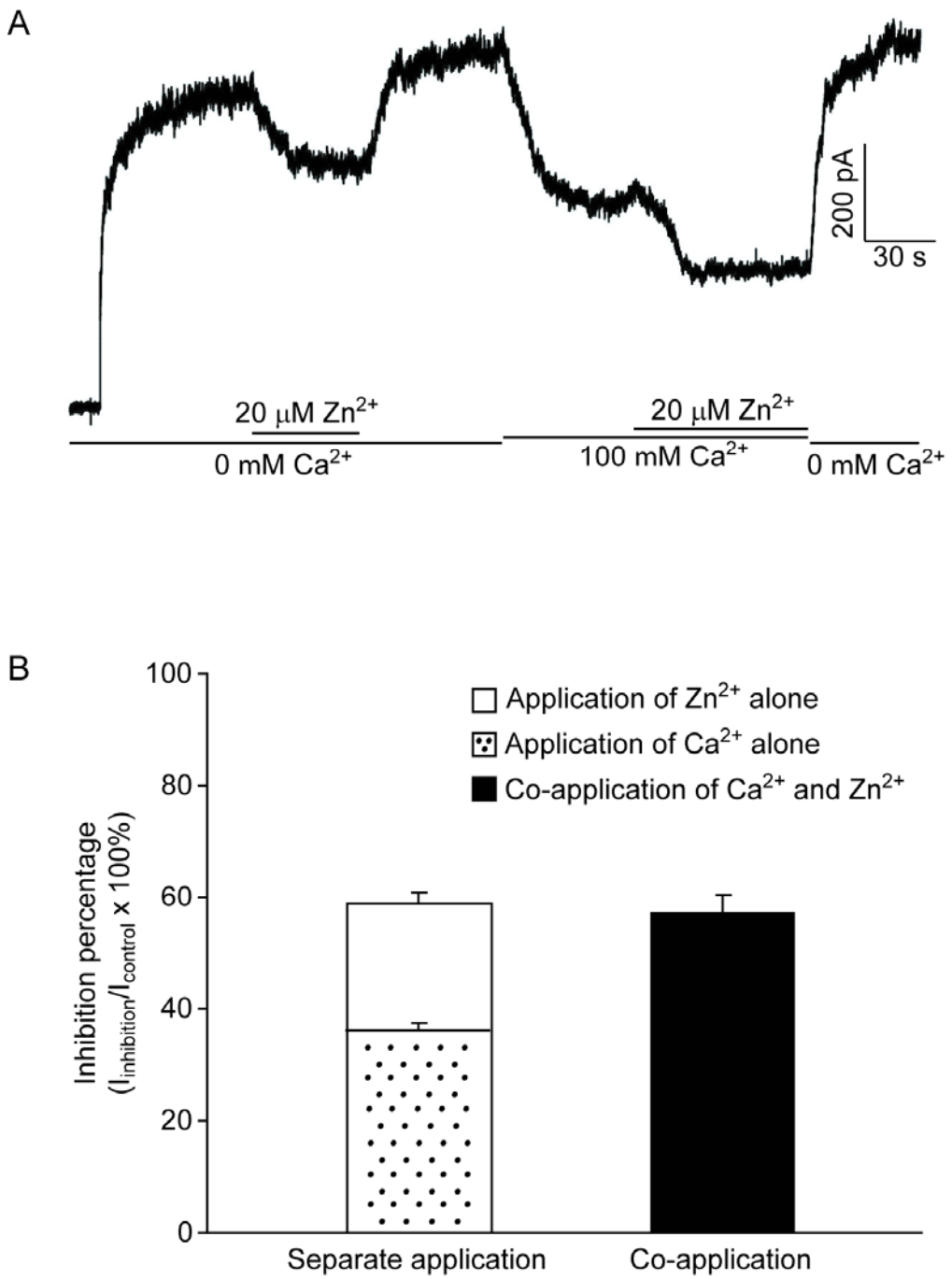

Figure 4-3. At low concentrations, Zn^{2+} and Ca^{2+} act on HGJ channels additively.

Figure 4-3. At low concentrations, Zn^{2+} and Ca^{2+} act on HGJ channels additively.

(A) In Ca^{2+}-free medium, HGJ channel currents were evoked by stepping the holding potential from 0 mV to +40 mV. 20 μM Zn^{2+} alone produced a 23.8% inhibition from 705 pA to 537 pA. 100 μM Ca^{2+} followed by 20 μM Zn^{2+} were perfused onto the cell.

(B) Average inhibition percentages resulting from the sum of individual application of Zn^{2+} (white bar) or Ca^{2+} (dotted bar), and resulting from the co-application of Zn^{2+} and Ca^{2+} (solid bar). Data were collected from 4 cells.

At high concentrations of Zn^{2+} and Ca^{2+}, especially those, at which the sum of separate inhibition exerted by Zn^{2+} or Ca^{2+} alone would exceed 100%, it becomes impossible to examine the action mode between Zn^{2+} and Ca^{2+} by comparing the inhibition of co-application with the sum of separate inhibitions. However, in this case, if Zn^{2+} and Ca^{2+} modulate HGJ channels independently, the fraction of inhibited channels by Zn^{2+} in Ca^{2+}-free medium should remain the same as in the presence of background Ca^{2+}. To test this hypothesis, we examined inhibitions by 60 μM Zn^{2+} (78 ± 3% inhibition in **Figure 4-1B**) on HGJ currents in the absence and in the presence of 100 μM Ca^{2+} (34 ± 2% inhibition in **Figure 4-1C**). As shown in **Figure 4-4A**, application of 60 μM Zn^{2+} reduced the HGJ channel current from 1000 pA to 200 pA, resulting in an 80% inhibition in Ca^{2+}-free medium. After washout with Ca^{2+}-free medium, 100 μM background Ca^{2+} was applied, and the current decreased to 640 pA. In the presence of the 100 μM Ca^{2+}, additional application of 60 μM Zn^{2+} further reduced the currents from 640 pA to 110 pA, producing an 83% inhibition, which is similar to that observed in Ca^{2+}-free medium. Again, statistical analyses showed no significant difference (**Figure 4-4B**) between the fraction inhibited by 60 μM Zn^{2+} in the absence (78 ± 3%) and in the presence (80 ± 3%) of 100 μM Ca^{2+} (*t* test, $P > 0.05$, n = 4). Similar results were obtained, when 550 μM Ca^{2+} was examined using 20 μM Zn^{2+} as background. As shown in **Figure 4-4C**, the inhibition of 550 μM Ca^{2+} without Zn^{2+} (65 ± 2%) remains the same as in the presence of 20 μM Zn^{2+} (64 ± 3%, *t*-test, $P > 0.05$, n = 4). These data indicate that at high concentrations, Zn^{2+} and Ca^{2+} modulate HGJ channel currents independently.

In addition, we also recorded HGJ channel currents at varying concentrations of Zn^{2+} in the presence of 100 μM Ca^{2+}. The dose response curve of Zn^{2+} in the presence of 100 μM Ca^{2+} exhibited an IC_{50} of 32 μM (data not shown), which is similar to the IC_{50} of Zn^{2+} in Ca^{2+}-free medium (37 μM), further supporting that Zn^{2+} and Ca^{2+} act on HGJ channels independently.

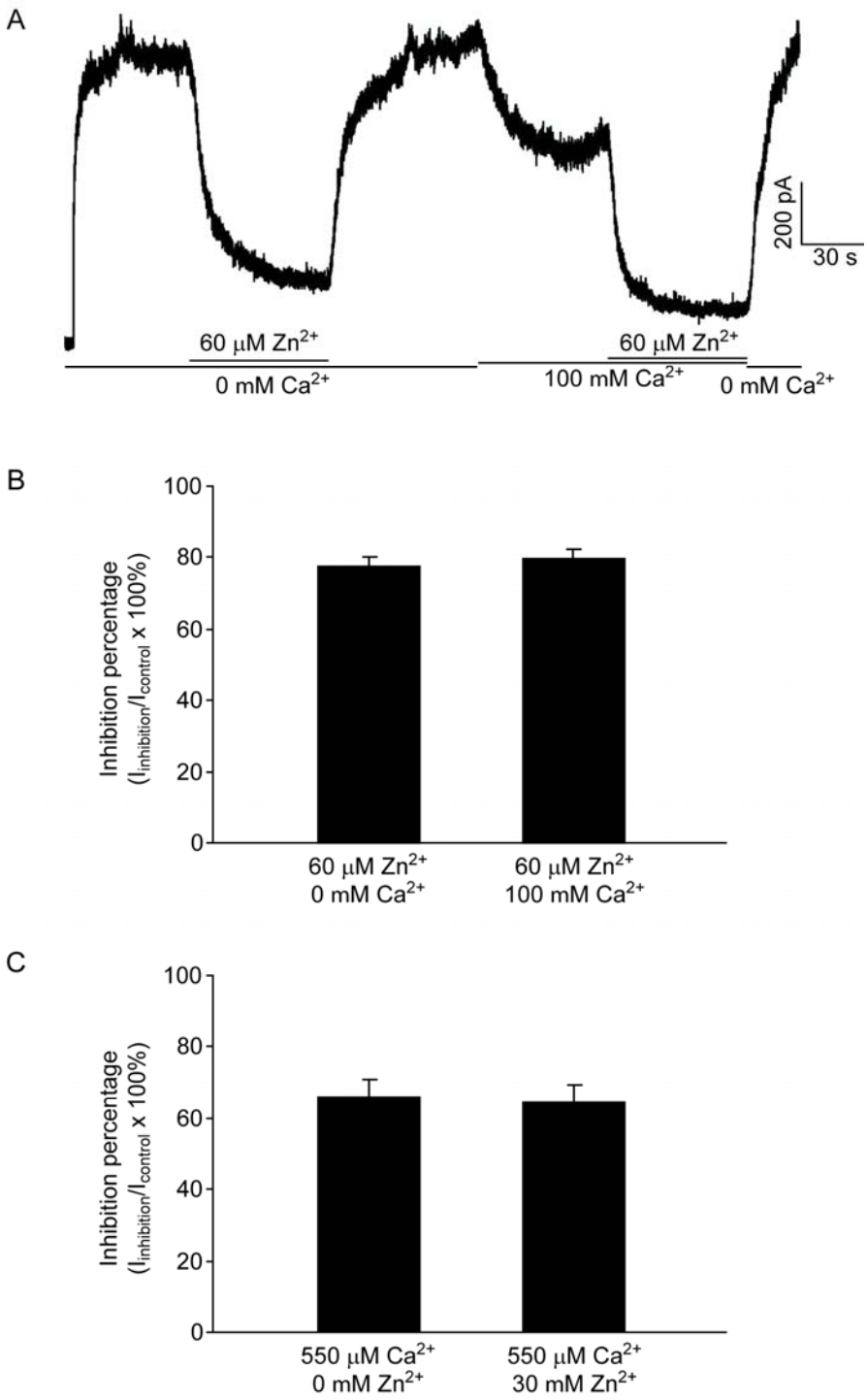

Figure 4-4. At high concentrations, Zn^{2+} or Ca^{2+} inhibits a constant proportion of current in co-application.

Figure 4-4. At high concentrations, Zn^{2+} or Ca^{2+} inhibits a constant proportion of current in co-application.

(A) In Ca^{2+}-free medium, outward HGJ channel currents were evoked by stepping from 0 to +40 mV. 60 μM Zn^{2+}, and then 100 μM Ca^{2+}, and additional application of 60 μM Zn^{2+} were perfused onto the cell.

(B) Average inhibition percentages of 60 μM Zn^{2+} in Ca^{2+}-free medium (left bar), and of 60 μM Zn^{2+} in the presence of 100 μM Ca^{2+} (right bar).

(C) Average inhibition percentages of 550 μM Ca^{2+} in Zn^{2+}-free medium (left bar), and of 550 μM Ca^{2+} in the presence of 30 μM Ca^{2+} (right bar). Data were collected from 4 cells.

Zinc inhibits HGJ channel currents via histidine not cysteine residues

The action of Zn^{2+} on proteins is generally mediated by complexing zinc ions with histidine or cysteine residues (Norregaard et al., 1998; Seebungkert and Lynch, 2001; Nevin et al., 2003; Connolly and Wafford, 2004). To test the hypothesis that the inhibition of connexin hemichannels by Zn^{2+} is mediated by binding to histidine/cysteine residues, the inhibition exerted by 50 μM Zn^{2+} was compared in the presence or absence of histidine or cysteine residue modifying agents. In control experiments, with no pre-treatment, 50 μM Zn^{2+} resulted in a 78 ± 2% inhibition of HGJ channel currents (n = 5, **Figure 4-5**). When the brominating agent N-bromosuccinimide (N-BrSuc) was used to modify the external histidine residues by pre-incubating HCs with 1 mM N-BrSuc for 30 min, the inhibitory effect exerted by 50 μM Zn^{2+} was significantly reduced to only 40 ± 2% inhibition (*t*-test $P < 0.001$, n = 5, **Figure 4-5**). I then tested whether cysteine residues are involved in mediating the action of Zn^{2+} on hemichannels. When HCs were pre-incubated with the fast-reacting, lipid-insoluble cysteine-modifier, 2-(trimethylammonium)ethyl methane thiosulfonate bromide (MTSET), no apparent effect was observed on the inhibition produced by 50 μM Zn^{2+} (75 ± 3% inhibition, n = 5, **Figure 4-5**) indicating that MTSET-accessible extracellular cysteines are not involved in Zn^{2+} action. To further confirm the lack of cysteine involvement, a non-charged, membrane-permeant cysteine modifier, N-ethylmaleimide (NEM), was tested, and similar results were obtained (74 ± 3%, n = 5, **Figure 4-5**).

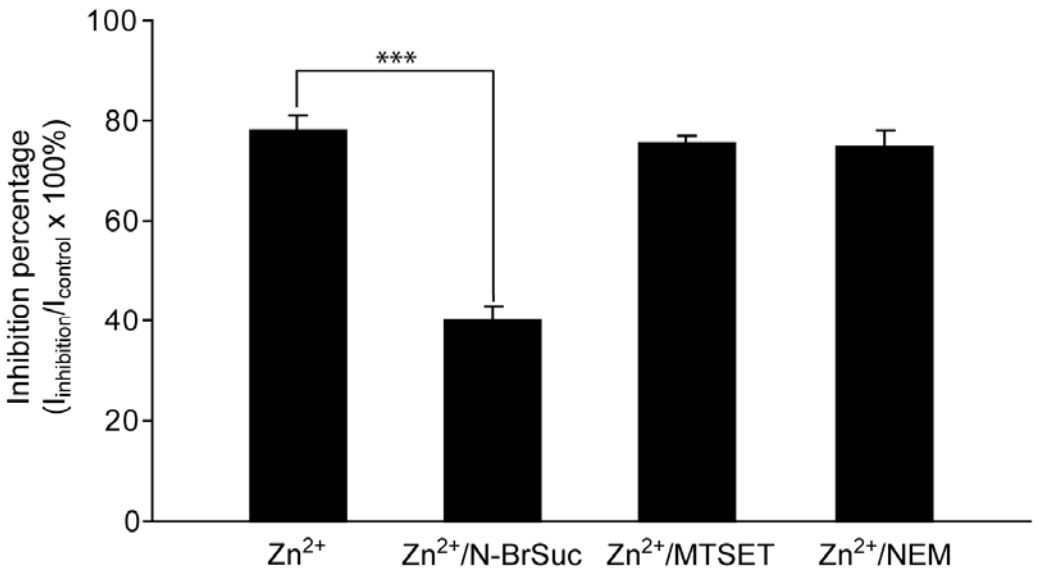

Figure 4-5. Effects of histidine and cysteine modification on zinc inhibition. Histogram shows 50 μM zinc inhibition of HGJ channels with or without pre-treating with histidine/cysteine modifying reagents. Asterisks indicate values significantly different from the control, *t* test, *** $p < 0.001$ (n = 5).

Zinc inhibits inward hemichannel currents

While positive holding potentials elicit high-amplitude, stable, HGJ currents that are advantageous for characterization of modulatory mechanisms, in the intact retina, HGJ channels are proposed to mediate electrotonic feedback to photoreceptors via inward currents generated at negative membrane potentials. Thus, I tested if HC HGJ currents could be elicited at potentials similar to those observed during HC light responses *in situ*, as well as to assess whether zinc could modulate these HGJ currents. When HCs were hyperpolarized from -30 mV to -80 mV (**Figure 4-6**, inset), such as would occur in a saturating light response in the intact retina, inward HGJ currents were elicited that partially inactivated within 100 to 150 ms (**Figure 4-6A**, upper panel). These currents were strongly suppressed by extracellular 100 μM Zn^{2+} (**Figure 4-6A** middle panel), and the suppression was reversed upon wash out with Ca^{2+}-free medium (**Figure 4-6A**, bottom panel). To exclude the possibility of contamination with inward Na^{+} currents, the Na^{+} channel blocker QX-314 (1 mM) was added to the pipette solution, and no significant difference was found (data not shown). As shown in **Figure 4-6B**, the amplitude of peak inward currents in Ca^{2+}-free medium was, on average, 92.5 ± 14.5 pA (n = 4), and 100 μM Zn^{2+} significantly suppressed the currents to 28.1 ± 3 pA (paired t-test, $P < 0.001$, n = 4).

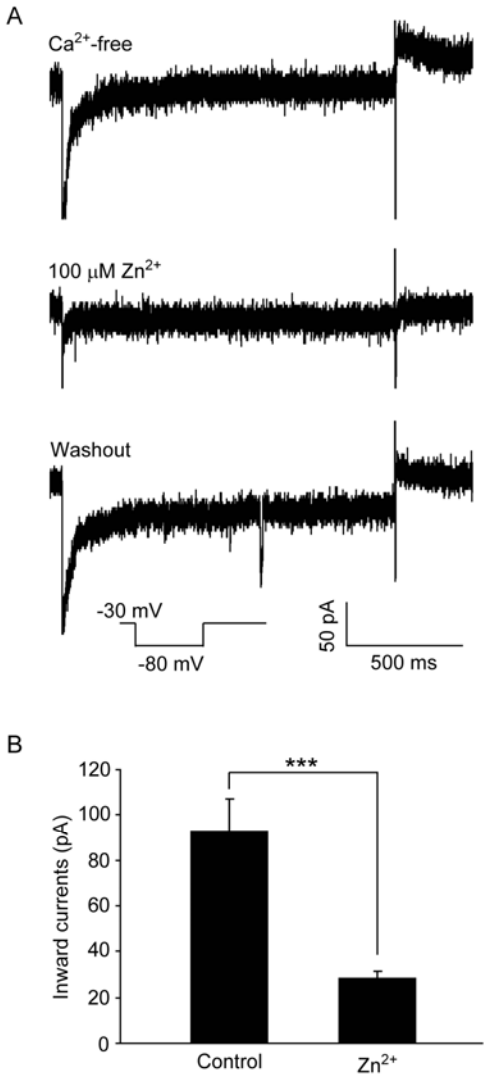

Figure 4-6. Suppression of inward hemichannel currents by Zn^{2+}.

(A) Representative current trace of inward hemichannel currents elicited in Ca^{2+}-free medium (upper), and suppressed by application of 100 μM Zn^{2+} (middle). The suppression by 100 μM Zn^{2+} was reversible (bottom). Voltage protocol shown as inset: inward hemichannel currents were induced by 1 s voltage stepping to -80 mV from a holding potential of -30 mV.

(B) Amplitudes of peak inward currents and inhibition effects by 100 μM Zn^{2+}. ***P < 0.001 (n=4).

Section 4.5: Discussion

I have characterized the effects of Zn^{2+} on HGJ channels of solitary retinal HCs, and our principal findings are: (1) Zn^{2+} inhibits HGJ channel currents at micromolar concentrations in a monophasic manner. (2) Zn^{2+} and Ca^{2+} modulate HGJ currents independently. (3) The inhibition of Zn^{2+} is mediated through histidine residues on the extracellular domain of hemichannels, while the contribution of cysteines is limited. Taken together, these data suggest that Zn^{2+} is a potent regulator of native HGJ channel currents.

Zinc acts monophasically and extracellularly

Previous studies showed that extracellular Zn^{2+} modulates perch Cx35 and human Cx26 HGJ channels expressed on *Xenopus* oocytes in a biphasic pattern, with low micromolar concentrations of Zn^{2+} enhancing HGJ currents, and high concentrations suppressing them (Chappell et al., 2003; Chappell et al., 2004). This biphasic action of Zn^{2+} has also been reported for other Zn^{2+}-binding proteins (Han and Wu, 1999). In contrast, in this study of native HC hemichannels, we found that Zn^{2+} suppressed HGJ channel currents at both low and high micromolar concentrations. This monophasic inhibitory effect of Zn^{2+} indicates that the Zn^{2+} modulation of bass HGJ channels is different from the biphasic model, which has two metal ion-binding sites with different affinities. It is interesting that a similar monotonic Zn^{2+} inhibition of AMPA-type glutamate receptors has also been reported in bass retinal HCs (Zhang et al., 2002).

The presence of 1 mM external Ca^{2+} did not affect the Zn^{2+} inhibition of HGJ currents, indicating that Zn^{2+} acts on HGJ channels via specific binding interactions, not due to non-specific cationic surface charge actions. Zn^{2+} suppressed HGJ currents at both positive and negative potentials, and this voltage-independence of Zn^{2+} modulation further suggested that the binding sites for Zn^{2+} are unlikely to be located within the pore of HGJ channels. Furthermore, no significant effect of extracellular Zn^{2+} on cell-to-cell coupling of bass HCs was observed (data not shown), indicating that the binding sites for Zn^{2+} are located on the extracellular surfaces exposed on unapposed HGJ channels. Taken together, these results suggest that the modulation of HGJ channels by Zn^{2+} occurs at specific binding sites on the extracellular surface as has been suggested for Cx46 hemichannels (Verselis and Srinivas, 2008). The distinct regulatory pattern and potency of Zn^{2+} observed on Cx35 and Cx26 HGJ channels heterologously expressed in oocytes (Chappell et al., 2003; Chappell et al., 2004) may be due to sequence differences in those connexin proteins compared to whatever bass HC connexin protein that forms the hemichannels we recorded, or differences in Zn^{2+} regulation of native HC versus heterologously expressed non-HC connexins.

Zinc acts independently of calcium

Previous studies have shown that Ca^{2+} has interactions with retinoic acid (Zhang and McMahon, 2001), and shares the same binding sites with Co^{2+} and Ni^{2+} in regulating HGJ channel currents (Srinivas et al., 2006). In this study, we found that at low concentrations

of both Zn^{2+} and Ca^{2+}, their actions were additive, while at high concentrations the fraction of current inhibited by one cation remains the same in the presence of the other. These results indicate that Zn^{2+} regulates HGJ channels by coordinating with binding sites that are distinct from the ones for Ca^{2+}. Furthermore, the IC_{50} of Zn^{2+} does not change significantly in the presence of Ca^{2+}, suggesting that the affinity of HGJ channels for Zn^{2+} remains the same under those conditions. All these data suggest that Zn^{2+} regulates HGJ channel currents in a Ca^{2+}-independent manner.

Zinc acts on histidine residues

Histidines and cysteines are the most common coordinating residues at Zn^{2+}-binding sites (Horenstein and Akabas, 1998; Norregaard et al., 1998; Katz and Luong, 1999; Seebungkert and Lynch, 2001; Nevin et al., 2003; Connolly and Wafford, 2004). Although the specific sequences of the bass HC connexins mediating hemi-channel currents have not been identified, connexin proteins possess conserved cysteine residues on the extracellular loops that stabilize the folding and cell-cell interactions of connexin proteins (Foote et al., 1998; Richard et al., 1998; Toyofuku et al., 1998). Histidine residues have also been found conserved in many different connexins (Stergiopoulos et al., 1999; Beahm and Hall, 2002). Our data show that Zn^{2+} inhibition was significantly attenuated by pre-treating cells with a histidine modifier N-BrSuc, a common brominating agent used to modify histidines in different proteins (Poe et al., 1979; Mancini et al., 1992), indicating that the Zn^{2+} inhibition involves binding to one or more exposed histidine residues. To

assess the contribution of cysteine residues to the Zn^{2+} inhibition, the effects of two cysteine-modifiers, a membrane-impermeant agent MTSET and a membrane-permeant agent NEM, were also examined, and neither exerted significant influence on Zn^{2+} modulation of HGJ currents. Overall, these results suggest that histidines are the major residues for coordinating Zn^{2+}, while cysteine residues contribute little to this inhibition. Interestingly, conserved histidine residues on HGJ channels have been identified on the extracellular domains of connexin proteins (Beahm and Hall, 2002). However, since the modification of histidine residues did not block the Zn^{2+} inhibition completely, our data do not exclude the possibility that other residues might also contribute to the coordination of Zn^{2+}.

Physiological relevance of zinc modulation on HGJ channels

Endogenous Zn^{2+} has been shown to be highly concentrated in the synaptic terminals of photoreceptors (Wu et al., 1993; Lee et al., 2008). Recently, both intracellular re-distribution of Zn^{2+} and depolarization-induced Zn^{2+} release have been reported in isolated zebrafish photoreceptors (Redenti et al., 2007). Furthermore, Zn^{2+} has also been shown to modulate $GABA_C$ and AMPA receptors in teleost retinal HCs, indicating that Zn^{2+} can potentially regulate visual signal processing within retinal circuits (Dong and Werblin, 1996; Zhang et al., 2002).

Chelation of endogenously released retinal zinc results in depolarization of the HC membrane potential (Zhang et al., 2002). This effect is consistent with both relief of zinc

inhibition of HC glutamate receptors (also high μM IC_{50}), as shown previously (Zhang et al., 2002), and with relief of the zinc inhibition of HC HGJ channels mediating currents shown here. The modulation of HGJ currents by Zn^{2+} provides a potential mechanism by which the HC membrane current could be regulated by Zn^{2+} release from photoreceptors. Thus, these experiments with isolated HCs, which allow direct measurement of native hemichannel currents not possible in HCs in intact retinas, have established novel aspects of HC HGJ currents and their modulation by zinc as well as the potential for these mechanisms to contribute to the regulation of HC membrane potential and processing of visual information in the distal retina.

CHAPTER V

SUMMARY

Hemi-gap-junction (HGJ) channels composed of connexin (Cx) proteins have long been known as the structural precursors of gap junctions on coupled cell membranes, and have now been shown to be active on unpaired plasma membranes as independent functional units (Goodenough and Paul, 2003). Retinal horizontal cells (HCs) are widely coupled to each other via gap junctions (Kaneko, 1971; McMahon et al., 1989) and the specific HGJ channels in HCs are proposed to mediate the negative feedback pathway from HCs to photoreceptors (Kamermans et al., 2001b). These studies suggest that the Cx channels expressed in retinal HCs are important not only for visual signal amplification and propagation, but also for visual signal refinement. In the current thesis project, I sought to examine the key question: whether HGJ channels in HCs could serve a proposed role in the negative feedback pathway. The answer should lie in studies of HGJ channels natively expressed in retinal HCs. However, pivotal information such as gating properties and molecular composition of native HGJ channels in retinal HCs is largely unknown.

To answer the key question, I focused my work on the Cx-forming HGJ channels, which are expressed in teleost retinal HCs. Patch-clamp electrophysiology, gene manipulation methods and immunocytochemistry were used to investigate biophysical

properties, molecular composition and potential physiological roles of functional HGJ channels in cultured retinal HCs. In summary, there are six major findings in this study. First, both outward hemichannel currents elicited at positive potentials and inward hemichannel currents induced at negative potentials are observed in cultured solitary zebrafish retinal HCs, indicating that functional HGJ channels are expressed in native uncoupled HCs. Second, outward and inward hemichannel currents show distinct properties in many aspects, including voltage and Ca^{2+} gating properties, pharmacological regulation, and single channel properties, indicating that different types of HGJ channels are present in native HCs, which may account for different functions *in vivo*. Third, inward hemichannel currents elicited at negative potentials exhibit unique channel properties, which persist under physiological conditions and satisfy the requirement of ephaptic communications in the feedback pathway. Fourth, both Cx52.6 and Cx55.5 are specifically expressed in the cell body and dendrite processes of cultured HCs from wild type zebrafish. Fifth, inward hemichannel currents may be mediated by the Cx55.5-formed channels, while outward hemichannel currents may be contributed by both Cx55.5 and Cx52.6 formed channels, which provide a molecular basis for the distinct properties observed between outward and inward hemichannel currents. Sixth, in bass retinal HCs, micromolar Zn^{2+} significantly inhibits both outward and inward hemichannel currents in a monophasic mode, which is likely mediated by extracellular histidine residues of HGJ channels and is independent of Ca^{2+}.

Gating and regulation properties of HGJ channels in retinal HCs

According to the ephaptic feedback model, HGJ channels must form a current sink by which the extrasynaptic potential could be modulated. In this view, HGJ channels located in HC dendrite tips should remain open within the physiological range of membrane potentials and Ca^{2+} concentrations (Kamermans and Fahrenfort, 2004). However, these opening properties are inconsistent with those of most documented HGJ channels. In addition, previous data on HGJ channels is contradictory or ambiguous, which may be due to the diverse Cx protein isoforms and their ability to form heteromeric channels. Therefore, it is possible that different HGJ channels in retinal HCs composed of distinct Cx proteins could satisfy all of these prerequisites for the ephaptic model.

To determine whether the native HGJ channels in zebrafish HCs could serve a putative role in the feedback pathway in the outer retina, I first examined the gating and pharmacological properties of HGJ channels using patch-clamp electrophysiological methods. Whole cell patch-clamp recordings showed that both macroscopic outward and inward hemichannel currents can be elicited at positive and negative potentials, respectively. Of particular interest, inward hemichannel currents are active within the physiological voltage range of HCs from -40 mV to -80 mV. In addition, compared to outward hemichannel currents, inward hemichannel currents exhibit distinct sensitivity to extracellular Ca^{2+} and persist at physiological Ca^{2+} concentrations from 1 mM to 1.5 mM. I then examined the properties of HGJ channel currents from the single-channel level using outside-out voltage clamp configuration. Outward and inward hemichannel currents

are elicited at the single-channel level, and significant differences are observed in unitary conductance and total channel open probability between these two types of currents. These data indicate that outward and inward hemichannel currents may be mediated by different Cx proteins, and that HGJ channels formed by distinct Cx protein may mediate unique inward currents and ephaptic communications. However, to answer whether and how these inward hemichannel currents mediate negative feedback *in vivo*, whole mount retinal recordings combined with specific gene ablation still need to be performed to provide direct evidence.

Based on previous studies in goldfish, it is estimated that the resistance of cone intersynaptic space is 6-60 MΩ and the hemichannel-mediated ephaptic inhibition induces a Ca^{2+} current shift of about -10 mV (Vandenbranden et al., 1996; Kamermans et al., 2001b). Therefore, there should be about 1.6 pA ~ 16 pA currents generated by HGJ channels to satisfy this negative feedback in each cone synapse. Based on this study, if the membrane potential of HCs hyperpolarizes from -30 mV to -80 mV upon light stimulation, each HC will produce an increased inward hemichannel current of 30 pA to 45 pA at 1.5 mM Ca^{2+}. Although the number of HGJ channels in each cultured HC is not known, the increased amplitude of inward hemichannel currents is relevant to the hemichannel feedback hypothesis.

Since the blockage of HGJ channels by carbenoxolone, a non-specific gap junction blocker, has been utilized to test the ephaptic hypothesis (Kamermans et al., 2001b; de Groot et al., 2003), I examined the effect of 100 μM carbenoxolone on outward and

inward hemichannel currents. I found that only the outward currents are significantly suppressed by carbenoxolone, while the inward currents are almost unaffected. Since pharmacological properties of hemichannels are primarily determined by the Cx subunits that form them. Different Cx proteins could confer different properties to the channels. Thus, it is possible that the Cx isoforms that form the inward current-carrying channels are insensitive to carbenoxolone. Another reagent, low concentration Co^{2+}, is also commonly used to test the role of hemichannels in the feedback pathway (Fahrenfort et al., 2004). Therefore, I examined the effect of Co^{2+} on hemichannel currents. 100 μM Co^{2+} significantly blocks both outward and inward hemichannel currents, suggesting that it can be used in whole mount retina recordings to further test the physiological role of inward hemichannel currents. So far, the lack of specific blockers of HGJ channels is one of the biggest obstacles in this research field.

Zn^{2+} has been shown to be highly concentrated in the synaptic terminals of photoreceptors and co-released with glutamate from photoreceptors to HCs (Akagi et al., 2001; Ugarte and Osborne, 2001). To understand how Zn^{2+} performs its regulatory function on HGJ channels and what physiological role it may play in HC network adaptation, the effect of Zn^{2+} on HGJ channels and the underlying mechanism were investigated in bass retinal HCs. Compared to other divalent cations, Zn^{2+} showed strong inhibitory effects on hemichannel currents by inhibiting HGJ channel currents at micromolar concentrations in a monophasic manner. The inhibition by Zn^{2+} is mediated through histidine residues on the extracellular domain of hemichannels in a

Ca^{2+}-independent way. Most interestingly, the inward hemichannel currents, which are proposed to be the key components in the ephaptic feedback model, are significantly inhibited by Zn^{2+}. Thus, the modulation of HGJ channel currents by Zn^{2+} in the photoreceptor synaptic cleft may provide a mechanism to regulate and limit the ephaptic feedback from HCs to photoreceptors.

Molecular composition and potential physiological role of HGJ Channels in retinal HCs

In this study, outward and inward hemichannel currents are shown to exhibit different properties, which indicates that different Cx proteins may contribute to different hemichannel currents in zebrafish HCs. Previous studies showed that Cx52.6 and Cx55.5 are specifically expressed in HCs in zebrafish retinal slices with different distribution patterns (Shields et al., 2007). However, the physiological role and the molecular composition of these two Cx proteins in zebrafish HCs are not fully understood. In particular, which Cx protein is responsible for the special inward hemichannel currents?

To analyze the composition of zebrafish HC HGJ channels, immunocytochemical staining, *cx55.5* mutant zebrafish and morpholino-based gene knockdown techniques were utilized in this study. First, immunocytochemistry was performed to verify that Cx52.6 and Cx55.5 are expressed in cultured solitary HCs from WT zebrafish. Consistent with reported results, both Cx55.5 and Cx52.6 proteins are present in the cell body and dendrite processes of HCs, indicating that the hemichannel currents recorded by

patch-clamp may be mediated by HGJ channels on the cell body or the dendrites of HCs. Next, studies on *cx55.5* mutant zebrafish show that inward hemichannel currents decrease substantially in the mutant, but it is not clear whether the inward hemichannel currents are specifically contributed by Cx55.5, since both Cx55.5 and Cx52.6 expression reduced dramatically in *cx55.5* mutant zebrafish. On the other hand, the intracellular recording from whole mount retina samples show that *cx55.5* mutant zebrafish exhibit significant decrease in inhibitory feedback signals (the Kamermans lab, ARVO 2008). Taken together, these data suggest that inward hemichannel currents mediate, at least in part, negative feedback communication. Next I examined the molecular basis of inward hemichannels currents. To facilitate this study, an intraocular injection and electroporation method was used to introduce different morpholinos into HCs to target specific *cx* genes for knockdown *in vivo*. The results demonstrate that Cx55.5, but not Cx52.6, is responsible for the inward hemichannel currents, while both Cx55.5 and Cx52.6 are required for outward hemichannel currents. These data suggest that inward hemichannel currents may be mediated by the Cx55.5 homomeric HGJ channels, while outward hemichannel currents may be mediated by the Cx55.5/Cx52.6 heteromeric HGJ channels. In addition, according to previous studies, although both Cx55.5 and Cx52.6 are involved in the formation of HGJ channels, they show different distribution patterns in HCs. Generally, only Cx55.5 is found on the dendrites of HCs, which invaginate into the cone terminals, while HGJ channels composed of Cx52.6 are mostly distributed on the cell body of HCs (Shields et al., 2007). Furthermore, HGJ channels are known as

low-selective and high-permeable ion channels, which permit most ions and biological molecules to pass through the cell membrane. Therefore, it may be critical for HGJ channels with distinct compositions to exhibit different distribution patterns in order to perform the specified functions and avoid fatal leakage. Taken together, inward hemichannel currents may be mediated by the Cx55.5 HGJ channels, which are mostly restricted to the dendrites of HCs. In this case, although Cx55.5 hemichannels remain open upon hyperpolarization under physiological conditions, the cell volume and ion balance of HCs will not be affected. In contrast, the Cx55.5/Cx52.6 heteromeric hemichannels may be responsible for outward hemichannel currents, which are mostly closed under physiological conditions and serve as the structural precursor of gap junctions between HCs.

Functional model of the ephaptic feedback pathway at zebrafish cone terminals

In summary, my study supports the ephaptic hypothesis of the negative feedback pathway at the first visual synapse. The modified functional model is described as follows (**Figure 5-1**). At cone terminals, HCs and bipolar cells are postsynaptic to cones in a lateral and central position, respectively. The dendrites of HCs are embedded deeply in the cone pedicle. The word “ephaptic” describes the communication between anatomically and electrically proximate neurons through the modulation of the extracellular potential where the electric fields generated by a specific neuron can alter the excitability of neighboring neurons (Kamermans and Fahrenfort, 2004). Since the

dendrites of HCs are deeply embedded in the cone pedicle with resultant narrow intercellular spaces, the resistance of the extracellular space is relatively high, which provides the structural basis of ephaptic communication within the cone-HC synapses.

In zebrafish retina, the Cx55.5 homomeric HGJ channels are specifically expressed at the dendrites of HCs, along with the glutamate receptors which are apposed to the voltage-sensitive Ca^{2+} channels in the cone pedicle. The Cx52.6/Cx55.5 heteromeric HGJ channels are mostly present on the cell body of HCs. At the cone terminal, glutamate- and Zn^{2+}-containing synaptic vesicles are distributed along the synaptic ribbons, which are close to the Ca^{2+} channels.

In the dark, glutamate is continuously released from depolarized cones to HCs, resulting in current influx into HCs from intersynaptic spaces through the glutamate receptors, which keeps the HCs depolarized at around -40 mV. Upon spatially broad light stimulation, glutamate release is reduced, resulting in a hyperpolarization of HCs to about -80 mV. The negative membrane potential change of HCs from -40 mV to -80 mV leads to increased Cx55.5 hemichannel-mediated currents (inward hemichannel currents) flowing into HCs from the intersynaptic cleft. Since these currents pass through high intersynaptic resistance, the extracellular potential in the intersynaptic cleft becomes more negative. The voltage-sensitive Ca^{2+} channels then sense a depolarized membrane potential, leading to an increased Ca^{2+} influx into the cone and increased glutamate release. In this way, Cx55.5 hemichannels at the dendrites of HCs can mediate ephaptic feedback at the cone terminals.

During the light response, Zn^{2+} release from photoreceptors is reduced, partially relieving the Zn^{2+} suppression of HGJ channels. Thus, *in situ*, Zn^{2+}-mediated modulation of HGJ channel currents may serve to increase the amplitude or duration of inward hemichannel currents in response to hyperpolarization, strengthening electrotonic feedback from HCs to photoreceptors.

Finally, since inward hemichannel currents are substantially suppressed by 100 μM Co^{2+} and extracellular acidification, these conditions can be used to test the ephaptic feedback model in the intact zebrafish retina.

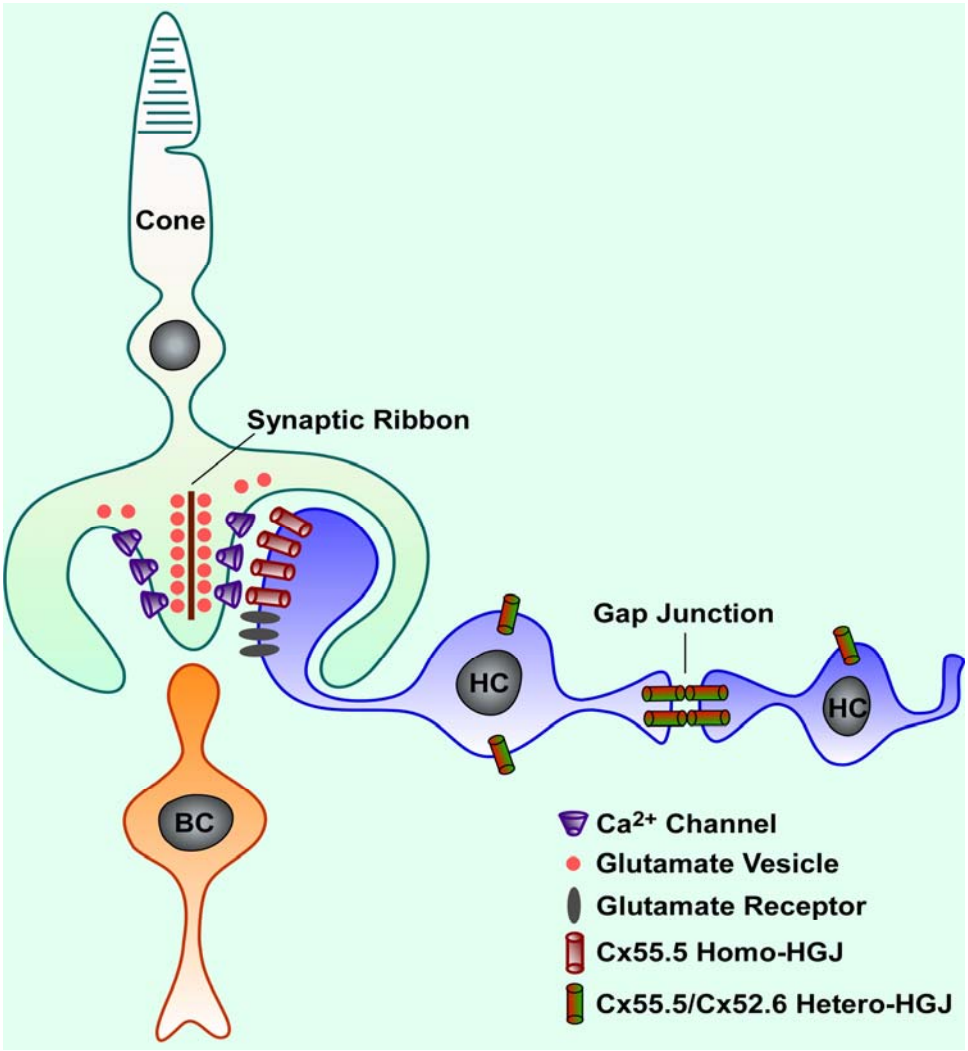

Figure 5-1. Functional model of the ephaptic feedback pathway at zebrafish cone terminals.

Figure 5-1. Functional model of the ephaptic feedback pathway at zebrafish cone terminals.

At the cone synapse, horizontal cells (HCs) and bipolar cells are postsynaptic with the cone in a lateral and central position, respectively. The dendrites of HCs are deeply embedded in the cone pedicle, which provides the structural basis of ephaptic communication between cones and HCs.

In zebrafish retina, Cx55.5 proteins are specifically expressed at HC dendrite tips, which form the homomeric hemi-gap-junction (HGJ) channels, along with the glutamate receptors which are apposed to the voltage-sensitive Ca^{2+} channels in the cone pedicle. On the other hand, the Cx52.6/Cx55.5 heteromeric HGJ channels are mostly present on the cell body of HCs.

In the dark, glutamate is continuously released from depolarized cones to HCs, keeping HCs depolarized at around -40 mV. Upon spatially broad light stimulation, glutamate release is reduced, resulting in a hyperpolarization of HCs to about -80 mV. The negative membrane potential change of HCs from -40 mV to -80 mV leads to increased Cx55.5 hemichannel-mediated currents (inward hemichannel currents) flowing into HCs from the intersynaptic cleft. Since these currents pass through high intersynaptic resistance, the extracellular potential in the intersynaptic cleft becomes more negative. The voltage-sensitive Ca^{2+} channels then sense a depolarized membrane potential, leading to an increased Ca^{2+} influx into the cone and increased glutamate release. In this way, Cx55.5 hemichannels at the dendrites of HCs can mediate ephaptic feedback at the cone terminals.

APPENDIX

FUTURE DIRECTIONS

Although the current study has greatly improved our understanding of the functional properties and molecular composition of hemi-gap-junction (HGJ) channels and the mechanism underlying the negative feedback pathway between horizontal cells (HCs) and photoreceptors, the contributions of other connexin (Cx) isoforms to HGJ channels and the potential role of protons in mediating the inhibitory feedback signal still need to be investigated.

Explore the contributions of other Cx isoforms to the native hemichannel currents in zebrafish retinal HCs

Although Cx52.6 and Cx55.5 are specifically expressed in zebrafish retinal HCs, previous studies indicate that other Cx isoforms may also exist in zebrafish retinal HCs. For example, outward hemichannel currents are significantly increased in HCs from *cx55.5* mutant zebrafish, where Cx52.6 and Cx55.5 expression are both decreased dramatically, compared to WT zebrafish. Interestingly, two new *cx* genes (*cx52.7* and *cx52.9*) have been cloned and identified in zebrafish retina. These *cx* genes are homologous in protein sequence to Cx52.6 and Cx55.5, respectively (Eastman et al., 2006). Although the localization and physiological functions of these new Cx proteins

need to be further investigated, the identification of two pairs of related *cx* genes is consistent with genome duplication as well as the complexity of Cx channel function. It is also possible that these two new Cx isoforms may be expressed in different subtypes of HCs since Cx52.6 and Cx55.5 are expressed only in H_A-HCs, but not in other HC types in zebrafish retina (Shields et al., 2007).

To explore possible contributions of Cx52.7 and Cx52.9 to native hemichannel currents in zebrafish retinal HCs, electrophysiological recordings and morpholino-based gene knockdown techniques will be used. Morpholinos that target four different *cx* genes in 25 bases of 5' untranslated regions (5'-UTR) will be designed and used to specifically inhibit the translation of the Cx mRNA into protein (From Gene Tools, Philomath, OR):

Anti-Cx52.6 morpholino: CACATGGCCTAAAACTGGAAGAGTG;

Anti-Cx52.7 morpholino: CACCGCCACATGTCAGTGCTTCATT;

Anti-Cx55.5 morpholino: TACTCGGGCTTTTTTGTGTCTGTAA;

Anti-Cx52.9 morpholino: CACGCCGGAGGACCCCTGAGATCAA.

These different anti-sense morpholinos will be introduced into adult zebrafish retinas via intraocular injection and electroporation. Four days after morpholino transfection, the protein level of individual Cx proteins will be examined by immunocytochemistry (anti-Cx52.7 antibody and anti-Cx52.9 antibodies have been generated by the Kamermans lab and will be shared with us). Morpholino-treated retinas will be dissected and cultured HCs will be used for patch-clamp recording. In this way, I can investigate the contributions of various Cx isoforms to native hemichannel currents.

I expect that Cx52.7 and Cx52.9 will also be involved in hemichannel formation. Since their amino acid sequences are very similar to Cx52.6 and Cx55.5, they may pair and form functional HGJ channels in a similar pattern to Cx52.6 and Cx55.5. As for the distribution, it is possible that Cx52.7 and Cx52.9 may only show low level expression in all HCs under normal conditions and may be up-regulated in a compensatory way. Alternatively, it is also possible that Cx52.7 and Cx52.9 may be expressed primarily in certain subtypes of HCs other than H_A type HCs.

Test a potential model that unites "proton" and "ephaptic" hypotheses by investigating pH-related properties of HGJ channels

Although the current study supports the "ephaptic" negative feedback model, previous reports also show that protons released in the synaptic cleft can modulate calcium currents in cones (DeVries, 2001) and the feedback pathway can be blocked by elevated extracellular pH buffering (Vessey et al., 2005). According to the proton hypothesis, hyperpolarization of HCs results in an increase in pH within the synaptic cleft, which then activates the Ca^{2+} current in cones, eventually enhancing transmitter release. Alternatively, the ephaptic hypothesis proposes that hyperpolarization of HCs leads to an increased influx of hemichannel currents, which in turn increases the calcium current in cones, and finally causes an increased release of transmitter (Kamermans et al., 2001b). However, these two hypotheses are not necessarily mutually exclusive. There are three possible ways to reconcile these two hypotheses. First, it is possible that the effect of

protons on the Ca^{2+} current is through modulation of HGJ channels. For example increased pH may increase the hemichannel mediated currents. Second, HEPES, Tris or other non-bicarbonate buffers, which have been applied in testing the proton hypothesis, may actually block the HGJ channels in HCs. Third, alkalinization within the intersynaptic cleft upon light stimulation may be partially contributed by the HGJ channels, which may carry the inward H^+ currents.

To address these possibilities, I will record hemichannel currents from cultured isolated zebrafish HCs using the patch-clamp electrophysiological method. A series of pharmacological reagents will be applied to change the intracellular pH or the extracellular pH buffering to assess their modulation of hemichannel currents, especially inward hemichannel currents. It is noteworthy that in all experiments performed for my studies, 10 mm HEPES was used as a buffer in both extracellular and intracellular solutions, and substantial inward hemichannel currents were still observed. However, from these experiments I cannot conclude whether there is an effect of HEPES on hemichannel currents. In a future study, HEPES buffers with different pH and concentrations, as well as other buffers (e.g. Tris and bicarbonate) will be tested. This series of experiments should resolve the first two possibilities. To test the last possibility, I will monitor and compare the extracellular pH change near the HC surface upon hyperpolarization between WT and *cx55.5* mutant zebrafish. If the last possibility is correct, a decreased alkalinization in the extracellular space of HCs isolated from *cx55.5* mutant zebrafish will be expected upon hyperpolarization compared to WT zebrafish HCs.

For this purpose, the extracellular membrane-bound fluorescent pH indicator 5-hexadecanoylaminofluorescein (HAF) will be used to monitor the surface pH change around HCs (Genz et al., 1999; Jouhou et al., 2007). In this way, whether the HGJ channels expressed in HCs could unite these two models can be assessed.

REFERENCES

Akagi T, Kaneda M, Ishii K, Hashikawa T (2001) Differential subcellular localization of zinc in the rat retina. J Histochem Cytochem 49:87-96.

Al-Ubaidi MR, White TW, Ripps H, Poras I, Avner P, Gomes D, Bruzzone R (2000) Functional properties, developmental regulation, and chromosomal localization of murine connexin36, a gap-junctional protein expressed preferentially in retina and brain. J Neurosci Res 59:813-826.

Assaf SY, Chung SH (1984) Release of endogenous Zn2+ from brain tissue during activity. Nature 308:734-736.

Baier H, Klostermann S, Trowe T, Karlstrom RO, Nusslein-Volhard C, Bonhoeffer F (1996) Genetic dissection of the retinotectal projection. Development 123:415-425.

Baldridge WH, Ball AK, Miller RG (1987) Dopaminergic regulation of horizontal cell gap junction particle density in goldfish retina. J Comp Neurol 265:428-436.

Barnes S, Merchant V, Mahmud F (1993) Modulation of transmission gain by protons at the photoreceptor output synapse. Proc Natl Acad Sci U S A 90:10081-10085.

Baylor DA, Fuortes MG, O'Bryan PM (1971) Receptive fields of cones in the retina of the turtle. J Physiol 214:265-294.

Beahm DL, Hall JE (2002) Hemichannel and junctional properties of connexin 50. Biophys J 82:2016-2031.

Berson DM, Dunn FA, Takao M (2002) Phototransduction by retinal ganglion cells that set the circadian clock. Science 295:1070-1073.

Berthoud VM, Minogue PJ, Laing JG, Beyer EC (2004) Pathways for degradation of connexins and gap junctions. Cardiovasc Res 62:256-267.

Bevans CG, Kordel M, Rhee SK, Harris AL (1998) Isoform composition of connexin channels determines selectivity among second messengers and uncharged molecules. J Biol Chem 273:2808-2816.

Bilotta J, Saszik S (2001) The zebrafish as a model visual system. Int J Dev Neurosci 19:621-629.

Bloomfield SA, Volgyi B (2009) The diverse functional roles and regulation of neuronal gap junctions in the retina. Nat Rev Neurosci 10:495-506.

Burkhardt DA (1977) Responses and receptive-field organization of cones in perch retinas. J Neurophysiol 40:53-62.

Burkhardt DA (1993) Synaptic feedback, depolarization, and color opponency in cone photoreceptors. Vis Neurosci 10:981-989.

Byzov AL, Shura-Bura TM (1986) Electrical feedback mechanism in the processing of signals in the outer plexiform layer of the retina. Vision Res 26:33-44.

Cao F, Eckert R, Elfgang C, Nitsche JM, Snyder SA, DF Hu, Willecke K, Nicholson BJ (1998) A quantitative analysis of connexin-specific permeability differences of gap junctions expressed in HeLa transfectants and Xenopus oocytes. J Cell Sci 111 (Pt 1):31-43.

Chappell RL, Zakevicius J, Ripps H (2003) Zinc modulation of hemichannel currents in Xenopus oocytes. Biol Bull 205:209-211.

Chappell RL, Qian H, Zakevicius J, Ripps H (2004) Histidine suppresses zinc modulation of connexin hemichannels. Biol Bull 207:188-190.

Cheng N, Tsunenari T, Yau KW (2009) Intrinsic light response of retinal horizontal cells of teleosts. Nature 460:899-903.

Connaughton VP, Dowling JE (1998) Comparative morphology of distal neurons in larval and adult zebrafish retinas. Vision Res 38:13-18.

Connaughton VP, Graham D, Nelson R (2004) Identification and morphological classification of horizontal, bipolar, and amacrine cells within the zebrafish retina. J Comp Neurol 477:371-385.

Connolly CN, Wafford KA (2004) The Cys-loop superfamily of ligand-gated ion channels: the impact of receptor structure on function. Biochem Soc Trans 32:529-534.

Contreras JE, Saez JC, Bukauskas FF, Bennett MV (2003) Gating and regulation of connexin 43 (Cx43) hemichannels. Proc Natl Acad Sci U S A 100:11388-11393.

Contreras JE, Sanchez HA, Veliz LP, Bukauskas FF, Bennett MV, Saez JC (2004) Role of connexin-based gap junction channels and hemichannels in ischemia-induced cell death in nervous tissue. Brain Res Brain Res Rev 47:290-303.

Cruciani V, Mikalsen SO (2007) Evolutionary selection pressure and family relationships

among connexin genes. Biol Chem 388:253-264.

de Groot JR, Veenstra T, Verkerk AO, Wilders R, Smits JP, Wilms-Schopman FJ, Wiegerinck RF, Bourier J, Belterman CN, Coronel R, Verheijck EE (2003) Conduction slowing by the gap junctional uncoupler carbenoxolone. Cardiovasc Res 60:288-297.

Dearry A, Burnside B (1984) Effects of extracellular Ca++, K+, and Na+ on cone and retinal pigment epithelium retinomotor movements in isolated teleost retinas. J Gen Physiol 83:589-611.

Dermietzel R, Kremer M, Paputsoglu G, Stang A, Skerrett IM, Gomes D, Srinivas M, Janssen-Bienhold U, Weiler R, Nicholson BJ, Bruzzone R, Spray DC (2000) Molecular and functional diversity of neural connexins in the retina. J Neurosci 20:8331-8343.

DeVries SH (2001) Exocytosed protons feedback to suppress the Ca2+ current in mammalian cone photoreceptors. Neuron 32:1107-1117.

DeVries SH, Schwartz EA (1989) Modulation of an electrical synapse between solitary pairs of catfish horizontal cells by dopamine and second messengers. J Physiol 414:351-375.

DeVries SH, Schwartz EA (1992) Hemi-gap-junction channels in solitary horizontal cells of the catfish retina. J Physiol 445:201-230.

Dixon DB, Takahashi K, Bieda M, Copenhagen DR (1996) Quinine, intracellular pH and modulation of hemi-gap junctions in catfish horizontal cells. Vision Res 36:3925-3931.

Dong CJ, Werblin FS (1996) Use-dependent and use-independent blocking actions of picrotoxin and zinc at the GABAC receptor in retinal horizontal cells. Vision Res 36:3997-4005.

Easter SS, Jr., Nicola GN (1996) The development of vision in the zebrafish (Danio rerio). Dev Biol 180:646-663.

Eastman SD, Chen TH, Falk MM, Mendelson TC, Iovine MK (2006) Phylogenetic analysis of three complete gap junction gene families reveals lineage-specific duplications and highly supported gene classes. Genomics 87:265-274.

Ebihara L, Steiner E (1993) Properties of a nonjunctional current expressed from a rat connexin46 cDNA in Xenopus oocytes. J Gen Physiol 102:59-74.

Ebihara L, Berthoud VM, Beyer EC (1995) Distinct behavior of connexin56 and connexin46 gap junctional channels can be predicted from the behavior of their hemi-gap-junctional channels. Biophys J 68:1796-1803.

Ebihara L, Beyer EC, Swenson KI, Paul DL, Goodenough DA (1989) Cloning and expression of a Xenopus embryonic gap junction protein. Science 243:1194-1195.

Elfgang C, Eckert R, Lichtenberg-Frate H, Butterweck A, Traub O, Klein RA, Hulser DF, Willecke K (1995) Specific permeability and selective formation of gap junction channels in connexin-transfected HeLa cells. J Cell Biol 129:805-817.

Fadool JM, Brockerhoff SE, Hyatt GA, Dowling JE (1997) Mutations affecting eye morphology in the developing zebrafish (Danio rerio). Dev Genet 20:288-295.

Fahrenfort I, Sjoerdsma T, Ripps H, Kamermans M (2004) Cobalt ions inhibit negative feedback in the outer retina by blocking hemichannels on horizontal cells. Vis Neurosci 21:501-511.

Fahrenfort I, Steijaert M, Sjoerdsma T, Vickers E, Ripps H, van Asselt J, Endeman D, Klooster J, Numan R, ten Eikelder H, von Gersdorff H, Kamermans M (2009) Hemichannel-mediated and pH-based feedback from horizontal cells to cones in the vertebrate retina. PLoS One 4:e6090.

Feigenspan A, Weiler R (2004) Electrophysiological properties of mouse horizontal cell GABAA receptors. J Neurophysiol 92:2789-2801.

Foote CI, Zhou L, Zhu X, Nicholson BJ (1998) The pattern of disulfide linkages in the extracellular loop regions of connexin 32 suggests a model for the docking interface of gap junctions. J Cell Biol 140:1187-1197.

Genz AK, v Engelhardt W, Busche R (1999) Maintenance and regulation of the pH microclimate at the luminal surface of the distal colon of guinea-pig. J Physiol 517 (Pt 2):507-519.

Gimlich RL, Kumar NM, Gilula NB (1988) Sequence and developmental expression of mRNA coding for a gap junction protein in Xenopus. J Cell Biol 107:1065-1073.

Glass AS, Dahm R (2004) The zebrafish as a model organism for eye development. Ophthalmic Res 36:4-24.

Golling G, Amsterdam A, Sun Z, Antonelli M, Maldonado E, Chen W, Burgess S, Haldi M, Artzt K, Farrington S, Lin SY, Nissen RM, Hopkins N (2002) Insertional mutagenesis in zebrafish rapidly identifies genes essential for early vertebrate

development. Nat Genet 31:135-140.

Gomez-Hernandez JM, de Miguel M, Larrosa B, Gonzalez D, Barrio LC (2003) Molecular basis of calcium regulation in connexin-32 hemichannels. Proc Natl Acad Sci U S A 100:16030-16035.

Goodenough DA, Paul DL (2003) Beyond the gap: functions of unpaired connexon channels. Nat Rev Mol Cell Biol 4:285-294.

Grahn BH, Paterson PG, Gottschall-Pass KT, Zhang Z (2001) Zinc and the eye. J Am Coll Nutr 20:106-118.

Han Y, Wu SM (1999) Modulation of glycine receptors in retinal ganglion cells by zinc. Proc Natl Acad Sci U S A 96:3234-3238.

Harris AL (2001) Emerging issues of connexin channels: biophysics fills the gap. Q Rev Biophys 34:325-472.

Hattar S, Liao HW, Takao M, Berson DM, Yau KW (2002) Melanopsin-containing retinal ganglion cells: architecture, projections, and intrinsic photosensitivity. Science 295:1065-1070.

Hirasawa H, Kaneko A (2003) pH changes in the invaginating synaptic cleft mediate feedback from horizontal cells to cone photoreceptors by modulating Ca2+ channels. J Gen Physiol 122:657-671.

Horenstein J, Akabas MH (1998) Location of a high affinity Zn2+ binding site in the channel of alpha1beta1 gamma-aminobutyric acidA receptors. Mol Pharmacol 53:870-877.

Huang EP (1997) Metal ions and synaptic transmission: think zinc. Proc Natl Acad Sci U S A 94:13386-13387.

Huber AM, Gershoff SN (1975) Effects of zinc deficiency on the oxidation of retinol and ethanol in rats. J Nutr 105:1486-1490.

Janssen-Bienhold U, Dermietzel R, Weiler R (1998) Distribution of connexin43 immunoreactivity in the retinas of different vertebrates. J Comp Neurol 396:310-321.

Janssen-Bienhold U, Schultz K, Gellhaus A, Schmidt P, Ammermuller J, Weiler R (2001) Identification and localization of connexin26 within the photoreceptor-horizontal cell synaptic complex. Vis Neurosci 18:169-178.

Jouhou H, Yamamoto K, Homma A, Hara M, Kaneko A, Yamada M (2007) Depolarization of isolated horizontal cells of fish acidifies their immediate surrounding by activating V-ATPase. J Physiol 585:401-412.

Kamermans M, Fahrenfort I (2004) Ephaptic interactions within a chemical synapse: hemichannel-mediated ephaptic inhibition in the retina. Curr Opin Neurobiol 14:531-541.

Kamermans M, van Dijk BW, Spekreijse H (1991) Color opponency in cone-driven horizontal cells in carp retina. Aspecific pathways between cones and horizontal cells. J Gen Physiol 97:819-843.

Kamermans M, Kraaij D, Spekreijse H (2001a) The dynamic characteristics of the feedback signal from horizontal cells to cones in the goldfish retina. J Physiol 534:489-500.

Kamermans M, Fahrenfort I, Schultz K, Janssen-Bienhold U, Sjoerdsma T, Weiler R (2001b) Hemichannel-mediated inhibition in the outer retina. Science 292:1178-1180.

Kaneko A (1971) Electrical connexions between horizontal cells in the dogfish retina. J Physiol 213:95-105.

Katz BA, Luong C (1999) Recruiting Zn2+ to mediate potent, specific inhibition of serine proteases. J Mol Biol 292:669-684.

Kay AR, Toth K (2008) Is zinc a neuromodulator? Sci Signal 1:re3.

Keeling PW, O'Day J, Ruse W, Thompson RP (1982) Zinc deficiency and photoreceptor dysfunction in chronic liver disease. Clin Sci (Lond) 62:109-111.

Kraaij DA, Kamermans M, Spekreijse H (1998) Spectral sensitivity of the feedback signal from horizontal cells to cones in goldfish retina. Vis Neurosci 15:799-808.

Kumar NM, Gilula NB (1986) Cloning and characterization of human and rat liver cDNAs coding for a gap junction protein. J Cell Biol 103:767-776.

Lam DM, Lasater EM, Naka KI (1978) gamma-Aminobutyric acid: a neurotransmitter candidate for cone horizontal cells of the catfish retina. Proc Natl Acad Sci U S A 75:6310-6313.

Lee SC, Zhong YM, Li RX, Yu Z, Yang XL (2008) Localization of zinc in the outer retina of carp: a light- and electron-microscopic study. Synapse 62:352-357.

Leure-duPree AE, McClain CJ (1982) The effect of severe zinc deficiency on the morphology of the rat retinal pigment epithelium. Invest Ophthalmol Vis Sci 23:425-434.

Malchow RP, Qian H, Ripps H (1993) Evidence for hemi-gap junctional channels in isolated horizontal cells of the skate retina. J Neurosci Res 35:237-245.

Malchow RP, Qian H, Ripps H (1994) A novel action of quinine and quinidine on the membrane conductance of neurons from the vertebrate retina. J Gen Physiol 104:1039-1055.

Malicki J, Neuhauss SC, Schier AF, Solnica-Krezel L, Stemple DL, Stainier DY, Abdelilah S, Zwartkruis F, Rangini Z, Driever W (1996) Mutations affecting development of the zebrafish retina. Development 123:263-273.

Mancini GM, Beerens CE, Galjaard H, Verheijen FW (1992) Functional reconstitution of the lysosomal sialic acid carrier into proteoliposomes. Proc Natl Acad Sci U S A 89:6609-6613.

Mangel SC, Ariel M, Dowling JE (1985) Effects of acidic amino acid antagonists upon the spectral properties of carp horizontal cells: circuitry of the outer retina. J Neurosci 5:2839-2850.

Mares-Perlman JA, Klein R, Klein BE, Greger JL, Brady WE, Palta M, Ritter LL (1996) Association of zinc and antioxidant nutrients with age-related maculopathy. Arch Ophthalmol 114:991-997.

McClain CJ, Van Thiel DH, Parker S, Badzin LK, Gilbert H (1979) Alterations in zinc, vitamin A, and retinol-binding protein in chronic alcoholics: a possible mechanism for night blindness and hypogonadism. Alcohol Clin Exp Res 3:135-141.

McLachlan E, White TW, Ugonabo C, Olson C, Nagy JI, Valdimarsson G (2003) Zebrafish Cx35: cloning and characterization of a gap junction gene highly expressed in the retina. J Neurosci Res 73:753-764.

McMahon DG (1994) Modulation of electrical synaptic transmission in zebrafish retinal horizontal cells. J Neurosci 14:1722-1734.

McMahon DG, Brown DR (1994) Modulation of gap-junction channel gating at zebrafish retinal electrical synapses. J Neurophysiol 72:2257-2268.

McMahon DG, Knapp AG, Dowling JE (1989) Horizontal cell gap junctions: single-channel conductance and modulation by dopamine. Proc Natl Acad Sci U S A 86:7639-7643.

Molina AJ, Verzi MP, Birnbaum AD, Yamoah EN, Hammar K, Smith PJ, Malchow RP (2004) Neurotransmitter modulation of extracellular H+ fluxes from isolated retinal horizontal cells of the skate. J Physiol 560:639-657.

Morrison SA, Russell RM, Carney EA, Oaks EV (1978) Zinc deficiency: a cause of abnormal dark adaptation in cirrhotics. Am J Clin Nutr 31:276-281.

Muto A, Orger MB, Wehman AM, Smear MC, Kay JN, Page-McCaw PS, Gahtan E, Xiao T, Nevin LM, Gosse NJ, Staub W, Finger-Baier K, Baier H (2005) Forward genetic analysis of visual behavior in zebrafish. PLoS Genet 1:e66.

Naka KI (1972) The horizontal cells. Vision Res 12:573-588.

Naka KI, Rushton WA (1967) The generation and spread of S-potentials in fish (Cyprinidae). J Physiol 192:437-461.

Neuhauss SC (2003) Behavioral genetic approaches to visual system development and function in zebrafish. J Neurobiol 54:148-160.

Nevin ST, Cromer BA, Haddrill JL, Morton CJ, Parker MW, Lynch JW (2003) Insights into the structural basis for zinc inhibition of the glycine receptor. J Biol Chem 278:28985-28992.

Norregaard L, Frederiksen D, Nielsen EO, Gether U (1998) Delineation of an endogenous zinc-binding site in the human dopamine transporter. Embo J 17:4266-4273.

Panda S, Sato TK, Castrucci AM, Rollag MD, DeGrip WJ, Hogenesch JB, Provencio I, Kay SA (2002) Melanopsin (Opn4) requirement for normal light-induced circadian phase shifting. Science 298:2213-2216.

Paul DL (1986) Molecular cloning of cDNA for rat liver gap junction protein. J Cell Biol 103:123-134.

Paul DL, Ebihara L, Takemoto LJ, Swenson KI, Goodenough DA (1991) Connexin46, a novel lens gap junction protein, induces voltage-gated currents in nonjunctional plasma membrane of Xenopus oocytes. J Cell Biol 115:1077-1089.

Plotkin LI, Bellido T (2001) Bisphosphonate-induced, hemichannel-mediated, anti-apoptosis through the Src/ERK pathway: a gap junction-independent action of connexin43. Cell Commun Adhes 8:377-382.

Plotkin LI, Manolagas SC, Bellido T (2002) Transduction of cell survival signals by connexin-43 hemichannels. J Biol Chem 277:8648-8657.

Poe M, Hoogsteen K, Matthews DA (1979) Proton magnetic resonance studies on Escherichia coli dihydrofolate reductase. Assignment of histidine C-2 protons in binary complexes with folates on the basis of the crystal structure with methotrexate and on chemical modifications. J Biol Chem 254:8143-8152.

Prochnow N, Hoffmann S, Vroman R, Klooster J, Bunse S, Kamermans M, Dermietzel R, Zoidl G (2009) Pannexin1 in the outer retina of the zebrafish, Danio rerio. Neuroscience 162:1039-1054.

Pujic Z, Omori Y, Tsujikawa M, Thisse B, Thisse C, Malicki J (2006) Reverse genetic analysis of neurogenesis in the zebrafish retina. Dev Biol 293:330-347.

Qian H, Li L, Chappell RL, Ripps H (1997) GABA receptors of bipolar cells from the skate retina: actions of zinc on GABA-mediated membrane currents. J Neurophysiol 78:2402-2412.

Redenti S, Ripps H, Chappell RL (2007) Zinc release at the synaptic terminals of rod photoreceptors. Exp Eye Res 85:580-584.

Retamal MA, Cortes CJ, Reuss L, Bennett MV, Saez JC (2006) S-nitrosylation and permeation through connexin 43 hemichannels in astrocytes: induction by oxidant stress and reversal by reducing agents. Proc Natl Acad Sci U S A 103:4475-4480.

Richard G, Smith LE, Bailey RA, Itin P, Hohl D, Epstein EH, Jr., DiGiovanna JJ, Compton JG, Bale SJ (1998) Mutations in the human connexin gene GJB3 cause erythrokeratodermia variabilis. Nat Genet 20:366-369.

Ripps H, Qian H, Zakevicius J (2002) Pharmacological enhancement of hemi-gap-junctional currents in Xenopus oocytes. J Neurosci Methods 121:81-92.

Ripps H, Qian H, Zakevicius J (2004) Properties of connexin26 hemichannels expressed in Xenopus oocytes. Cell Mol Neurobiol 24:647-665.

Robinson J, Schmitt EA, Harosi FI, Reece RJ, Dowling JE (1993) Zebrafish ultraviolet visual pigment: absorption spectrum, sequence, and localization. Proc Natl Acad Sci U S A 90:6009-6012.

Saez JC, Retamal MA, Basilio D, Bukauskas FF, Bennett MV (2005) Connexin-based gap junction hemichannels: gating mechanisms. Biochim Biophys Acta 1711:215-224.

Schwartz EA (2002) Transport-mediated synapses in the retina. Physiol Rev 82:875-891.

Seebungkert B, Lynch JW (2001) A common inhibitory binding site for zinc and odorants

at the voltage-gated K(+) channel of rat olfactory receptor neurons. Eur J Neurosci 14:353-362.

Shen Y, Yang XL (1999) Zinc modulation of AMPA receptors may be relevant to splice variants in carp retina. Neurosci Lett 259:177-180.

Shields CR, Klooster J, Claassen Y, Ul-Hussain M, Zoidl G, Dermietzel R, Kamermans M (2007) Retinal horizontal cell-specific promoter activity and protein expression of zebrafish connexin 52.6 and connexin 55.5. J Comp Neurol 501:765-779.

Sohl G, Willecke K (2004) Gap junctions and the connexin protein family. Cardiovasc Res 62:228-232.

Spray DC, Ye ZC, Ransom BR (2006) Functional connexin "hemichannels": a critical appraisal. Glia 54:758-773.

Srinivas M, Calderon DP, Kronengold J, Verselis VK (2006) Regulation of connexin hemichannels by monovalent cations. J Gen Physiol 127:67-75.

Stell WK, Lightfoot DO (1975) Color-specific interconnections of cones and horizontal cells in the retina of the goldfish. J Comp Neurol 159:473-502.

Stergiopoulos K, Alvarado JL, Mastroianni M, Ek-Vitorin JF, Taffet SM, Delmar M (1999) Hetero-domain interactions as a mechanism for the regulation of connexin channels. Circ Res 84:1144-1155.

Stone S, Witkovsky P (1987) Center-surround organization of Xenopus horizontal cells and its modification by gamma-aminobutyric acid and strontium. Exp Biol 47:1-12.

Stout CE, Costantin JL, Naus CC, Charles AC (2002) Intercellular calcium signaling in astrocytes via ATP release through connexin hemichannels. J Biol Chem 277:10482-10488.

Summerton J, Weller D (1997) Morpholino antisense oligomers: design, preparation, and properties. Antisense Nucleic Acid Drug Dev 7:187-195.

Sun Z, Zhang DQ, McMahon DG (2009) Zinc modulation of hemi-gap-junction channel currents in retinal horizontal cells. J Neurophysiol 101:1774-1780.

Tachibana M, Kaneko A (1984) gamma-Aminobutyric acid acts at axon terminals of turtle photoreceptors: difference in sensitivity among cell types. Proc Natl Acad Sci U S A 81:7961-7964.

Taylor JS, Van de Peer Y, Braasch I, Meyer A (2001) Comparative genomics provides

evidence for an ancient genome duplication event in fish. Philos Trans R Soc Lond B Biol Sci 356:1661-1679.

Taylor JS, Braasch I, Frickey T, Meyer A, Van de Peer Y (2003) Genome duplication, a trait shared by 22000 species of ray-finned fish. Genome Res 13:382-390.

Thompson RJ, Zhou N, MacVicar BA (2006) Ischemia opens neuronal gap junction hemichannels. Science 312:924-927.

Thoreson WB, Burkhardt DA (1990) Effects of synaptic blocking agents on the depolarizing responses of turtle cones evoked by surround illumination. Vis Neurosci 5:571-583.

Thummel R, Kassen SC, Montgomery JE, Enright JM, Hyde DR (2008) Inhibition of Muller glial cell division blocks regeneration of the light-damaged zebrafish retina. Dev Neurobiol 68:392-408.

Toyofuku T, Yabuki M, Otsu K, Kuzuya T, Hori M, Tada M (1998) Intercellular calcium signaling via gap junction in connexin-43-transfected cells. J Biol Chem 273:1519-1528.

Trexler EB, Bennett MV, Bargiello TA, Verselis VK (1996) Voltage gating and permeation in a gap junction hemichannel. Proc Natl Acad Sci U S A 93:5836-5841.

Twig G, Levy H, Perlman I (2003) Color opponency in horizontal cells of the vertebrate retina. Prog Retin Eye Res 22:31-68.

Ugarte M, Osborne NN (2001) Zinc in the retina. Prog Neurobiol 64:219-249.

Valiunas V, Mui R, McLachlan E, Valdimarsson G, Brink PR, White TW (2004) Biophysical characterization of zebrafish connexin35 hemichannels. Am J Physiol Cell Physiol 287:C1596-1604.

Vandenbranden CA, Verweij J, Kamermans M, Muller LJ, Ruijter JM, Vrensen GF, Spekreijse H (1996) Clearance of neurotransmitter from the cone synaptic cleft in goldfish retina. Vision Res 36:3859-3874.

Verselis VK, Srinivas M (2008) Divalent cations regulate connexin hemichannels by modulating intrinsic voltage-dependent gating. J Gen Physiol 132:315-327.

Verselis VK, Trexler EB, Bukauskas FF (2000) Connexin hemichannels and cell-cell channels: comparison of properties. Braz J Med Biol Res 33:379-389.

Verweij J, Kamermans M, Spekreijse H (1996) Horizontal cells feed back to cones by

shifting the cone calcium-current activation range. In: Vision Res, pp 3943-3953.

Verweij J, Hornstein EP, Schnapf JL (2003) Surround antagonism in macaque cone photoreceptors. J Neurosci 23:10249-10257.

Vessey JP, Stratis AK, Daniels BA, Da Silva N, Jonz MG, Lalonde MR, Baldridge WH, Barnes S (2005) Proton-mediated feedback inhibition of presynaptic calcium channels at the cone photoreceptor synapse. J Neurosci 25:4108-4117.

Wagner TL, Beyer EC, McMahon DG (1998) Cloning and functional expression of a novel gap junction channel from the retina of Danio aquipinnatus. Vis Neurosci 15:1137-1144.

White TW, Deans MR, O'Brien J, Al-Ubaidi MR, Goodenough DA, Ripps H, Bruzzone R (1999) Functional characteristics of skate connexin35, a member of the gamma subfamily of connexins expressed in the vertebrate retina. Eur J Neurosci 11:1883-1890.

Witkovsky P, Owen WG, Woodworth M (1983) Gap junctions among the perikarya, dendrites, and axon terminals of the luminosity-type horizontal cell of the turtle retina. J Comp Neurol 216:359-368.

Wu SM (1992) Feedback connections and operation of the outer plexiform layer of the retina. Curr Opin Neurobiol 2:462-468.

Wu SM, Qiao X, Noebels JL, Yang XL (1993) Localization and modulatory actions of zinc in vertebrate retina. Vision Res 33:2611-2616.

Yamada E, Ishikawa T (1965) The fine structure of the horizontal cells in some vertebrate retinae. Cold Spring Harb Symp Quant Biol 30:383-392.

Zhang DQ, McMahon DG (2000) Direct gating by retinoic acid of retinal electrical synapses. Proc Natl Acad Sci U S A 97:14754-14759.

Zhang DQ, McMahon DG (2001) Gating of retinal horizontal cell hemi gap junction channels by voltage, Ca2+, and retinoic acid. Mol Vis 7:247-252.

Zhang DQ, Sun Z, McMahon DG (2006) Modulation of A-type potassium currents in retinal horizontal cells by extracellular calcium and zinc. Vis Neurosci 23:825-832.

Zhang DQ, Ribelayga C, Mangel SC, McMahon DG (2002) Suppression by zinc of AMPA receptor-mediated synaptic transmission in the retina. J Neurophysiol 88:1245-1251.

Zhang L, Deng T, Sun Y, Liu K, Yang Y, Zheng X (2008) Role for nitric oxide in permeability of hippocampal neuronal hemichannels during oxygen glucose deprivation. J Neurosci Res 86:2281-2291.

Zoidl G, Kremer M, Zoidl C, Bunse S, Dermietzel R (2008) Molecular diversity of connexin and pannexin genes in the retina of the zebrafish Danio rerio. Cell Commun Adhes 15:169-183.

Zoidl G, Bruzzone R, Weickert S, Kremer M, Zoidl C, Mitropoulou G, Srinivas M, Spray DC, Dermietzel R (2004) Molecular cloning and functional expression of zfCx52.6: a novel connexin with hemichannel-forming properties expressed in horizontal cells of the zebrafish retina. J Biol Chem 279:2913-2921.